

A TRANSIENT ANALYSIS OF TEMPERATURES
AND THERMAL STRESSES IN GAMMA
HEATED MATERIALS

by

NORMAN KARL RUMPF

B. S., Lehigh University, 1959

A MASTER'S THESIS

submitted in partial fulfillment of the

requirements for the degree

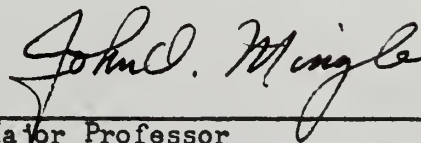
MASTER OF SCIENCE

Department of Nuclear Engineering

KANSAS STATE UNIVERSITY
Manhattan, Kansas

1963

Approved by:



Major Professor

TABLE OF CONTENTS

INTRODUCTION.....	1
NOMENCLATURE.....	4
THEORY.....	6
CALCULATIONS.....	13
The Single Plate with Constant Gamma Photon Flux and Radiative Heat Loss.....	13
The Single Plate with Time Dependent Gamma Photon Flux and Radiative Heat Loss.....	15
Two Parallel Plates with both Convection and Radiation Heat Loss in a Constant Gamma Photon Beam.....	17
DISCUSSION AND RESULTS.....	20
The Single Plate with Constant Gamma Photon Flux and Radiative Heat Loss.....	20
The Single Plate with Time Dependent Gamma Photon Flux and Radiative Heat Loss.....	39
Two Parallel Plates with both Convection and Radiation Heat Loss in a Constant Gamma Photon Beam.....	45
Conclusions.....	54
Suggestions for Further Work.....	57
ACKNOWLEDGEMENT.....	61
BIBLIOGRAPHY.....	62
APPENDICES.....	64
APPENDIX A: Derivation of the Temperature Distribution and Thermal Stresses in a Flat Plate with Insulation at One Face and Radiation Heat Loss at the Other Face.....	65
APPENDIX B: Derivation of the Temperature Distribution and Thermal Stresses in a Flat Plate with Decaying Internal Heat Generation.....	71

APPENDIX C:	Derivation of the Temperature Distribution in Parallel Plates with a Constant Gamma Photon Flux, Insulation at the Inner Face, Gas Flow Between the Plates and Radiation Heat Loss from the Outside Face.....	76
APPENDIX D:	Description and Explanation of the IBM 1620 FORTRAN Program to Find the Temperature Distribution and the Thermal Stresses in a Plate with Insulation at One Face and Radiative Heat Loss at the Other Face when Subjected to a Constant Gamma Photon Flux at the First Face.....	85
APPENDIX E:	Description and Explanation of the IBM 1620 FORTRAN Program to Calculate the Temperature Distribution and Thermal Stresses in a Plate with Insulation at One Face and Radiative Heat Loss at the Other Face, when Subjected to a Time Dependent Gamma Photon Beam at the First Face.....	102
APPENDIX F:	Description and Explanation of the IBM 1620 FORTRAN Program to Equate the Steady State Maximum Thermal Stress and Find the Temperature Distribution in the Outer Plate of Two Parallel Plates.....	110

INTRODUCTION

The advent of the space age, and the proposals for nuclear rockets which have naturally followed, has presented perplexing physical situations which have not been previously considered. One of the more prominent of these is that of the heating of materials by the attenuation of a beam of gamma photons of high flux intensity.

Such a physical situation would be found in the structural members of a nuclear rocket which are in the near proximity of the reactor. Although the problem of non uniform heat generation is somewhat unique, it is really the unusual boundary conditions which give rise to this new series of problems which are dissimilar from those which have been conventionally considered. Consequently, the mathematical models needed to analyze such systems have also needed alteration.

Two properties of special interest in such systems are the temperature and the thermal stresses in the materials subjected to this high intensity gamma photon flux. Structural members obviously will have their utility seriously impaired if the temperature of the material is allowed to approach the melting point or if the stresses arising in the material rise to such proportions that the member tends to buckle.

In keeping with the physical conditions under consideration, the availability of certain modes of heat transfer can be considered only in specific instances. The most prominent evidence of this is the absence of convection in regions of extremely low atmospheric density such as would occur in outer space. Consequently, the primary manner in which heat may be carried from a body is first through conduction to the surface and then by thermal radiation from the surface to the surroundings.

Since a limited amount of information is available in the literature with regard to such systems, it is necessary to construct mathematical models which closely approximate these conditions and then attempt to find solutions to the resulting equations and boundary conditions which are proposed.

A first approximation to a feasible physical system is that of an infinite plate with insulation at one face and radiative heat loss at the other face. Such a system easily yields a solution, especially in the steady state case, provided the flux is of a constant intensity. However, since radiative heat loss presents a non linear system of equations, it is necessary to approximate the true solution by forming an equivalent gray body convective radiation coefficient so that a linear system is created. Equating this to the true thermal radiation heat loss determines the value of the coefficient and subsequently the exact solution to the resulting system of equations.

During the operation of the reactor, the gamma flux can be considered to be of constant intensity. However, after shutdown the flux becomes a function of time and the problem of expressing the temperature of the plate with regard to its time dependency becomes considerably more complex. This complexity is significantly reduced by resorting to numerical techniques coupled with the use of a high speed digital computer. The primary significance of the considerations involved in such a situation is the knowledge of the time evolved in attaining the maximum temperature of the plate after the shutdown of the reactor and also the magnitude of this temperature. Of course the period of operation of the reactor and the type of material being considered are determining factors in such considerations.

In an attempt to keep the temperature and the maximum thermal stress well within the probable destructive limitations, it is possible to construct

a system whereby additional heat transfer can be made available. The construction considered here is that of two parallel plates which would have the same total thickness as a similar plate which has been previously considered. The inside face of the first plate is insulated and the outside face of the second plate loses heat to its surroundings only by thermal radiation. Between the two plates heat is lost by convection such as would occur if a gas were kept flowing through this channel.

An accurate evaluation of this system would involve an extremely detailed and complex mathematical model. However, a good indication of the behavior of the system can be obtained by assuming a single convective coefficient to be applicable over the entire face of the plate. Then by varying this convective coefficient over a fairly wide range, the temperature response of the system can be investigated. The minimization of the maximum thermal stress for each of the two plates is obtained by altering the size of both plates while keeping the total thickness constant until the average temperature in each of the plates is equivalent. This choice is determined by the fact that the maximum thermal stress is directly proportional to the temperature.

NOMENCLATURE

A	Area (ft ²)
c _p	heat capacity (Btu/lb, °F)
E	modulus of elasticity (psi)
h ₁ , h ₂	convection coefficient at the surface of plate one and two respectively in the double plate iteration (Btu/hr, ft ² , °F)
h _r	equivalent gray body convective radiation coefficient (Btu/hr, ft ² , °F)
H	volumetric heat generation rate (Btu/hr, ft ³)
I	gamma photon flux intensity (Btu/hr, ft ²)
k	thermal conductivity (Btu/hr, ft, °F)
L	thickness of the plate (ft)
$\mathcal{L} ()$	Laplace transform of the variable in parenthesis
q/A	heat flux (Btu/hr, ft ²)
s	Laplacian variable
t	time (hr; seconds in time dependent flux equation)
t _s	time of reactor operation (sec)
Δt	time increment between two successive calculations (hr)
T	temperature (°R)
V	volume (ft ³)
x	distance through the plate (ft)
Δx	spatial increment in finite difference calculations (ft) (=L/number of increments)
α	coefficient of thermal expansion
ε	emissivity
θ	temperature difference between the body and the heat sink (°F)
$\bar{\theta}$	Laplace transform of θ

θ_j^n	temperature difference between the body and the heat sink at the nth time increment and the jth mesh point across the plate in the finite difference calculations ($^{\circ}\text{F}$)
α	thermal diffusivity (ft^2/hr)
λ_n	eigenvalue which satisfies a transcendental equation for a particular set of boundary conditions (ft^{-1})
μ	linear energy absorption coefficient (ft^{-1})
ν	Poisson's ratio (ft/ft)
ρ	density (lb/ft^3)
σ	Steffan - Boltzmann constant ($\text{Btu}/\text{hr}, \text{ft}^2, ^{\circ}\text{R}^4$)
σ	(subscripted) - thermal stress (psi)
ψ	real constant used in the finite difference calculations
∇^2	Laplacian operator

THEORY

In order to find the thermal stresses in any body, it is necessary to investigate the resultant temperature distribution, preferentially determined as the temperature increase above some base temperature. These results are directly related to the type of heating to which the body is exposed and to the boundary conditions to which it is subjected. The following discussion considers a gamma photon heat source under two basic conditions:

- 1) A non time dependent gamma source, such as would occur during the steady state operation of a reactor.
- 2) A decaying gamma source, such as would occur after the shutdown of a reactor.

The partial differential equation describing the temperature distribution in a body with an internal heat source is*

$$k \nabla^2 T + H = \rho c_p \frac{\partial T}{\partial t} \quad (1)$$

where the thermal conductivity, k , and the density, ρ , have been assumed as being constant at the average temperature of the body. A more convenient way of writing this for an infinite plate is

$$\frac{\partial^2 \theta}{\partial x^2} + \frac{H}{k} = \frac{1}{\alpha} \frac{\partial \theta}{\partial t} \quad (2)$$

The first case considered will be that of a steady state gamma source, thus implying a heat source which has only spatial dependence. The assumption is made that the flat plate, which is under consideration, is exposed to a plane collimated beam of gamma photons. This is a reasonable assumption if

*see Nomenclature, p. 4.

the contribution from capture gammas can be ignored. A few elementary calculations, using Grotenhuis (9), Table 5.6, show that for a plate of one inch thickness this assumption is justified, since the capture gamma photon contribution is probably less than five percent of the total flux. The heat generation term is then written as

$$H = \mu I e^{-\mu x} \quad (3)$$

where the absorption coefficient has been adjusted to consider the minimal effect of buildup (3), (16). The equation to be solved thus becomes

$$\frac{\partial^2 \theta}{\partial x^2} + \frac{\mu I e^{-\mu x}}{k} = \frac{1}{\mathcal{H}} \frac{\partial \theta}{\partial t} \quad (4)$$

with the exact solution depending on the boundary conditions.

The first investigation is the idealized situation in which the side of the plate exposed to the gamma photon flux is perfectly insulated and the other side of the plate loses heat only by thermal radiation. It is also assumed that there is an initially flat temperature distribution at the same temperature as the heat sink to which the plate is radiating. Applying these conditions appropriately, it is found that the temperature distribution is given by (see Appendix A)

$$\theta = \frac{I}{h_r} (e^{-\mu L} - e^{-\mu x}) + \frac{I}{k} (L - x) + \frac{I}{h_r} (1 - e^{-\mu L}) \quad (5)$$

$$- \sum_{n=1}^{\infty} \frac{2\mu I \cos \lambda_n x}{k \lambda_n^2 (\lambda_n^2 + \mu^2)} \left[\frac{\mu (h_r + k^2 \lambda_n^2) + \lambda_n^2 (k h_r - k^2 \mu) e^{-\mu L} \sec \lambda_n L}{h_r L + k^2 \lambda_n^2 L + h_r k} \right] e^{-\lambda_n^2 t}$$

where λ_n are the n positive roots of the transcendental equation

$$\tan \lambda_n L = \frac{h_r}{k \lambda_n} \quad (6)$$

and h_r is an equivalent gray body convective radiation coefficient, such that

$$\frac{q}{A} = h_r (T - T_o) = \epsilon \sigma (T^4 - T_o^4) \quad (7)$$

Timoshenko and Goodier (21) show that the thermal stresses in the y and z directions of an unrestrained flat plate with a temperature distribution along the x axis are given by

$$\begin{aligned} \sigma_y = \sigma_z = & -\frac{\alpha E T(x)}{1-\nu} + \frac{1}{2(L/2)(1-\nu)} \int_{-L/2}^{L/2} \alpha E T(x) dx \\ & + \frac{3x}{2(L/2)^3(1-\nu)} \int_{-L/2}^{L/2} x \alpha E T(x) dx \end{aligned} \quad (8)$$

where T represents the temperature rise above some base temperature at which the plate is in an unstressed condition. If this base temperature is taken to be the same as the initial temperature of the plate, Eq.(8) may be written in terms of θ , derived above, provided the axis is shifted so as to permit integration from 0 to L . This is easily accomplished by replacing x in Eq.(8), by the quantity $(x - L/2)$. The equation then becomes

$$\sigma_y = \sigma_z = \frac{\alpha E}{1-\nu} \left\{ -\theta + \frac{1}{L} \int_0^L \theta dx + \frac{12(x-L/2)}{L^3} \int_0^L (x-L/2)\theta dx \right\} \quad (9)$$

Performing the indicated operations for the case of the temperature distribution shown in Eq.(5) yields (see Appendix A)

$$\begin{aligned} \sigma_y = \sigma_z = & \frac{\alpha E}{1-\nu} \left\{ (e^{\mu L} - 1) \left(1 + \frac{12(x-L/2)}{\mu L^2} \right) \left(\frac{I}{k\mu^2 L} \right) \right. \\ & + \frac{I}{k\mu} e^{\mu x} + \frac{6I(x-L/2)(1+e^{\mu L})}{k\mu^2 L^2} \\ & \left. + \sum_{n=1}^{\infty} \left[G_n \cos \lambda_n x - \frac{\sin \lambda_n L}{\lambda_n L} - \frac{12(x-L/2)}{L^3} \left(\frac{L \sin \lambda_n L}{2\lambda_n} + \frac{\cos \lambda_n L - 1}{\lambda_n^2} \right) \right] \right\} \end{aligned} \quad (10)$$

where G_n is defined as

$$G_n = \frac{2\mu I e^{-\lambda_n^2 t}}{k \lambda_n^2 (\lambda_n^2 + \mu^2)} \left[\frac{\mu (h_r^2 + \lambda_n^2 k^2) + \lambda_n^2 (k h_r - k^2 \mu) e^{-\mu L} \sec \lambda_n L}{h_r L + k^2 \lambda_n^2 L + h_r k} \right] \quad (11)$$

After shutdown, the gamma flux becomes time dependent. Lottes (12) gives this dependency as

$$I(t) = I(0) \left\{ \left[0.1(t+10)^{-0.2} - 0.087(t+2 \times 10^7)^{-0.2} - 0.0025 e^{-\left(\frac{t}{2040}\right)} - 0.0013 e^{-\left(\frac{t}{270,000}\right)} \right] \right. \\ \left. - \left[0.1(t+t_s+10)^{-0.2} - 0.087(t+t_s+2 \times 10^7)^{-0.2} - 0.0025 e^{-\left(\frac{t+t_s}{2040}\right)} - 0.0013 e^{-\left(\frac{t+t_s}{270,000}\right)} \right] \right\} \quad (12)$$

where t is the time of reactor operation and t_s is the time after shutdown, all time units being in seconds.

Because of this time dependency, the most convenient analytical solution to this problem is through the use of the Laplace transformation. However, this leads to an equation in the Laplace domain which is quite unwieldy. Consequently, it was deemed advisable to resort to the use of numerical techniques. Though such a system is not precisely accurate, it can be made to give answers to accuracies as close as desired by choosing variables of proper magnitude. Expressing Eq.(4) in finite difference form, the temperature at the $(n+1)$ th time increment at distance $x = j\Delta x$ from the side of the plate is represented by

$$\frac{\psi (\theta_{i,j}^{n+1} - 2\theta_{i,j}^n + \theta_{i,j}^{n-1})) + (1-\psi)(\theta_{i,j}^n - 2\theta_{i,j}^n + \theta_{i,j}^{n-1}))}{(\Delta x)^2} + \frac{\mu I e^{-\mu j \Delta x}}{k} \\ = \frac{1}{\Delta t} (\theta_{i,j}^{n+1} - \theta_{i,j}^n) \quad (13)$$

where ψ is a real constant $0 \leq \psi \leq 1$. If $\frac{1}{2} \leq \psi \leq 1$, the system is stable and can be solved for any choice of Δx and Δt . If $0 \leq \psi \leq \frac{1}{2}$, the system

is stable only when

$$\frac{2\chi\Delta t}{(\Delta x)^2} \leq \frac{1}{1-2\psi} \quad (14)$$

Richtmyer (18) shows that such a system converges to the analytical solution most rapidly and is always stable when

$$\psi = \frac{1}{2} - \frac{(\Delta x)^2}{12\chi\Delta t} \quad (15)$$

This system yields a set of equations which may be put in matrix form and easily solved for the temperature distribution with the aid of a high speed digital computer. The system of equations is described in detail in Appendix B.

The final area to be considered is that of two parallel plates with a space between them. This space is assumed to act as a channel through which a flow of gas is kept moving. As a first approximation, an element of the two plates is considered, between which there is a constant convective heat transfer coefficient. The object of such an arrangement would be to keep the total thickness of the two plates constant and then vary the individual thickness in such a way as to equalize the average steady state temperatures. The inner plate would be subjected to the same boundary conditions as existed in the case of the single plate, except that the radiation coefficient would be replaced by a true convection coefficient. Examination of Eq.(5) shows that the resulting equation is

$$\begin{aligned} \theta_1 = & \frac{I_1}{k_1\mu_1} (e^{\mu_1 L_1} - e^{-\mu_1 x_1}) + \frac{I_1}{k_1} (L_1 - x_1) + \frac{I_1}{h_1} (1 - e^{-\mu_1 L_1}) \\ & - \sum_{n=1}^{\infty} \frac{2\mu_n I_1 \cos \lambda_n x_1}{k_1 \lambda_n^2 (\lambda_n^2 + \mu_1^2)} \left[\frac{\mu_1 (h_1^2 + k_1 \lambda_n^2) + \lambda_n^2 (k_1 h_1 - k_1 \mu_1) e^{-\mu_1 L_1} \sec \lambda_n L_1}{h_1^2 L_1 + k_1^2 L_1 \lambda_n^2 + h_1 k_1} \right] e^{-\lambda_n^2 x_1} \end{aligned} \quad (16)$$

where the subscript 1 refers to the first plate. The second plate loses heat by convection from its inner face and by radiation from its outer face. The resulting temperature distribution in this plate is found to be

$$\begin{aligned}
 \theta_2 = & \left\{ R_1 e^{\mu_1 x_1} + R_2 x_2 + R_3 \right\} - \sum_{n=1}^{\infty} \left[\left\{ \frac{h_2}{k_2 \lambda_{n2}} \sin \lambda_{n2} x_2 + \cos \lambda_{n2} x_2 \right\} e^{-\lambda_{n2}^2 t} \right. \\
 & \cdot \left\{ \cos \lambda_{n2} L_2 \left[-\frac{R_2 h_2}{k_2 \lambda_{n2}^2} + R_2 \left(\frac{1}{\lambda_{n2}^2} - \frac{h_2 L_2}{\lambda_{n2}^2 k_2} \right) - \frac{R_1 e^{-\mu_1 L_1}}{(\lambda_{n2}^2 + \mu_1^2)} \left(\mu_2 + \frac{h_2}{k_2} \right) \right] + \frac{R_1 (\mu_1 + \frac{h_2}{k_2})}{(\lambda_{n2}^2 + \mu_1^2)} \right. \\
 & + \sin \lambda_{n2} L_2 \left[\frac{R_2}{\lambda_{n2}} + R_2 \left(\frac{L_2}{\lambda_{n2}} - \frac{h_2}{k_2 \lambda_{n2}^2} \right) + \frac{R_1 e^{-\mu_1 L_1}}{(\lambda_{n2}^2 + \mu_1^2)} \left(\lambda_{n2} - \frac{\mu_2 h_2}{k_2 \lambda_{n2}} \right) + \frac{R_2 h_2}{k_2 \lambda_{n2}} - \frac{R_2}{\lambda_{n2}} \right] \\
 & \cdot \left. \left\{ \frac{1}{2 \lambda_{n2}} \left[\frac{L_2}{k_2^2} (\lambda_{n2}^2 k_2^2 + h_2^2) + \frac{(\lambda_{n2}^2 k_2^2 + h_2^2)(h_r)}{k_2 (\lambda_{n2}^2 k_2 + h_r)} + \frac{h_2}{k_2} \right] \right\} \right] \quad (17)
 \end{aligned}$$

where

$$\left. \begin{aligned}
 R_1 &= -\frac{I_2}{k_2 \mu_1} \\
 R_2 &= -\left[\frac{h_r h_2 \frac{I_2}{k_2 \mu_1} (1 - e^{-\mu_1 L_1}) + I_2 (h_2 e^{-\mu_1 L_1} + h_r)}{k_2 h_r + k_2 h_2 + h_2 h_r L_2} \right] \\
 R_3 &= -R_2 \left(\frac{k_2}{h_r} + L_2 \right) + I_2 e^{-\mu_1 L_1} \left(\frac{1}{k_2 \mu_1} - \frac{1}{h_r} \right)
 \end{aligned} \right\} \quad (18)$$

and λ_{n2} is given by

$$\tan \lambda_{n2} L_2 = \frac{k_2 \lambda_{n2} (h_r - h_2)}{k_2^2 \lambda_{n2}^2 + h_r h_2} \quad (19)$$

and I_2 , the flux incident on the second plate is given by

$$I_2 = I_1 e^{-\mu_1 L_1} \quad (20)$$

Each of the constants in Eq.(16) and (17) have been subscripted to denote which plate is being analyzed. Since each plate is at a different average temperature, the physical constants are different for each plate.

CALCULATIONS

The Single Plate with Constant Gamma Photon Flux and Radiative Heat Loss

The temperature rise within a flat plate is a function of the energy absorbed within the plate from the gamma photon flux incident upon it. Since a complete energy spectrum of gamma photons is emitted from a reactor, it is expedient, for purposes of calculation, to divide the spectrum into several discrete energy groups. A set of flux data taken from the reactor of a prototype nuclear power plant was employed (17). The spectrum is divided into eight energy groups, and all subsequent calculations are based on these data.

For a steel plate at a point 1.5 meters from the reactor, the data presented are shown in Table 1. The absorption coefficients for both steel and aluminum are also given in this table.

Table 1. Flux data from a prototype nuclear power plant and energy absorption coefficients of steel and aluminum at these corresponding energies.

Energy (Mev)	Heat flux (1000 Btu/hr, ft ²)	Energy absorption coefficient (ft ⁻¹)*	
		Steel	Aluminum
6.50	3.05293	5.5839	1.5377
4.72	4.95276	5.4913	1.5978
3.40	16.66158	5.3675	1.7044
2.06	24.02722	5.5260	1.8983
1.26	16.25520	5.9802	2.1269
0.71	13.51214	6.7056	2.3180
0.41	10.87067	7.0744	2.3613
0.15	5.28294	19.4066	2.3287

* see reference (9).

Since the number of mean free paths through any of the steel plates considered is small, the effect of buildup will be minimal (3). Hence, the amount of Compton scattering is small and the linear energy absorption

coefficient gives a reasonably accurate description of the attenuation of the gamma photons in the plate. Therefore, in the solution to Eq.(5), the first step is to sum the flux and absorption coefficient over each of the eight energy groups. It is then possible to iterate for the value of the equivalent gray body convective coefficient, h_r , by successively solving Eq.(6), (5) and (7). This procedure is outlined in greater detail in Appendix D.

A complete investigation of the temperature of a $1/4$, $1/2$, $3/4$, and 1 inch plate, from zero time until the steady state temperature distribution had been reached, was undertaken. For each calculation made in this study the base temperature was assumed to be 500°R . The free plate thermal stress distribution was also calculated at various times. The time increment chosen was 0.01 hr., and the stipulation was made that this increment would be doubled each time the inside temperature was less than 15°F higher than that of the previous time considered at this same position. Steady state was considered to have been reached when the inside temperature was within 10°F of the steady state component of the temperature in Eq.(5).

Besserer (2) has presented data on the physical properties of steel. Many of these properties were found to be temperature dependent, and hence, it was necessary to alter the value of these physical constants as the temperature of the plate increased. Rather than fit the curves which Besserer presents, accurately, a linear approximation was employed. The only deviation from this procedure occurred in the case of the modulus of elasticity which was approximated by two connecting linear curves. The properties considered to be temperature dependent were the coefficient of thermal expansion, the thermal conductivity, the emissivity, the density and the modulus of elasticity. The density was found from volumetric considerations (19), and

is given by

$$\rho(\tau) = \frac{\rho_0}{(1 + 3\alpha(\tau - \tau_0))} \quad (21)$$

where ρ_0 is the density at some base temperature T_0 . The heat capacity and Poisson's ratio were considered to be non temperature dependent. In each case the temperature chosen for alteration of the constants was the average temperature of the plate at the time of interest.

For the case of aluminum, a point was chosen at which the level of the flux was 1/30 of the level at 1.5 meters. The energy distribution at such a location was not available; consequently the previous data were employed, with the intensity of each energy group reduced by a factor of 30.

Since the absorption coefficient of aluminum is significantly less than that of iron, the buildup is negligible and the linear energy absorption coefficient was again used. For aluminum, the only thicknesses considered were one half and one inch. Because of the low absorption coefficient and because of the low emissivity, the temperature rose at a much slower rate than was found for steel, but for a corresponding flux level the steady state temperature was higher in aluminum. Thus the first time increment considered for this reduced flux is 0.1 hr. It was also found that each of the temperature dependent physical quantities could be approximated by the same type curves as were used for steel.

The Single Plate with Time Dependent Gamma Photon Flux and Radiative Heat Loss

In considering the temperature distribution in a metal plate when it is subjected to a time dependent gamma photon flux, it is convenient to employ the use of finite differences. Hence, it is essential that the size of

the time increment be carefully considered before attempting to find a solution. It was found that in the case of steel, a time increment of 0.01 hr. was small enough to give answers which were in excellent agreement with those obtained from the analytic calculations for a 1/4 inch plate. Small values of the ratio $\Delta t/\Delta x$ tend to give the most accurate results (18). In these calculations ten subdivisions were considered for all plate thicknesses. Hence, the accuracy of the calculations for a 1/4 inch plate were sufficient to insure good results for thicker plates.

Maienschein, et al. (13) present data on the emission of gamma photons and their energy distribution from fission products formed, after various times of reactor operation. The graphs presented show that the amount of higher energy radiation present decreased very rapidly for all periods of reactor operation. Since there is a higher concentration of photons of a lower energy present, it would be possible to bracket the photons of all energies into a single energy group at the average energy, provided this average energy is close to the energy peak (7).

The average energy for each of several periods of reactor operation was calculated. This was done by using Simpson's rule (20) for energy increments of 0.125 Mev. in the range 0.25 to 5.50 Mev. The average energy for the fission products of different periods of reactor operation varied from 1.02 to 1.29 Mev., with the fission products of longer operating time having the lower average energy. This was also found to be near the energy peak, especially for the longer periods of reactor operation. Hence, the use of a single energy group at the average energy for the purpose of calculation is justified.

The longest operating time considered in the above data is about 25 minutes. Operating times of longer than about 12 minutes yield essentially the same average energy photons. Since the operating times considered were longer

than 12 minutes, a single energy of 1.05 Mev. was used for obtaining the absorption coefficient. Using this procedure, it was also more expedient to consider the total energy flux in preference to taking a summation over each of the eight energy groups.

A continuous description of the temperature in the plate was obtained by employing the analytic expression described above, until the time of reactor shutdown. The period of reactor operation was varied, and for each of the several cases considered, the equations in finite difference form were used to find the temperature distribution at the succeeding time increments. The choice of the point of termination of these calculations is completely arbitrary and depends on how closely the system is desired to be investigated. At each succeeding time increment the flux was found from the equations presented by Lottes (12) and inserted into the matrix.

As has been previously discussed, the temperature dependent constants in the matrix must be changed after each iteration. Since no analytic expression for the temperature distribution was available, it was not possible to directly calculate the average temperature. Instead, this was done by using Simpson's rule with the temperature distribution found from the numerical solution to the matrix.

Two Parallel Plates with both Convection and Radiation Heat Loss in a Constant Gamma Photon Beam

In attempting to provide additional cooling by the use of two parallel plates with gas flow between them, only the steady state case was considered. It was felt that the operation of the reactor for lesser periods of time would not raise the temperature or the thermal stress levels to abnormal proportions. The investigation of the effect of a number of convection coefficients on the

magnitude of the temperature in steel plates and the distribution of the two plate thicknesses necessary to keep the average temperature of the plates equal, was made. The range of convection coefficients used was from 1 to 25 Btu/hr, ft², °F.

It was again necessary to alter the temperature dependent physical properties of each of the two plates as the average temperatures changed. However, it was noted that the sign of some of these properties changed if the temperature became too high. This phenomenon occurs because the linear approximations used are invalid at excessively high temperatures, especially near the melting point. Since some original division of the plate thickness was necessary, it was possible that for low convection coefficients the temperature of the inside plate would be abnormally high until its thickness had been reduced enough to lower the temperature to a reasonable level. Therefore, some of the physical constants would not be represented by their true values. In general this would not hinder the iteration. However, as the thickness of the inside plate is reduced, there exists a point at which a change in the sign of the physical constants occurs. In the case of the thermal conductivity, one segment of the equation involved in the calculation of the temperature, contains its reciprocal so that when it arrives at the point where the sign changes, the value of this portion of the equation varies from a high positive to a high negative number. Consequently, this iteration would probably never converge. If the average temperature of the plate reached this unrealistic level, it was set equal to the steady state average temperature of a single plate of equivalent thickness, for the purpose of altering the physical constant involved. From this point the calculations proceeded in a normal manner until the average temperatures of the two plates

were within the limits specified. The limits set were that the temperature difference between the plates, divided by their combined average temperature, be less than 10^{-4} .

DISCUSSION AND RESULTS

The Single Plate with Constant Gamma Photon Flux and Radiative Heat Loss

Figures 1 and 2 show the theoretically predicted temperature responses of two different sized plates of steel and aluminum to a constant gamma photon flux. The calculations on the aluminum plate were made with the flux level of each of the eight energy groups being $1/30$ of the flux level to which the steel plate was exposed.

The temperature rise in both the $1/4$ inch and the one inch steel plates shown in Fig. 1 is quite rapid. In the $1/4$ inch plate the average heat generation rate is somewhat higher and the initial temperature rise is greater than in the one inch plate. However, after a short period of time, the thinner plate is able to conduct a greater percentage of the heat generated within it to the surface. Consequently, its rate of ascension quickly begins to fall while the temperature in the one inch plate continues to rise in almost a linear manner. This is also true because of the lesser amount of total heat capable of being stored within a plate of smaller dimensions.

An indication of the effect of the thermal conductivity on the rate of heat removal can be obtained by examining the change in the temperature distribution in each of the two plates as the period of exposure to the gamma flux progresses. This is done in Tables 2 and 3. The time of the first distribution shown in each case, occurs during the period when there is a linear temperature rise and the last distribution is at steady state. At first, both the plates move slowly from the initially flat temperature distribution. However, the temperature differential between the inside and outside temperatures in the one inch plate increases quite rapidly compared to the

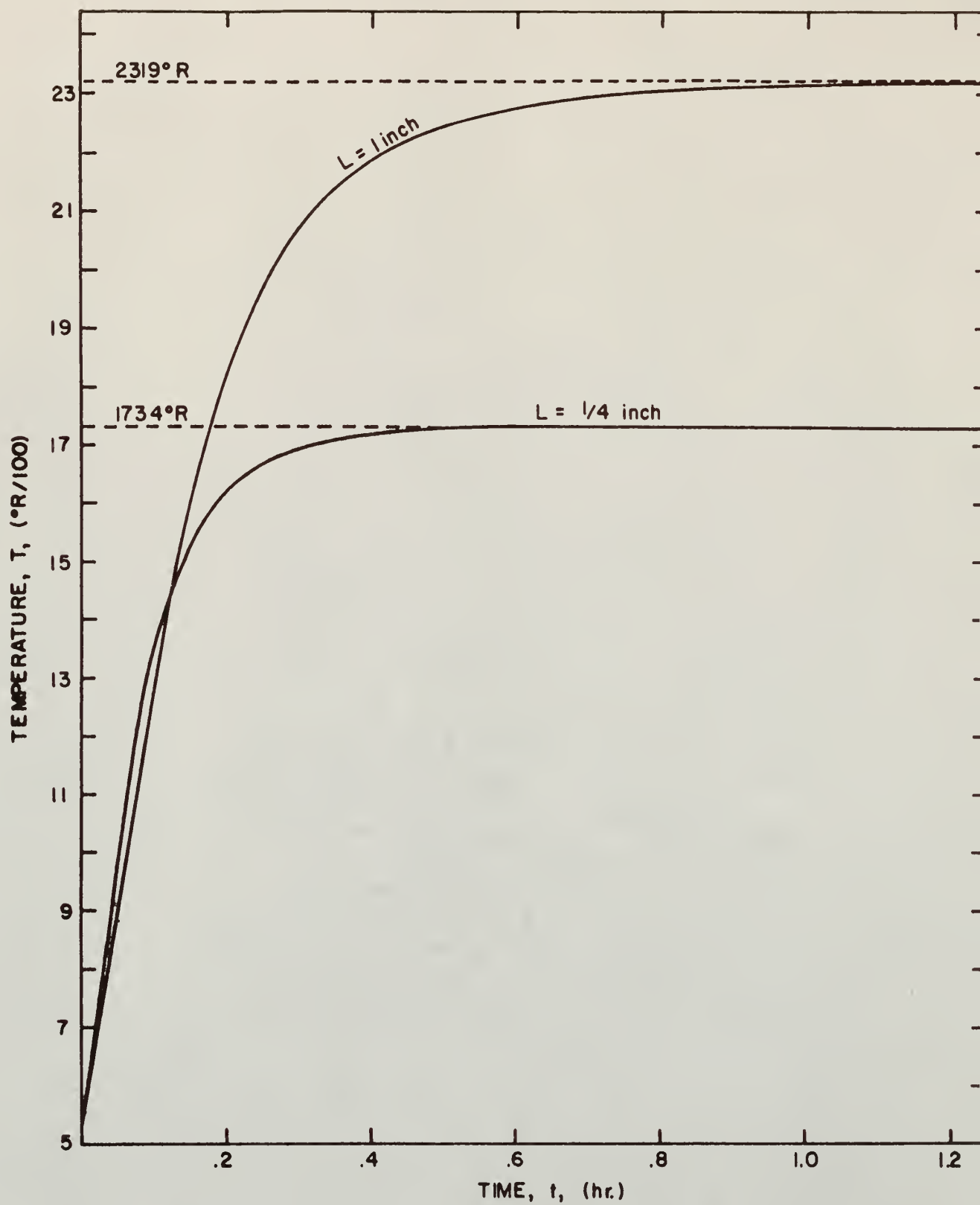


FIG. 1.. EFFECT OF CONSTANT GAMMA FLUX ON SURFACE TEMPERATURE OF STEEL PLATE

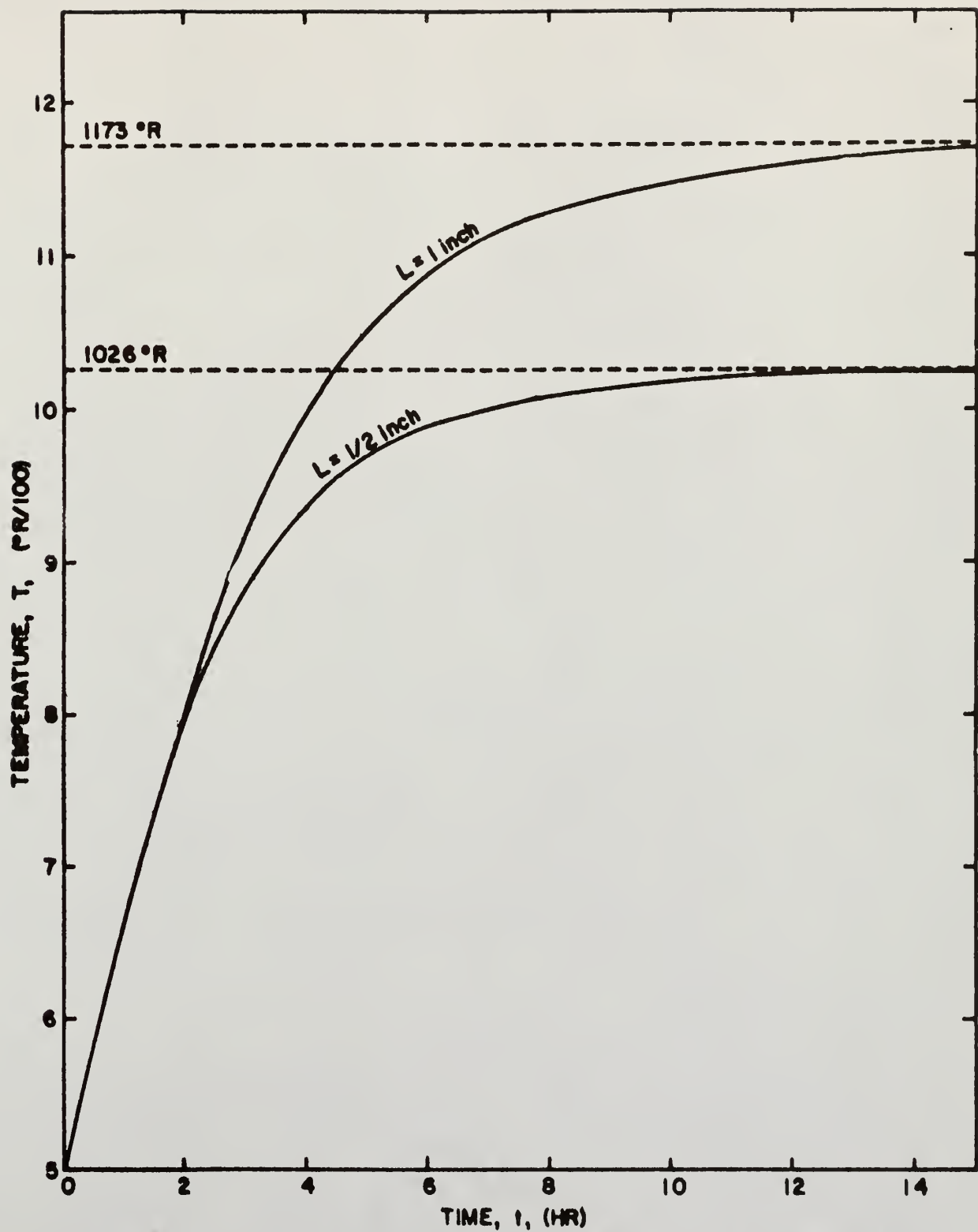


FIG. 2. EFFECT OF CONSTANT GAMMA FLUX ON SURFACE TEMPERATURE OF ALUMINUM PLATE

Table 2. Temperature distribution in a 1/4 inch steel plate after irradiation by a constant gamma photon beam for various times

Distance through the plate (ft)	Temperature (°R)	Time of reactor operation (hr)
0.020833	601.818	0.01
0.018750	601.827	
0.016667	601.842	
0.014583	601.859	
0.012500	601.880	
0.010417	601.890	
0.008333	601.922	
0.006250	601.941	
0.004167	601.955	
0.002083	601.966	
0	601.969	
0.020833	1344.598	0.10
0.018750	1344.972	
0.016667	1345.315	
0.014583	1345.624	
0.012500	1345.897	
0.010417	1346.134	
0.008333	1346.331	
0.006250	1346.489	
0.004167	1346.603	
0.002083	1346.673	
0	1346.697	
0.020833	1707.216	0.34
0.018750	1708.341	
0.016667	1709.357	
0.014583	1710.261	
0.012500	1711.051	
0.010417	1711.725	
0.008333	1712.282	
0.006250	1712.719	
0.004167	1713.033	
0.002083	1713.224	
0	1713.288	
0.020833	1734.257	steady state
0.018750	1735.469	
0.016667	1736.563	
0.014583	1737.536	
0.012500	1738.385	
0.010407	1739.110	
0.008333	1739.708	
0.006250	1740.177	
0.004167	1740.515	
0.002083	1740.719	
0	1740.788	

Table 3. Temperature distribution in a one inch steel plate after irradiation by a constant gamma photon beam for various times

Distance through the plate (ft)	Temperature ($^{\circ}$ R)	Time of reactor operation (hr)
0.083333	579.270	0.01
0.075000	579.429	
0.066667	579.834	
0.058333	580.436	
0.050000	581.178	
0.041667	582.006	
0.033333	582.853	
0.025000	583.649	
0.016667	584.327	
0.008333	584.797	
0	584.974	
0.083333	1291.625	0.10
0.075000	1293.035	
0.066667	1294.622	
0.058333	1296.325	
0.050000	1298.076	
0.041667	1299.804	
0.033333	1301.430	
0.025000	1302.868	
0.016667	1304.027	
0.008333	1304.805	
0	1305.090	
0.083333	2131.287	0.34
0.075000	2145.108	
0.066667	2157.941	
0.058333	2169.698	
0.050000	2180.286	
0.041667	2189.598	
0.033333	2197.524	
0.025000	2203.941	
0.016667	2208.714	
0.008333	2211.696	
0	2212.729	
0.083333	2319.233	steady state
0.075000	2340.928	
0.066667	2360.878	
0.058333	2378.980	
0.050000	2395.123	
0.041667	2409.188	
0.033333	2421.043	
0.025000	2430.550	
0.016667	2437.555	
0.008333	2441.893	
0	2443.382	

differential for the 1/4 inch plate. A more detailed description of this response is shown in Fig. 3.

For the case of the aluminum plates shown in Fig. 2, the temperature rise is considerably slower than that of steel. In fact, for the magnitude of the flux considered, the time necessary to approach steady state is about ten times as great for the aluminum plate as for the steel plate. Calculations show that when the aluminum plate is subjected to the same gamma flux as the steel plate, it reaches temperatures of several hundred degrees Fahrenheit higher than the steel plate for all the sizes of plates examined. However, the temperature rise remains considerably slower in the aluminum.

This phenomenon is a result of several of the physical properties involved. Because the aluminum has a significantly lower absorption cross section than steel (see Table 1), the amount of heat generated within a comparable volume of aluminum is distinctly less than that generated in steel during any given time increment. Consequently, the temperature has a tendency to ascend at a much slower rate in aluminum. However, the temperature rise is also affected by the thermal conductivity and the emissivity of the material involved. The high thermal conductivity of aluminum allows the heat generated within the plate to reach the surface far more rapidly than is the case for steel. But since the emissivity of aluminum is low, the heat has a reduced chance to be radiated once it reaches the surface.

By far, the overriding difference between aluminum and steel during the early portion of the heating period is the low absorption cross section of aluminum. The amount of heat generated is not nearly enough to cause as rapid a temperature rise as is found in steel. However, because of the low emissivity of aluminum, it retains a significantly greater percentage of the heat generated within it. Consequently, when the aluminum plate finally

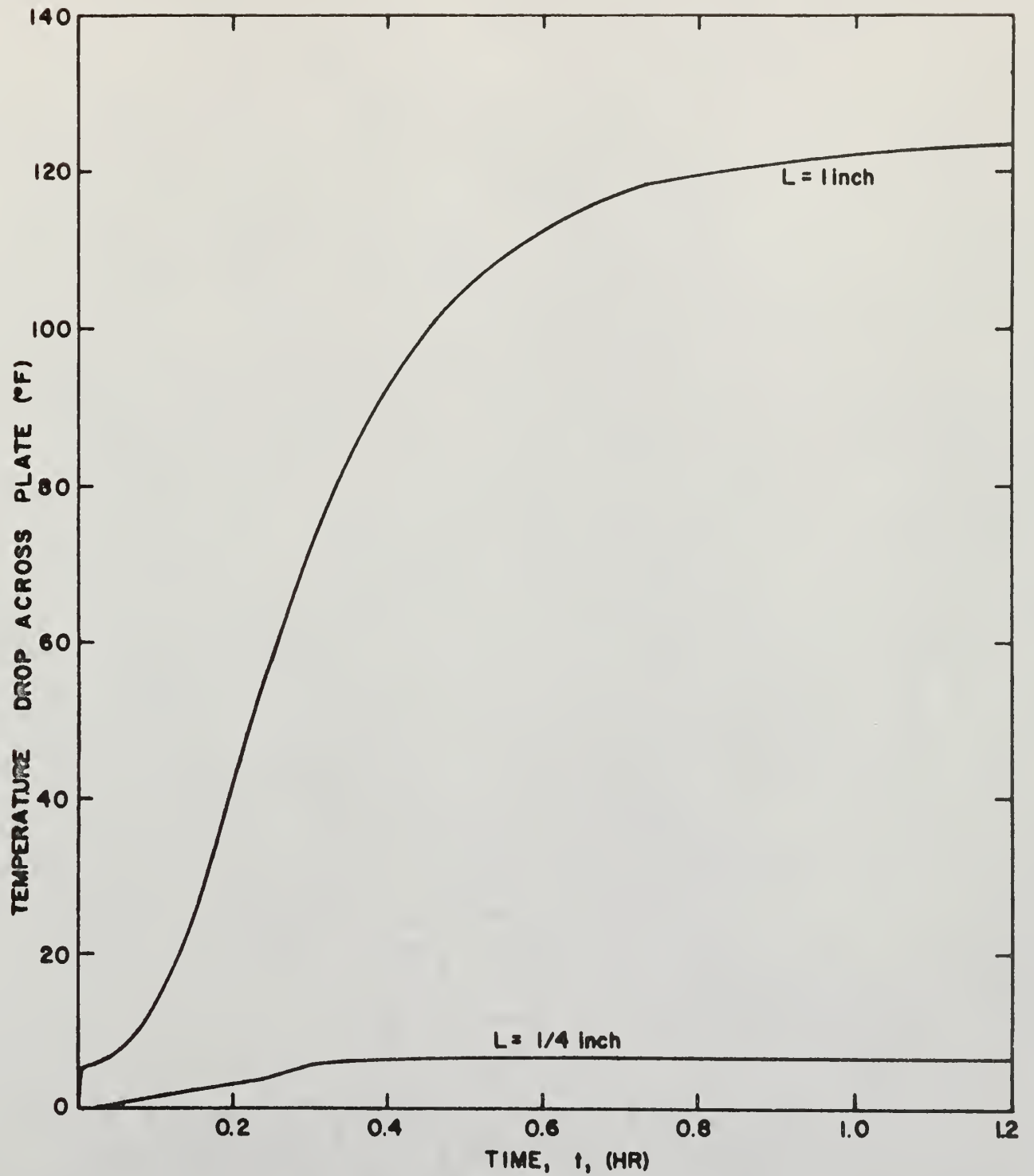


FIG. 3. RELATIONSHIP OF TEMPERATURE DROP ACROSS STEEL PLATE AS A FUNCTION OF TIME

reaches an equilibrium condition, the total amount of heat retained within it is greater than for similar conditions in steel. Thus, the temperature in aluminum reaches a higher steady state value.

It is also seen from Fig. 2, that for all practical purposes, the temperature of both the one half inch and one inch aluminum plates is the same for a period of two hours. This can be attributed in part to the high thermal conductivity of the aluminum, which allows a more rapid flow of heat across any thickness of plate. The significance of this high conductivity is attested by the fact that the temperature drop across a one inch aluminum plate at the steady state temperature distribution is less than one degree Fahrenheit, while for steel this temperature differential exceeds 100°F.

This high conductivity of the aluminum approximates one of the stipulations for the "thin body" temperature transients discussed by Unterberg (22). Such a system assumes zero internal resistance to heat flow, so that no temperature gradient exists within the material. This assumption is satisfied by an infinite (k/x), and removes the spatial temperature variation from the system. Hence, the heat balance for the case of radiation heat loss is given by

$$V\rho c_p \frac{dT}{dt} = HV - A\sigma\epsilon (T^4 - T_o^4) \quad (22)$$

where V is the volume of the body and A is the area of the surface radiating to the surroundings.

The steady state case is then given by $(dT/dt) = 0$, whence

$$T_{max} = \left(\frac{W}{Z} \right)^{\frac{1}{4}} \quad (23)$$

where

$$W = \frac{H}{\rho c_p} + \frac{A\sigma\epsilon T_o'}{V\rho c_p} \quad (24)$$

$$Z = \frac{A\sigma\epsilon}{V\rho c_p} \quad (25)$$

If a quantity, p , is defined as

$$p = \left(\frac{Z}{W}\right)^{1/4} \quad (26)$$

the temperature is given by the transcendental equation

$$ZpWt = \eta(pT) - \eta(pT_o) \quad (27)$$

where

$$\eta(pT) = \tanh^{-1}(pT) + \tan^{-1}(pT) \quad (28)$$

Solution of Eq.(23) for a one half inch aluminum plate, shows the steady state "thin body" temperature to be 1337°R. For a one inch plate this temperature is 1553°R. The exact solution for these temperatures, shows them to be 1026°R and 1173°R respectively. The temperature rise for the "thin body" aluminum takes on the same relative shape, but as the temperature increases, the departure from the exact solution becomes more apparent. Thus, the "thin body" approximation for the aluminum plates examined starts to approach the exact solution, but does not give accurate answers except at temperatures only slightly above the base temperature.

It is possible to consider the thermal stresses expressed in Eq.(8) by using the equation in its entirety or by considering any of its several parts. The simplest case is to examine the first term of Eq.(8) alone. This is

equivalent to holding the ends of the plate in perfect restraint, and gives the maximum thermal stress to which the plate may be subjected (21). Although this condition could probably not be precisely reconstructed in a nuclear rocket, a sketch of the physical representation is given in Fig. 3a. Here, the plate is pinned at the two ends to supports which remain fixed. Consequently, the plate can neither expand longitudinally nor bend about either end to relieve the applied stresses. If the physical constants involved in this calculation are assumed to be constant, the maximum thermal stress is a linear function of the temperature.

Figure 4 shows the maximum yield stress for 4130 steel. The calculation of the maximum thermal stress for steel shows it to exceed the maximum yield stress by the time the temperature has risen more than 200°F above the base temperature. For the one inch plate, which has the slowest initial temperature rise of any of the cases investigated, the time necessary to attain this temperature is less than two minutes. Since it is highly illogical that any nuclear rocket power plant would feasibly remain in operation for that short a period of time, provisions must obviously be made to allow for expansion of the system involved. Since the maximum thermal stress attains a value of five times the yield stress within ten minutes, this consideration is extremely important.

In examining the maximum thermal stress in aluminum, the results are found to be considerably different than for steel, as is shown in Fig. 5. The point at which the maximum thermal stress first exceeds the yield stress for 7075-T6 aluminum with the flux level considered, does not occur until almost two hours have elapsed. Thus for periods of reactor operation in the 15 to 30 minute range, the thermal stresses in aluminum when subjected to the heating level discussed, are well within the destructive limits.

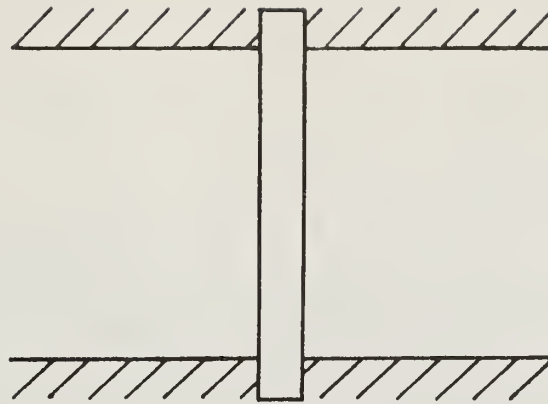


FIG. 3a: SKETCH OF FLAT PLATE HELD IN PERFECT RESTRAINT.

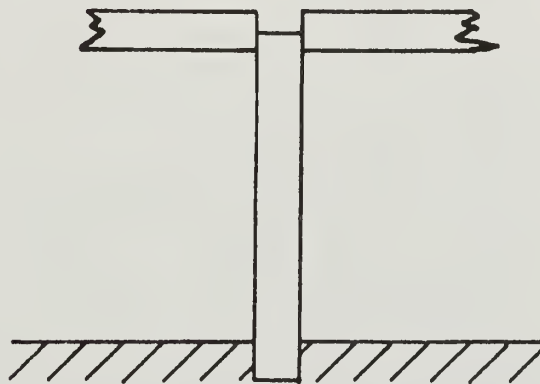


FIG. 3b: SKETCH OF FLAT PLATE RESTRAINED ONLY IN BENDING.

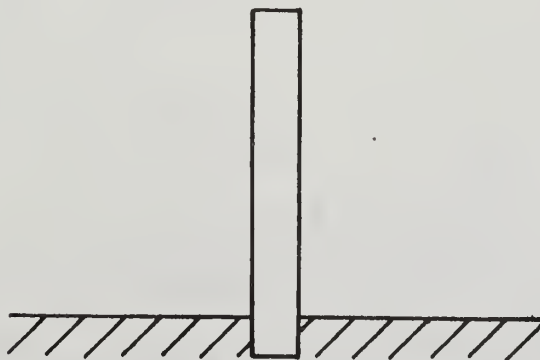


FIG. 3c: CANTILEVER ARRANGEMENT IN WHICH PLATE MAY MOVE IN ANY DIRECTION.

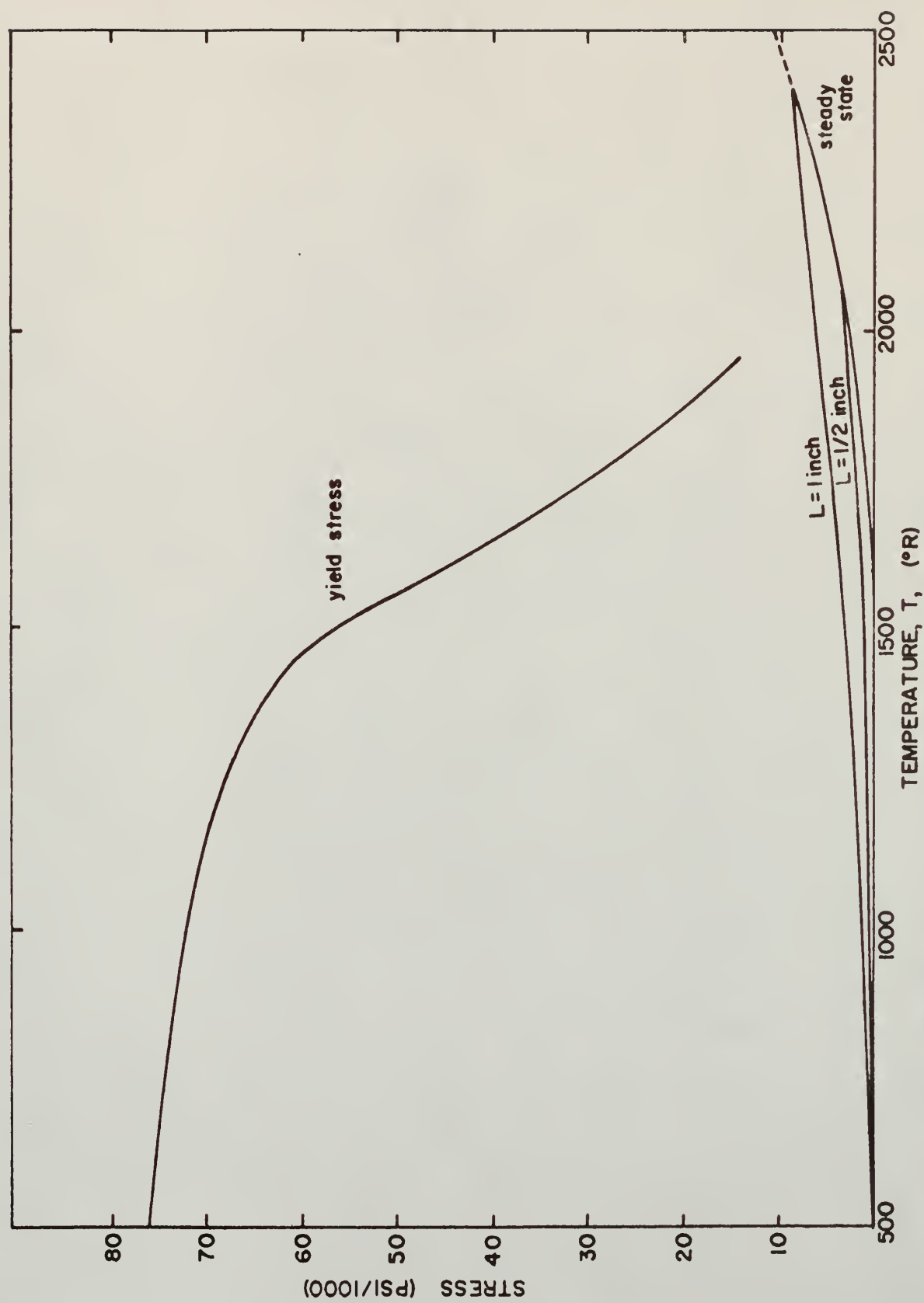


FIG. 4. RELATIONSHIP OF YIELD STRESS TO MAXIMUM THERMAL STRESS FOR 4130. STEEL PLATE RESTRAINED IN BENDING

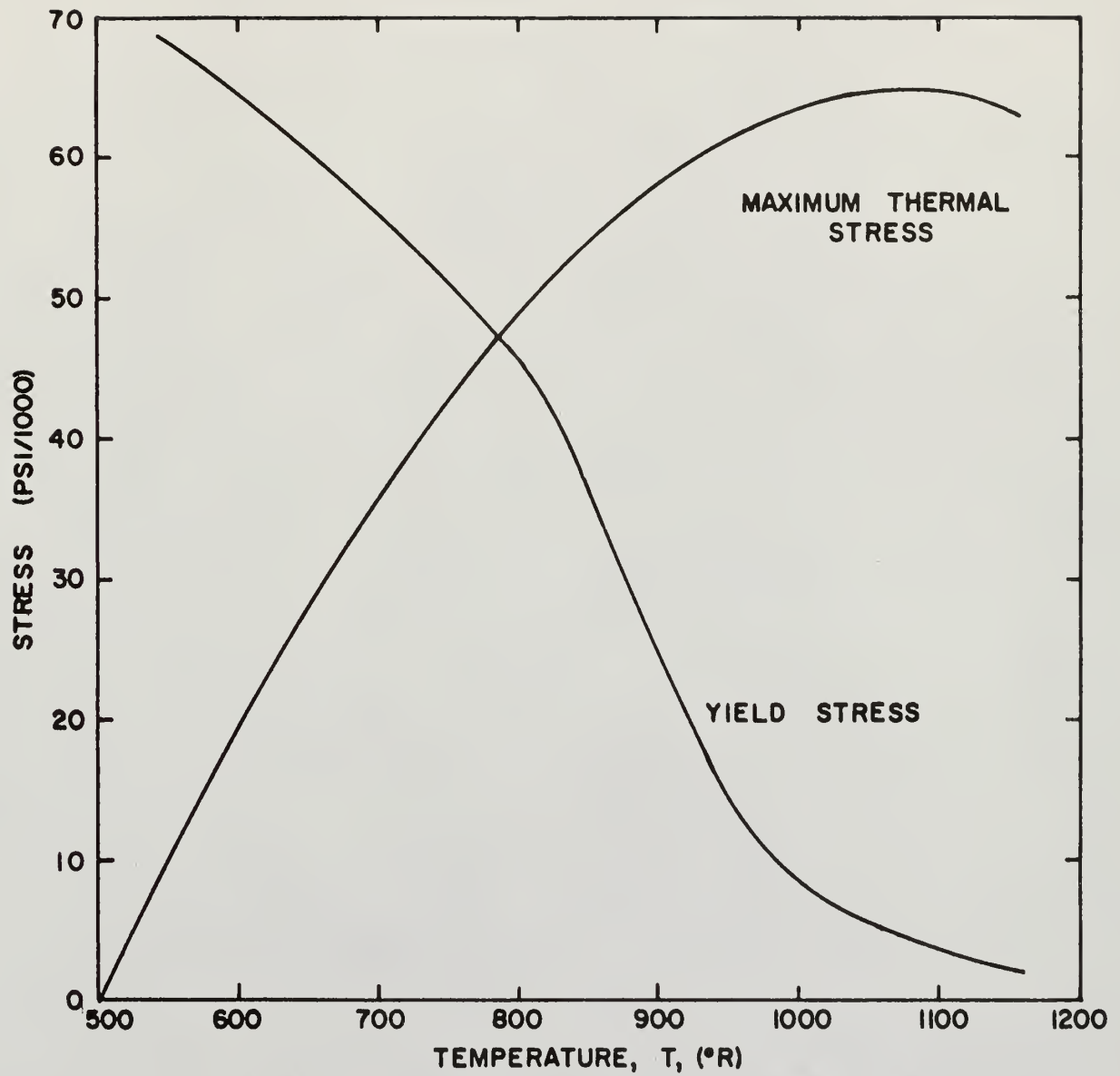


FIG. 5. TEMPERATURE DEPENDENCY OF MAXIMUM THERMAL STRESS AND YIELD STRESS IN ALUMINUM

It is also possible to consider the thermal stress produced in a plate which is restrained in bending. This is done by evaluating the first two terms in Eq.(8). Further examination shows that this equation is simply

$$\sigma_{no\ bend} = \frac{\alpha E}{1-\nu} (\theta_{av} - \theta) \quad (29)$$

where θ_{av} represents the average temperature differential above the base temperature. This case is represented schematically in Fig. 3b. This is a cantilever type arrangement in which the unattached end of the plate is free to expand longitudinally, but is held between two immovable guides so that it may not bend about its fixed end. The quantity which is of primary interest here is again the maximum possible thermal stress. This is found by considering the point at which the largest departure from the average temperature exists.

Figure 6 shows the maximum thermal stress of several different sizes of steel plates which are restrained in bending. For each of these plates the maximum thermal stress exists at the outer extremity of the plate. Also, the stress is always found to be one of tension at this point in the plate. It is seen that as the plate becomes thicker, the maximum thermal stress increases at a rapid rate, especially at higher temperatures. Thus, in the case of thermal stresses there is a definite size of plate which may be used if it is desired to keep the thermal stresses in the range which is well below the yield stress of steel.

It should be noted in Fig. 4, however, that the maximum thermal stress for a plate restrained in bending does not begin to seriously approach the yield stress in steel until the temperature of the plate has risen above 2000°R. For the flux levels which were considered here, this case does not

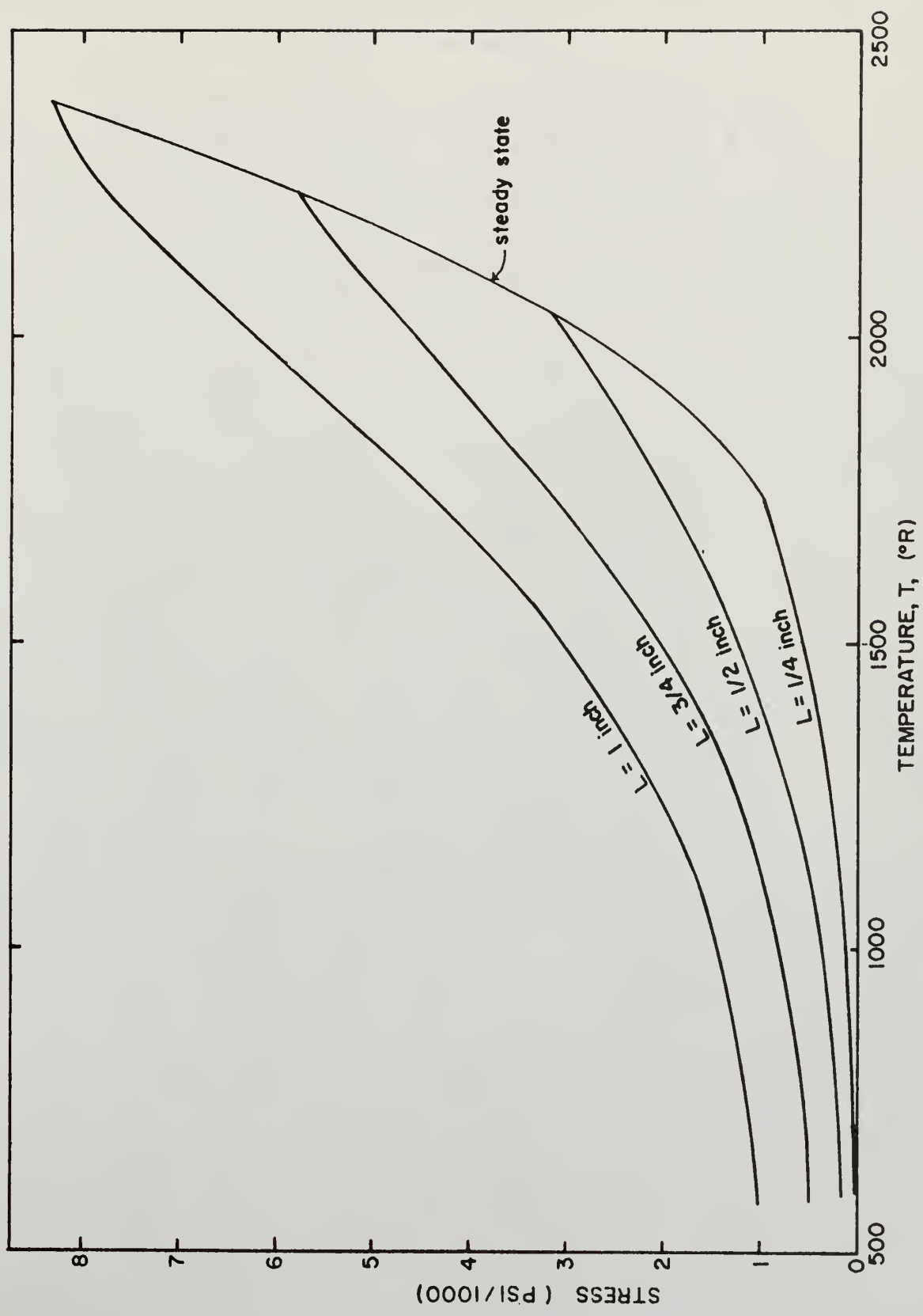


FIG. 6. THERMAL STRESS IN A STEEL PLATE RESTRAINED IN BENDING

arise until the thickness of the plate is approximately one half inch. For plates of this and greater thicknesses, a temperature of 2000°R is reached in approximately 15 minutes. For plates of the thicknesses examined, this maximum thermal stress never exceeds the yield stress. However, plates of larger thickness would undoubtedly tend to have their maximum thermal stresses increase at an increasing rate. This is evidenced by the rate of increase of the temperature differential across the plate as the thickness is increased (see Fig. 3). This rate of increase can also be seen by examining the steady state line in Fig. 6, which gives a more detailed description of the maximum thermal stress for a plate restrained in bending for each of the thicknesses considered.

In Fig. 4, the steady state line has been extrapolated slightly beyond the calculated data in an attempt to give some indication of the maximum thermal stress of a plate larger than those discussed here. However, it must be remembered at this point, that one of the assumptions used in the calculations of this study was that the plates under consideration were thin enough so that Compton scattering could be neglected. This assumption begins to rapidly break down, especially for the lower energy groups, if calculations are made on thicker plates. When the amount of Compton scattering begins to increase significantly, the total energy release predicted by the equations derived in this study is seriously underestimated. Applying this information to the thermal stresses under consideration, the magnitude of these thermal stresses would increase at an even more rapid rate than is predicted by the equations presently employed.

In the case of aluminum, the temperature differential across the plate was found to be almost non existent. As previously discussed, this is due to the high thermal conductivity of aluminum. Consequently, the maximum

thermal stress for either of the plates considered, when restrained in bending, lies in the range of zero to ten psi. This can be considered as negligible for all practical purposes. The ratio of the maximum thermal stress for an aluminum plate restrained in bending to the yield stress is 10^{-3} or less, so that the plate essentially does not "feel" the thermal stress which exists within it. The "thin body" approximation then seems to gain a slight degree of stature since it predicts a zero stress in all cases except that of perfect restraint.

The final manner in which the thermal stress may be examined is to consider a free plate. In this case Eq.(8) is used in its entirety. The representation of such a physical construction is shown in Fig. 3c. The one end of the plate is fixed with the plate free to expand in any direction from this end. Such a system is evidenced in any simple cantilever arrangement. Figure 7 gives an indication of the thermal stress response of a $1/4$ inch steel plate. In attempting to explain this unusual transient response, it is helpful to examine the individual terms which determine the free plate stress.

The second term in this equation is simply a constant. The last term is linear with position, and is zero at the midpoint of the plate. The first term is simply a constant times the negative of the temperature distribution. Figure 8 shows the temperature distribution at three different times. After the higher order transient terms of Eq.(5) have died out, the temperature profile begins to closely approximate a cosine distribution. The free plate thermal stress for such a distribution has the appearance of the curve shown for $t = 0.12$ hr. in Fig. 7.

Examination of the temperature profile for $t = 0.01$ hr. shows an inflection point. Consequently, this temperature profile has the appearance

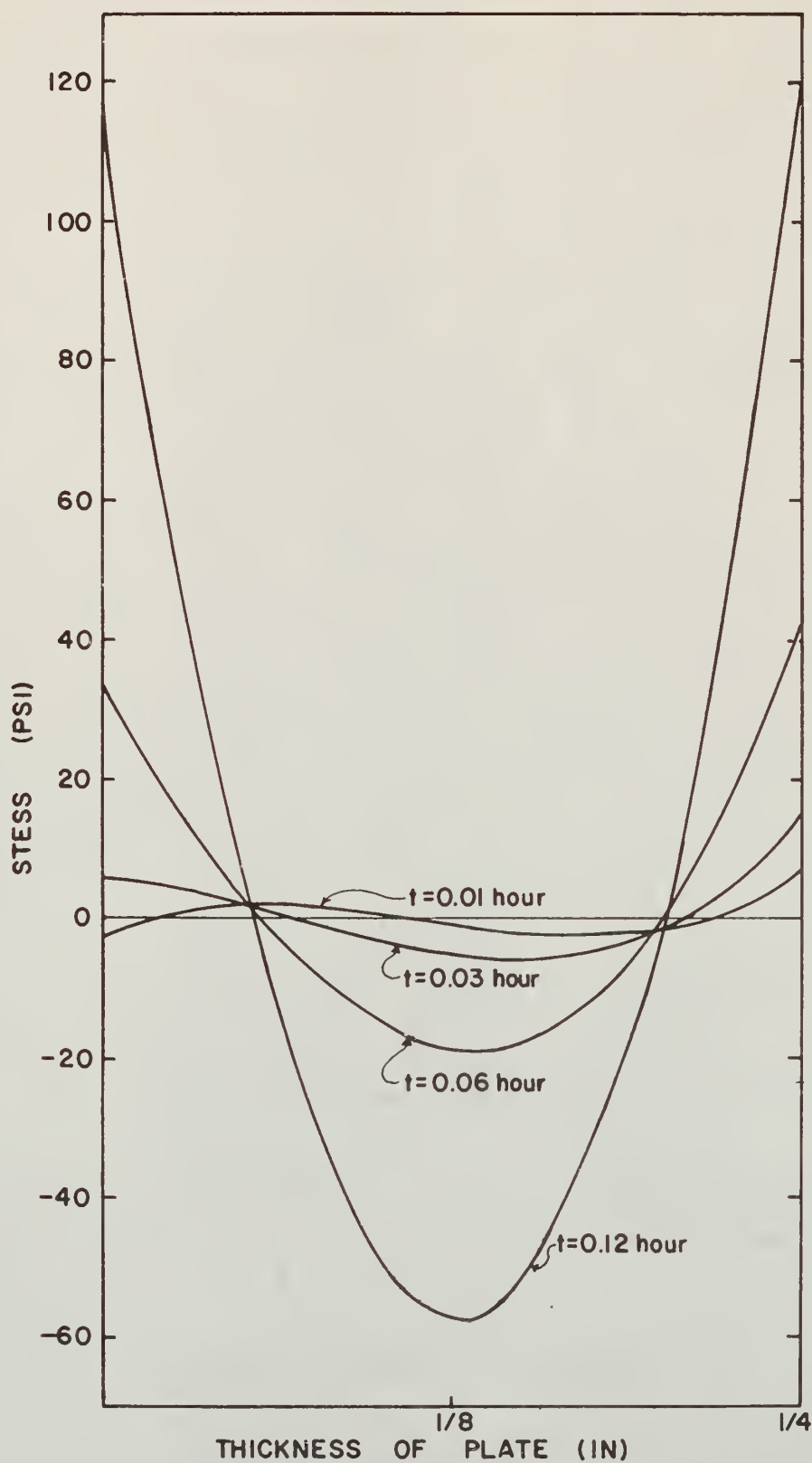


FIG. 7. TRANSIENT FREE PLATE THERMAL STRESS DISTRIBUTION IN STEEL PLATE

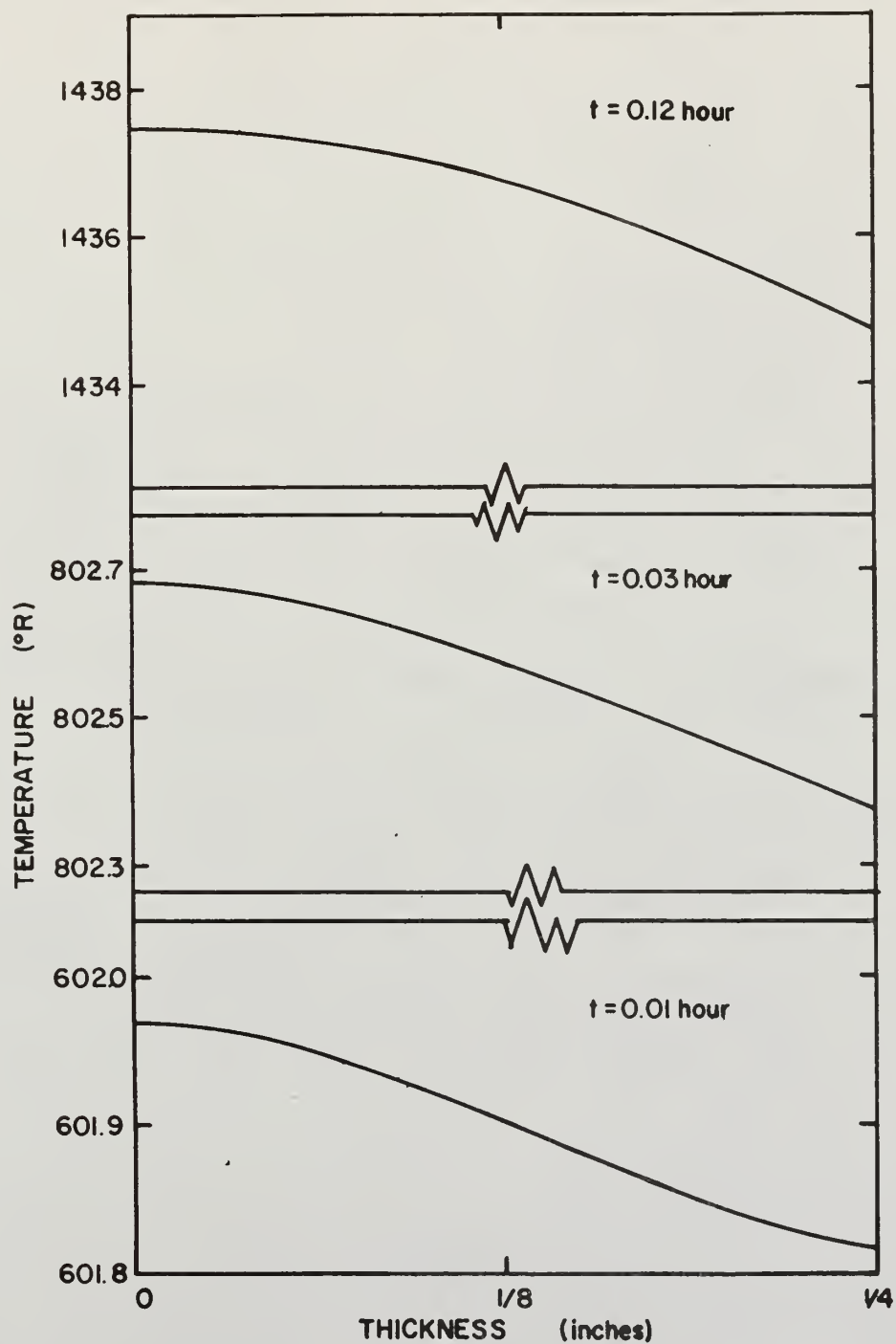


FIG. 8. TEMPERATURE PROFILE FOR 1/4 INCH PLATE AT VARIOUS TIMES

of nearly 180° of a cosine curve. The resultant thermal stress also extends through two quadrants of the normal cosine-type distribution. Within a very short time inflection point disappears from the temperature profile and the free plate thermal stress distribution begins to again take on the appearance of a simple cosine-type distribution. Although these curves are rather interesting to investigate, they do not present any serious physical difficulties with regard to structural considerations.

The one inch plate exhibits the same cosine type distribution as the $1/4$ inch plate, but it takes slightly longer before the higher order temperature transient terms have been sufficiently damped to cause the thermal stress curve to show a simple cosine determined distribution. The magnitude of the maximum thermal stress in a free plate is about 2000 psi for a one inch steel plate at steady state. In no case does the maximum free plate stress exceed that of a plate which is completely restrained in bending. Thus, this former stress should be of little consequence in considering the structural feasibility of any rocket construction.

As would be expected from the case of the steel plate just discussed, the maximum free plate thermal stress in aluminum is also less than the maximum thermal stress for a plate restrained in bending. The free plate stresses exhibit the same type distribution as was evidenced in steel, however, these are so small that they can be completely neglected. The maximum thermal stress for any of the cases examined in aluminum was found to be less than one psi.

The Single Plate with Time Dependent Gamma Photon Flux and Radiative Heat Loss

It is to be expected that a time dependent investigation of the

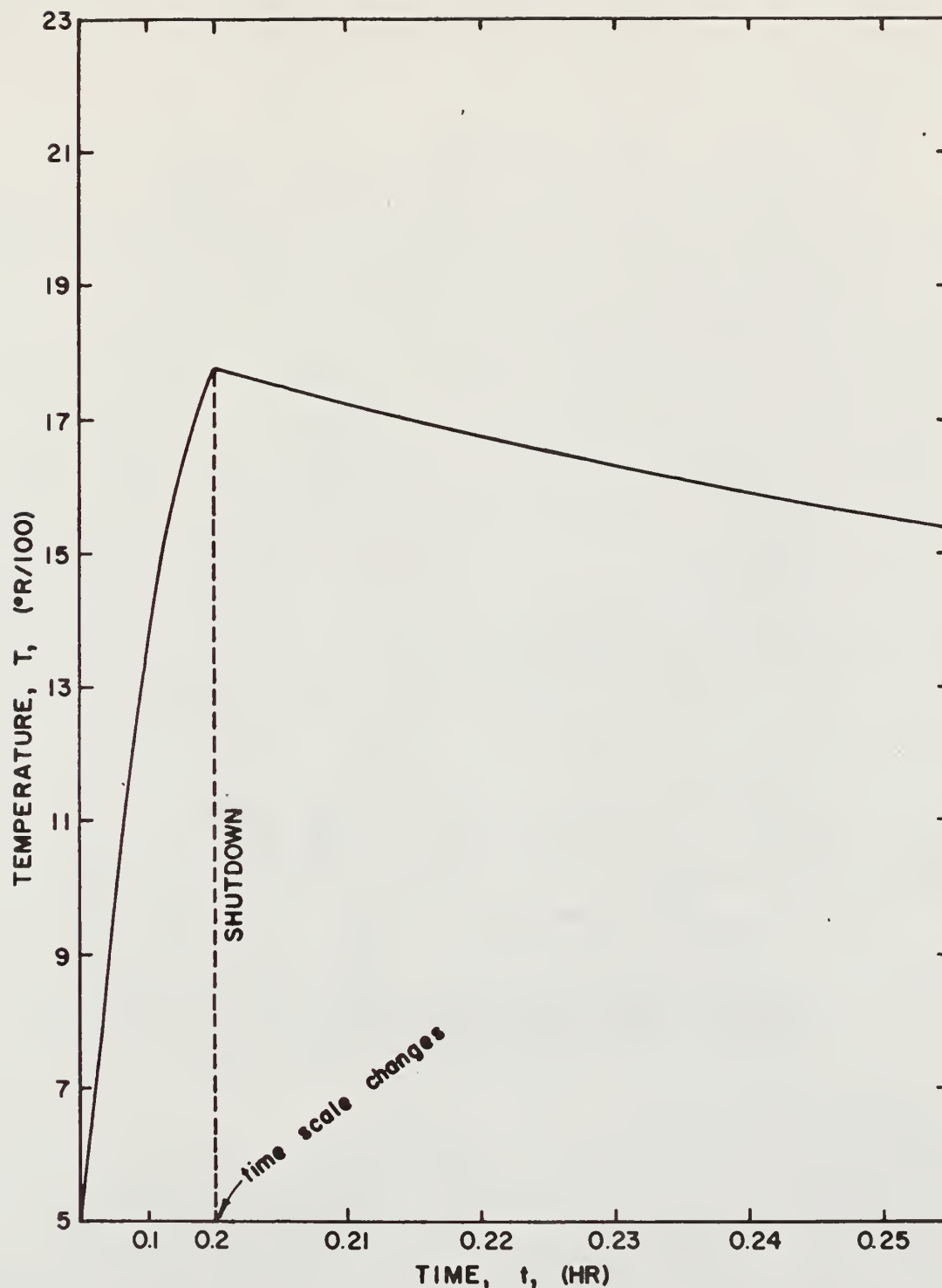


FIG. 9. OUTSIDE TEMPERATURE OF 1/2 INCH STEEL PLATE AFTER SHUTDOWN WHEN SUBJECTED TO TIME DEPENDENT GAMMA PHOTON FLUX

temperature within a flat plate will present a smooth curve. Figure 9 shows the curve for the case of shutdown after 12 minutes of reactor operation. The time scale after shutdown has been expanded in an attempt to give a more distinct appraisal of the temperature during this period. Because of the large temperature increments necessary to plot this graph, it is difficult to distinguish that for a short period the curve is concave downward, after which it goes through an inflection point and reverses itself. For the time increments chosen, the curve appears to show a discontinuity. Table 4 gives the actual temperature distribution immediately before and 0.001 hr. after shutdown for two different times of reactor operation. It is most probable that this apparent discontinuity would be eliminated by choosing a time increment small enough. However, the increment could not be shortened below 0.1 seconds since this is the endpoint of the graph for the time dependent flux equation given by Lottes (12).

A comparison was also made of the temperature of a steel plate using the time dependent flux equation of Lottes and also assuming zero flux immediately after shutdown. Tables 5 and 6 show these temperatures for several different times after shutdown. The operating time of the reactor was taken as about 22 minutes, at which time the rate of increase of the temperature has slowed considerably from the original rate of ascension. Examination of these tables shows that after a period of two to three minutes the difference in the temperatures between the two cases is about five degrees Fahrenheit.

Thus the amount of heating provided by the gamma photons after shutdown is quite minimal when compared to the heating during reactor operation. For the case of zero flux after shutdown, the temperature would asymptotically

Table 4. Temperature distribution in a 1/2 inch steel plate at shutdown and 0.001 hours after shutdown for operating times of 0.20 and 0.37 hours

Distance through the plate (ft)	Temperature (°R)	Time (hr)
0.041667	1779.283	0.200
0.037500	1782.052	
0.033333	1784.592	
0.029167	1786.888	
0.025000	1788.929	
0.020833	1790.699	
0.016667	1792.184	
0.012500	1793.368	
0.008333	1794.236	
0.004167	1794.770	
0	1794.952	
0.041667	1773.911	0.200 + 0.001
0.037500	1776.749	
0.033333	1779.271	
0.029167	1781.490	
0.025000	1783.409	
0.020833	1785.030	
0.016667	1786.354	
0.012500	1787.379	
0.008333	1788.104	
0.004167	1788.535	
0	1788.675	
0.041667	1963.272	0.370
0.037500	1967.730	
0.033333	1971.786	
0.029167	1975.426	
0.025000	1978.636	
0.020833	1981.400	
0.016667	1983.702	
0.012500	1985.524	
0.008333	1986.849	
0.004167	1987.659	
0	1987.933	
0.041667	1954.915	0.370 + 0.001
0.037500	1959.471	
0.033333	1963.526	
0.029167	1967.095	
0.025000	1970.185	
0.020833	1972.798	
0.016667	1974.933	
0.012500	1976.590	
0.008333	1977.767	
0.004167	1978.467	
0	1978.698	

Table 5. Temperature distribution in a 1/2 inch steel plate for various times after reactor shutdown at 0.37 hours without additional heating after shutdown

Distance through the plate (ft)	Temperature (°R)	Time after shutdown (hr)
0.041667	1954.616	0.001
0.037500	1959.168	
0.033333	1963.219	
0.029167	1966.783	
0.025000	1969.867	
0.020833	1972.474	
0.016667	1974.604	
0.012500	1976.255	
0.008333	1977.428	
0.004167	1978.125	
0	1978.354	
0.041667	1881.357	0.010
0.037500	1885.130	
0.033333	1888.510	
0.029167	1891.502	
0.025000	1894.104	
0.020833	1896.312	
0.016667	1898.123	
0.012500	1899.533	
0.008333	1900.539	
0.004167	1901.141	
0	1901.340	
0.041667	1750.670	0.030
0.037500	1753.335	
0.033333	1755.728	
0.029167	1757.843	
0.025000	1759.677	
0.020833	1761.230	
0.016667	1762.502	
0.012500	1763.493	
0.008333	1764.202	
0.004167	1764.629	
0	1764.773	
0.041667	1649.840	0.050
0.037500	1651.851	
0.033333	1653.657	
0.029167	1655.251	
0.025000	1656.633	
0.020833	1657.804	
0.016667	1658.762	
0.012500	1659.508	
0.008333	1660.042	
0.004167	1660.363	
0	1660.472	

Table 6. Temperature distribution in a 1/2 inch steel plate for various times after reactor shutdown at 0.37 hours when exposed to a time dependent gamma photon beam

Distance through the plate (ft)	Temperature (°R)	Time after shutdown (hr)
0.041667	1954.915	0.001
0.037500	1959.471	
0.033333	1963.526	
0.029167	1967.095	
0.025000	1970.185	
0.020833	1972.798	
0.016667	1974.933	
0.012500	1976.590	
0.008333	1977.767	
0.004167	1978.467	
0	1978.698	0.010
0.041667	1883.638	
0.037500	1887.434	
0.033333	1890.837	
0.029167	1893.850	
0.025000	1896.470	
0.020833	1898.693	
0.016667	1900.516	
0.012500	1901.935	
0.008333	1902.950	
0.004167	1903.558	0.030
0	1903.759	
0.041667	1754.832	
0.037500	1757.528	
0.033333	1759.947	
0.029167	1762.085	
0.025000	1763.941	
0.020833	1765.514	
0.016667	1766.802	
0.012500	1767.806	
0.008333	1768.524	0.050
0.004167	1768.957	
0	1769.102	
0.041667	1655.241	
0.037500	1657.283	
0.033333	1659.111	
0.029167	1660.729	
0.025000	1662.135	
0.020833	1663.326	
0.016667	1664.302	
0.012500	1665.062	
0.008333	1665.605	0.050
0.004167	1665.930	
0	1666.037	

approach the base temperature of the plate. If a plate were subjected to a time dependent gamma flux such as occurred after shutdown of a reactor, it would show some transient temperature response. For the case examined, where the plate is first heated by a constant gamma flux during reactor operation, the transient temperature analysis will first show a rapid cooling period. However, the temperature will eventually approach the values predicted for a plate which had not been subjected to the gamma flux during reactor operation. After a period of one or two hours this flux would not be significant enough to keep the temperature of the plate much above the base temperature.

Two Parallel Plates with both Convection and Radiation
Heat Loss in a Constant Gamma Photon Beam

In attempting to minimize the thermal stresses in each of two parallel plates which have a gas flowing between them, the minimization of the maximum thermal stress of a plate perfectly restrained at the ends was chosen. This is accomplished by simply equating the average temperature in each of the two plates. However, it does not necessarily follow that the maximum thermal stress of a free plate or of a plate restrained only in bending will also be minimized.

In all cases examined for both a steel and an aluminum plate, only the steady state temperatures and thermal stresses were calculated. Rather than seeking the transient nature of the double plate problem, an attempt was made to correlate the resultant temperature and thermal stresses to the magnitude of the convection coefficients used.

Figure 10 shows the relationship for the outside steel plate, steady state temperature to the convection coefficient. When the convection coefficient reaches a value of zero, the temperature will be the same as was

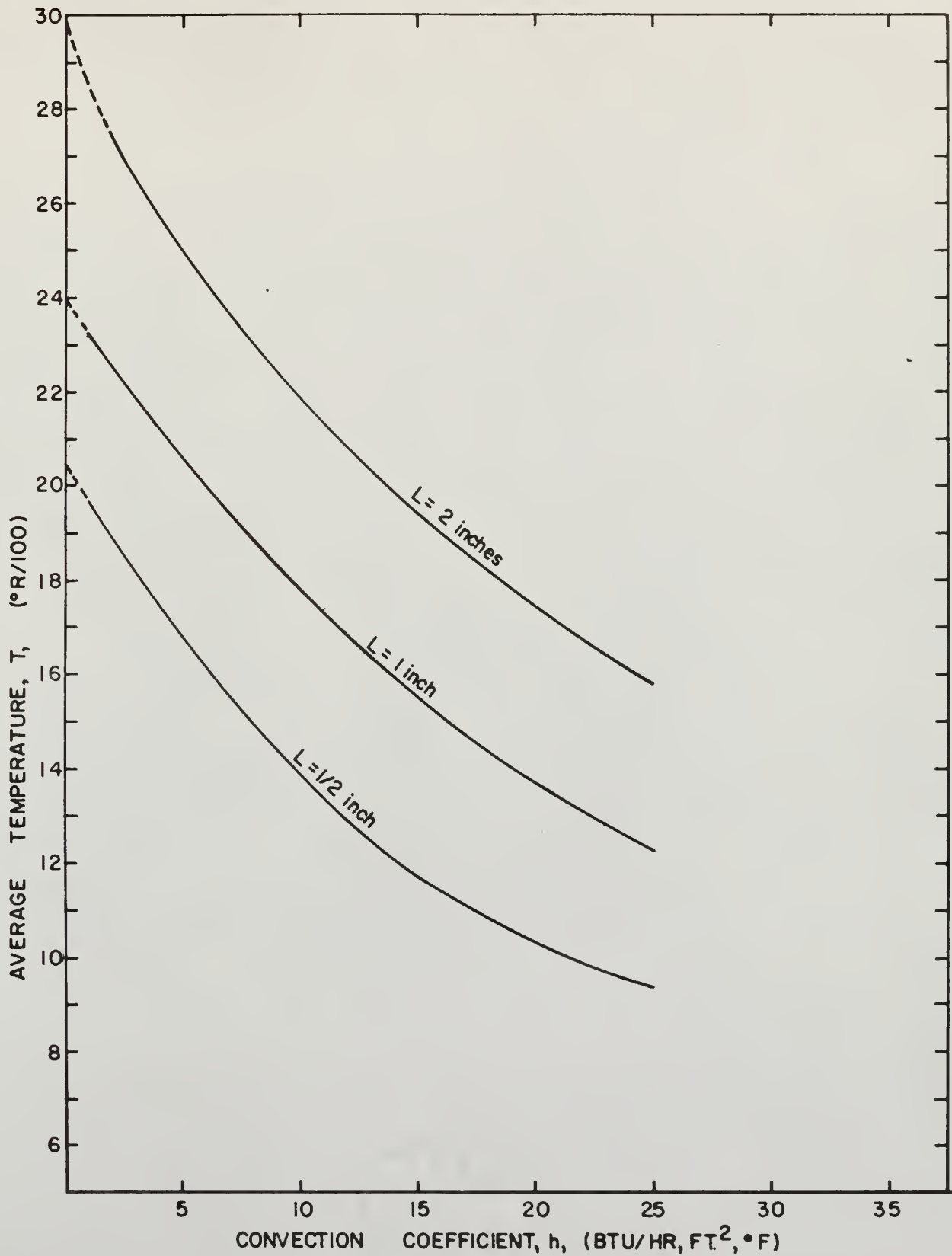


FIG.10 EFFECT OF CONVECTION COEFFICIENT ON AVERAGE STEADY STATE TEMPERATURE IN A STEEL PLATE

found for a single plate of the same total thickness. Because this condition would require the reduction of one of the plates to zero thickness, this case could not be directly calculated. However, Fig. 10 has been extrapolated to the actual single plate steady state temperature and the curve appears to be smooth, thus giving at least some partial verification to the calculations performed. The calculations made for aluminum show similar type curves which smoothly approach the single plate steady state temperature, as is shown in Fig. 11.

Figure 12 shows the percentage of the total steel plate thickness which is contained in the outside plate. For a convection coefficient of zero, each plate examined will have its entire thickness in the outside plate. Consequently, these curves were also extrapolated to that value.

Figure 13 shows the same type data just described, when obtained for an aluminum plate. The flux level chosen to compute this data was $1/10$ the flux level to which the steel plate was exposed. This level is quite arbitrary and was chosen simply to keep the temperature below the melting point of aluminum. It can be seen that the relationship of the plates of different thickness to each other on this graph are essentially the same as were found for steel. However, the graphs are quite dissimilar in other respects.

The two outstanding differences between aluminum and steel are that the division of the aluminum plate is much more nearly equal than the steel plate, and furthermore retains this near equality until the convection coefficient becomes almost zero. Both these differences can be attributed to the combined effect of the high conductivity of aluminum and the availability of an additional mode of heat transfer.

In considering the aluminum plate with radiation heat loss only, the low emissivity of the aluminum was found to retain the heat, despite the

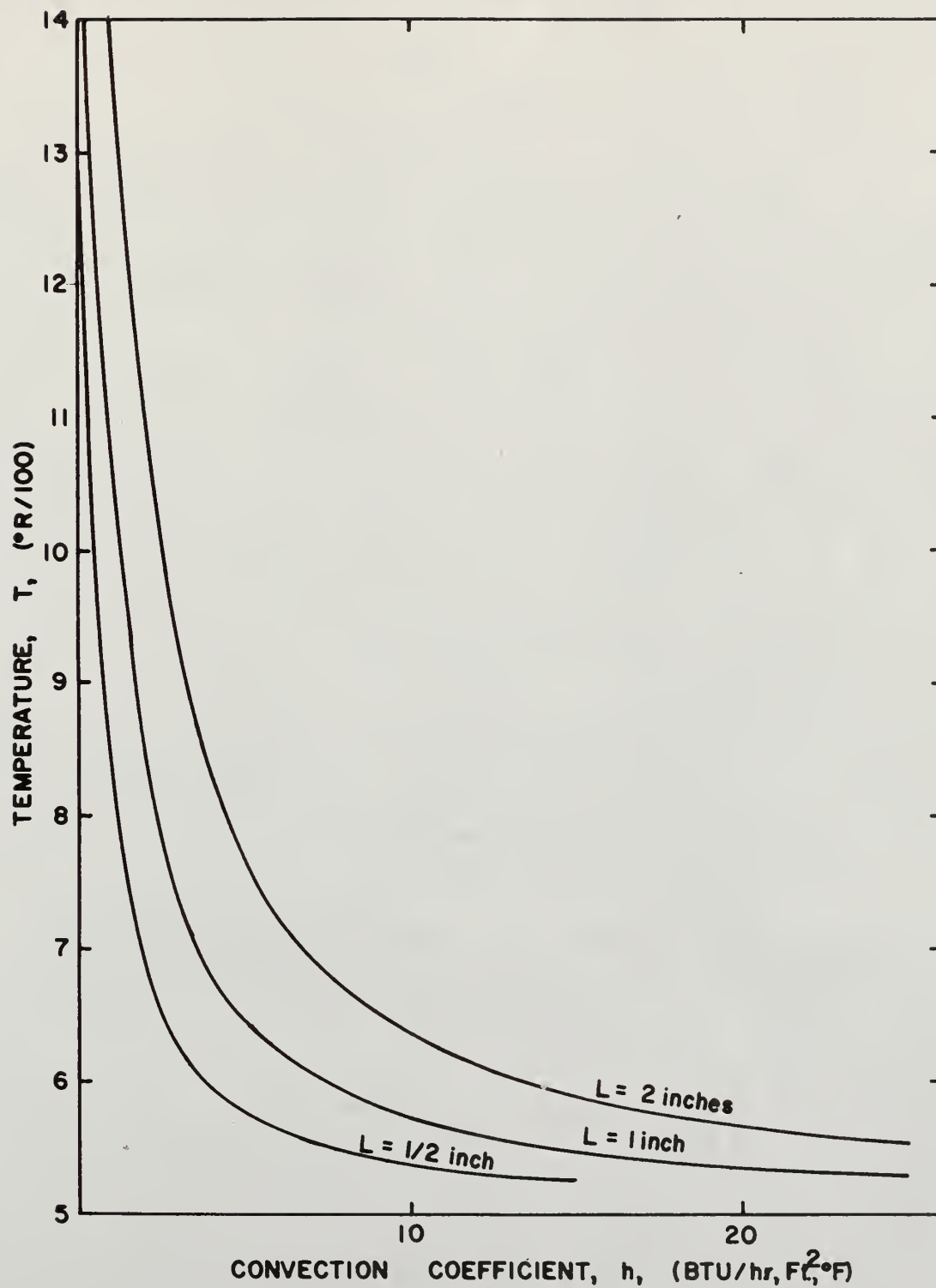


FIG. II EFFECT OF CONVECTION COEFFICIENT ON AVERAGE STEADY STATE TEMPERATURE IN AN ALUMINUM PLATE

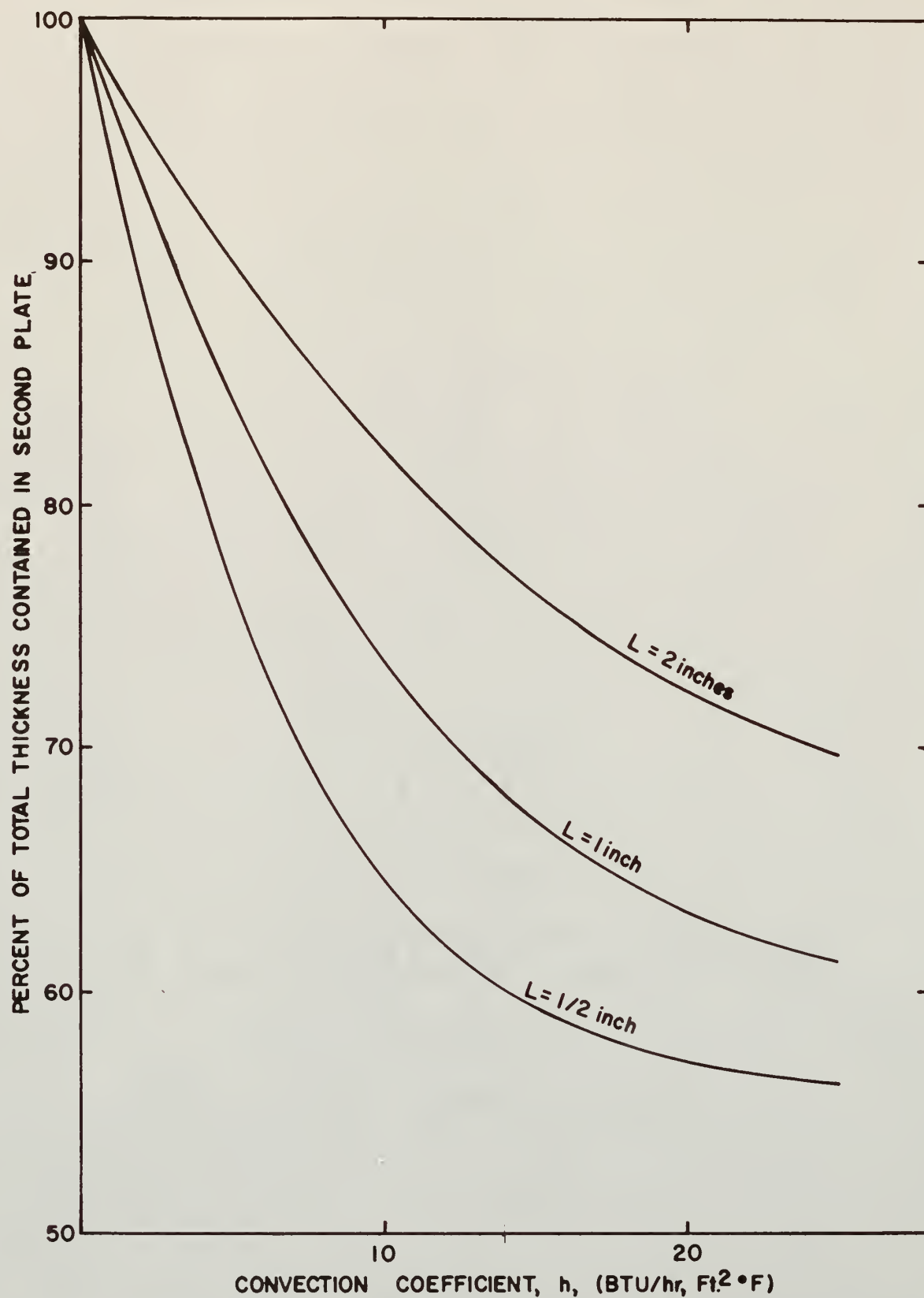


FIG.12. PERCENTAGE OF TOTAL THICKNESS IN OUTSIDE PLATE AT DIFFERENT CONVECTION COEFFICIENTS WHEN AVERAGE STEEL PLATE TEMPERATURES ARE EQUAL

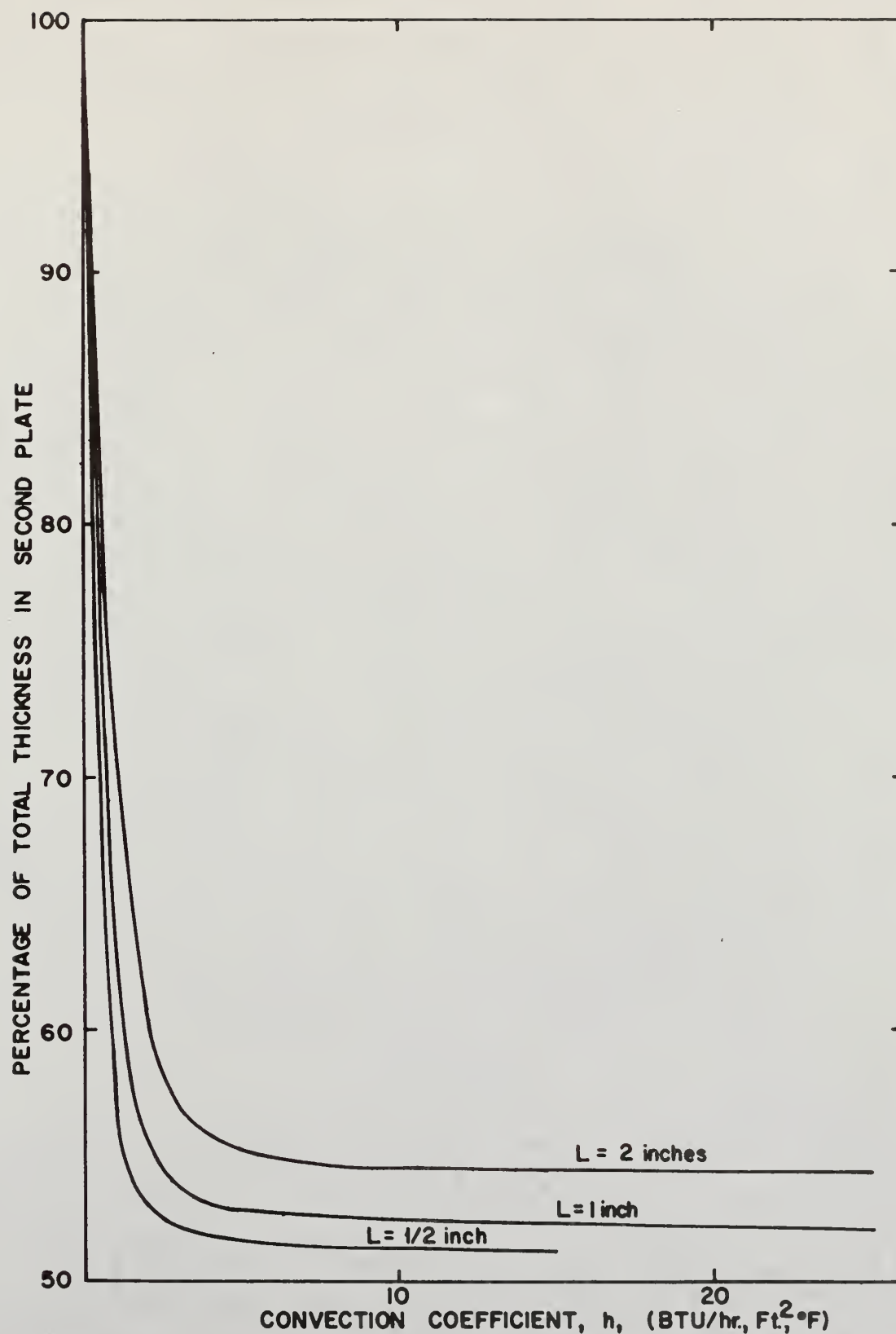


FIG.13. PERCENTAGE OF TOTAL THICKNESS IN OUTSIDE PLATE AT DIFFERENT CONVECTION COEFFICIENTS WHEN AVERAGE ALUMINUM PLATE TEMPERATURES ARE EQUAL

fact that the high conductivity allowed this heat to be rapidly transferred to the surface. It was also found that the temperature of both a one-half and one inch aluminum plate were nearly identical. Consequently, it was expected that the division of the plates would also be nearly identical since the resistance to the heat flow does not vary by a great amount.

When convection heat transfer is made available, the amount of heat flow through the inner surface of the outside plate apparently exceeds that through the radiating surface of the plate by some considerable amount, except for low convection coefficients, as can easily be seen in Fig. 11. Thus it is entirely expected that the percentage division of the aluminum plate will remain relatively constant until the convection coefficient attains a low value. When the heat has been rapidly transferred to the surface, the presence of an expeditious heat transfer medium, through the availability of convection, allows this heat to be removed from the system.

With regard to the maximum thermal stress of a plate which is held in perfect restraint, Fig. 5 may again be utilized. The temperature at which the maximum thermal stress first exceeded the yield stress for 7075-T6 aluminum was about 790°R . Examination of Fig. 11 shows that when convection is made available to the aluminum, the steady state temperature does not exceed 790°R until the convection coefficient has reached approximately $5 \text{ Btu/hr, ft}^2, ^{\circ}\text{F}$, with the exact value varying slightly with the plate thickness. Since there is a good probability that the temperature of a gas flowing in a channel such as has been postulated here, will be lower than the assumed value of 500°R , and since the convection coefficient will almost surely be greater than $5 \text{ Btu/hr, ft}^2, ^{\circ}\text{F}$, the aluminum can be subjected to a much higher flux level than was found for a plate with radiation heat loss only, without endangering its structural stability.

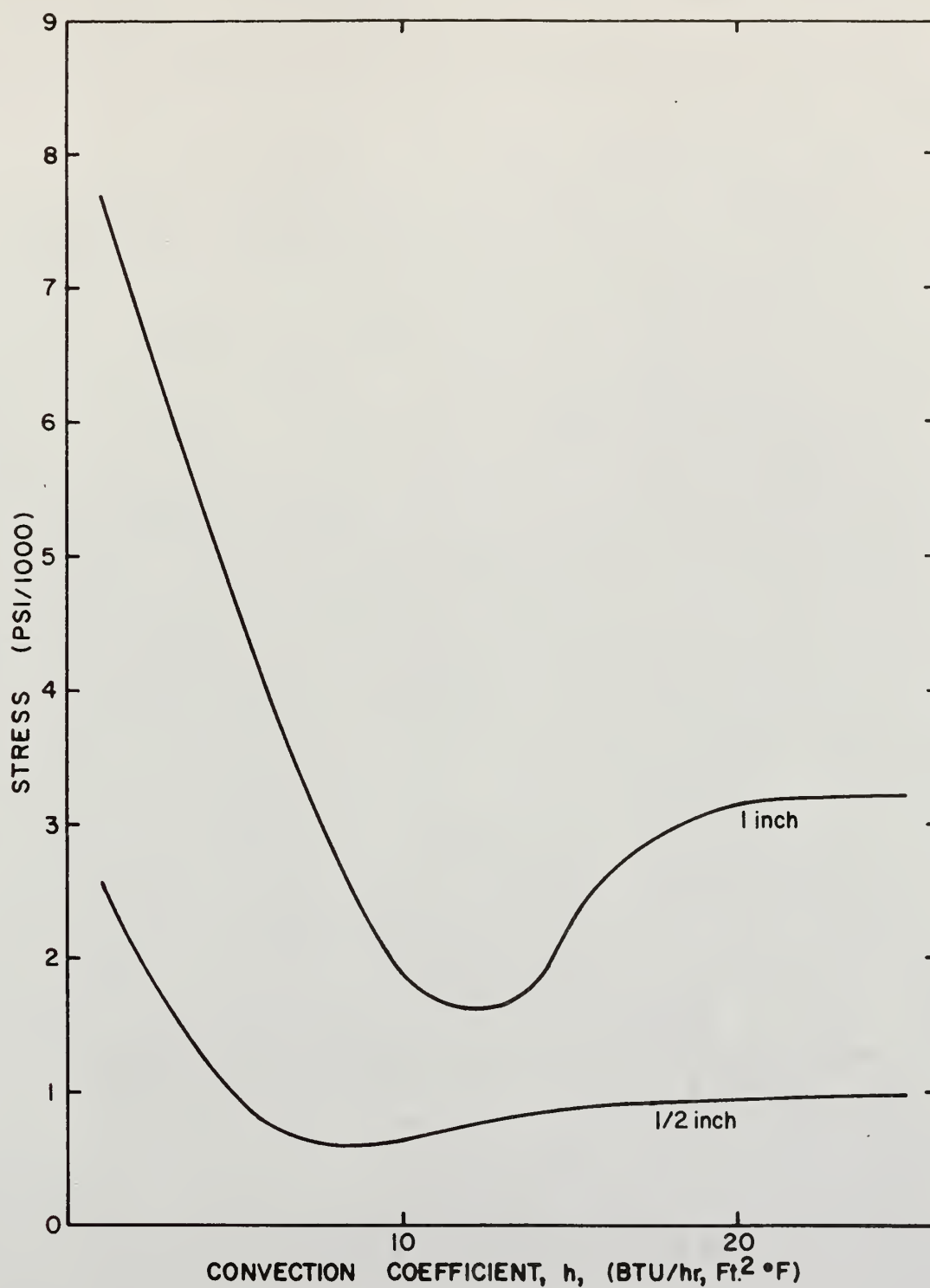


FIG. 14. RELATION OF MAXIMUM THERMAL STRESS FOR STEEL PLATE RESTRAINED IN BENDING TO CONVECTION COEFFICIENT

Figure 14 shows the relation of the maximum thermal stress in a steel plate restrained in bending to the convection coefficient. This curve is seen to exhibit a distinct minimum as the thickness of the plate increases. In the present instance, the stresses for a two inch plate were not plotted. For this case the temperatures for the lower convection coefficients reached values for which the elastic properties of steel are no longer considered to be completely valid (3). The presence of this minimum is the result of the availability of a mode of heat transfer from both surfaces of the plate and also the relative importance of each mode.

The maximum thermal stress for a plate restrained in bending is found at the edge of the plate for each of the cases considered. Furthermore, this stress is always found to be one of tension. For a steel plate at a relatively high convection coefficient, the greater amount of heat is lost from the inner face of the second plate. Consequently, the temperature at this face is lower than the temperature at the face losing heat by radiation, and the quantity $(T_{av} - T)$ is greater at the inner face. Thus there is also a higher thermal stress at this face. However, the heat lost from the outer face by radiation soon begins to become more significant as the convective heat transfer coefficient is lowered. Thus the difference between the temperature at the inside face and the average temperature of the plate becomes less, while the difference at the outside face becomes greater. This also causes a lowering of the thermal stress at the inside face of the plate while the stress at the outside face is rising.

When the equivalent gray body convective coefficient is equal to the convection coefficient at the inside face, the temperatures at both the inside and the outside face are equal. At this point the maximum thermal stress for a plate restrained in bending reaches a minimum. For any lower

convection coefficient, the temperature difference ($T_{av} - T$) becomes greater at the outside face and continues to rise at a rapid pace as the radiation heat loss takes on continuously greater significance. Consequently, the maximum thermal stress also rises rapidly as is shown in Fig. 14.

For an aluminum plate, Fig. 15 does not seem to exhibit the same property just discussed for steel. However, further examination of the equivalent gray body convective coefficient shows it to be below a value of one Btu/hr,ft²,°F for all the steady state cases considered. Thus the minimum point has not been reached within the range of convection coefficients investigated.

As was found to be the case for the single plate, the maximum thermal stress for a plate restrained in bending is not of such a magnitude that it becomes significant in the structural considerations for any of the cases which have been presently examined. Although this is true, the presence of the minimum which has been discussed above should be kept in mind in considering the presence of thermal stresses in other materials not examined in this study.

Conclusions

When radiation heat transfer is available to a flat plate subjected to a high intensity gamma photon flux with a magnitude of 94500 Btu/hr,ft², the temperatures remain in a range where its structural utility is not seriously impaired. In the case of steel, a temperature of about 2000°R is reached in approximately 15 minutes for each of the thicknesses considered except for a 1/4 inch plate. In that instance the steady state temperature does not reach 2000°R. In contrast to the nature of this temperature rise,

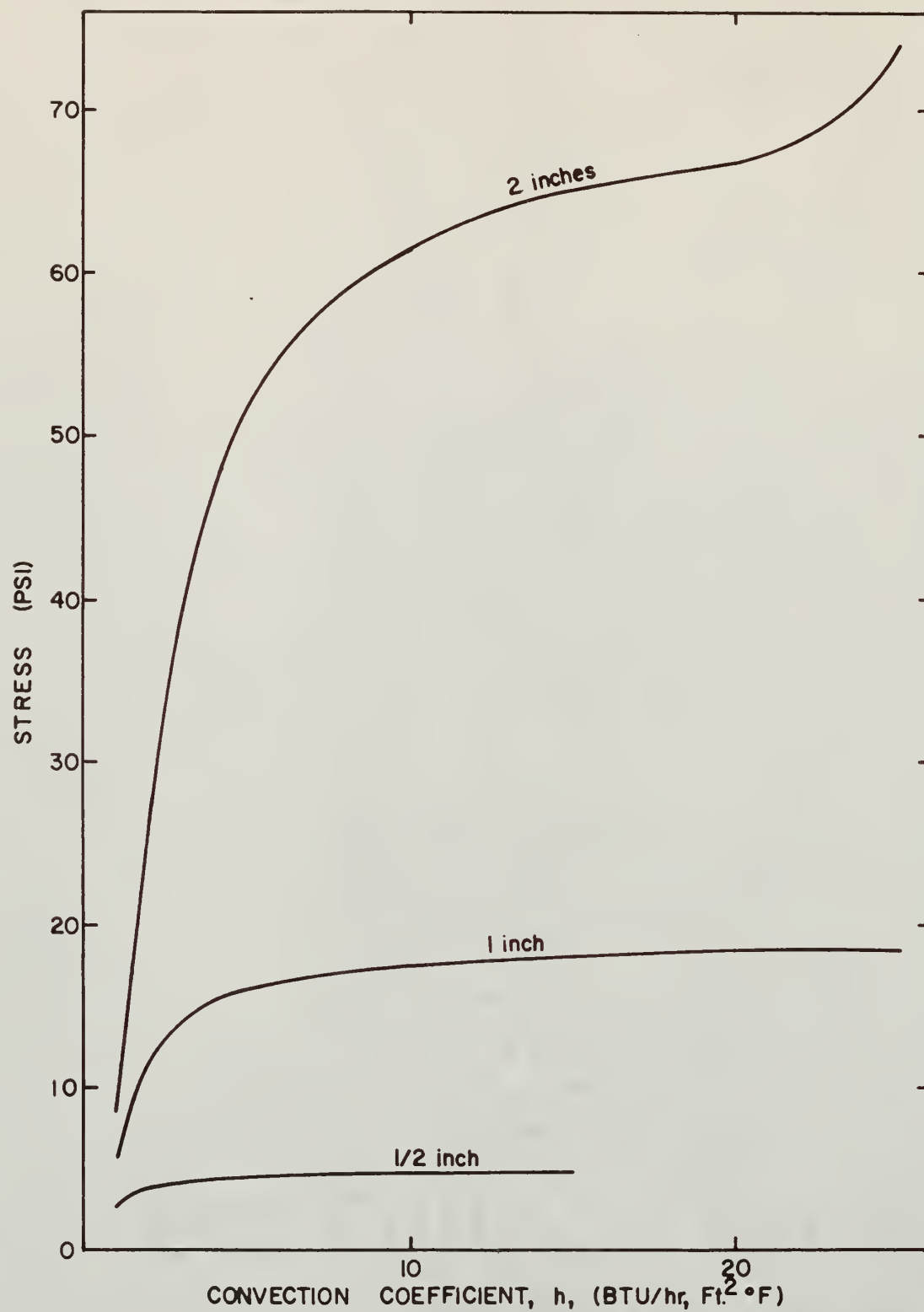


FIG.15. RELATION OF MAXIMUM THERMAL STRESS FOR ALUMINUM PLATE RESTRAINED IN BENDING TO CONVECTION COEFFICIENT

aluminum is found to approach the steady state much more slowly. Hence, even if aluminum were exposed to the same intensity flux as steel, the danger of nearing the melting point would be negligible for a period of reactor operation in the range of 15 to 30 minutes.

After shutdown, the temperature of the plate cools quite rapidly despite the presence of a time dependent gamma photon source from the fission products. The difference between this cooling and that for no heat generation after shutdown remains nearly the same for a period of several minutes. The continuous nature of the temperature as a function of time immediately after shutdown is difficult to exhibit and is probably more evident in the consideration of extremely small time increments. However, this is of little or no consequence to a macroscopic investigation of the present nature.

When additional modes of heat transfer are made available to a flat plate, the steady state temperature can be significantly lowered. For steel, the additional convection heat transfer becomes significant at about 10 Btu/hr,ft²,°F. At this point, approximately the same amount of heat is lost by both convection and radiation. For convection coefficients below this value, the steady state temperature rises rapidly. In aluminum, the critical value for the convection coefficient is below one Btu/hr,ft²,°F. The rise of the steady state temperature for convection coefficients below this critical value is also considerably more severe than for steel.

The only apparent thermal stress damage which might occur for any of the cases considered, is for a steel plate which is perfectly restrained. This physical situation is somewhat unlikely, however, since almost all the structural members in a nuclear rocket would be subjected to a high intensity gamma photon flux and would have a tendency to expand simultaneously.

Although such a system would still remain restrained in bending, the maximum thermal stresses of this type are small compared to the elastic limits of the systems examined. It is significant that subjection of an aluminum plate to a maximum thermal stress of the type encountered in perfect restraint, does not present difficulties until the plate has been irradiated by the gamma flux for a period in excess of the 15 to 30 minutes which might be considered normal for the operating time of a nuclear rocket. Furthermore, by providing even minimal additional modes of heat transfer, the steady state maximum thermal stress of an aluminum plate can be kept well below the yield stress.

Finally the case of a plate with heat transfer available at both faces exhibits a distinct minimum for the maximum thermal stress of a plate restrained in bending. For all the metals and conditions which have been examined in this study, the magnitude of this type of thermal stress is small enough not to be of danger to structural members. However, there are undoubtedly some metals for which the minimum exhibited by this curve could be of primary importance in the design of a nuclear rocket.

Suggestions for Further Work

The availability of further data in the areas discussed in this study lies principally in refinements of calculational techniques and in the variation of certain parameters to obtain a more accurate description of the systems under consideration. All the calculations which have been presented, used the basic assumption that there was no Compton scattering in the plates examined. Of course, even for the thinnest plate, this assumption is not precisely accurate. A more exact evaluation of the mode of gamma

photon absorption could be obtained by use of the moments method (8). This could serve to set limits on the thickness of a plate which is reasonably approximated by the method employed. Also, it would give a more accurate description of the temperature response of materials of greater thickness than have been considered.

Another interesting study would be a closer investigation of some of the parameters involved in the calculations. Rather than consider some specific metal, it would be possible to choose some reasonable set of physical constants and then vary each one individually while holding the others steady. In this respect it would also be possible to vary the temperature dependence of each of these physical constants after assuming several initial values. Those constants which would be of special interest in both the temperature and thermal stress equations are the density, the heat capacity, the emissivity, the coefficient of thermal expansion and the thermal conductivity.

The thermal conductivity would be of special interest because of its effect on the use of the "thin body" approximation. A more thorough investigation of the magnitude of the conductivity, coupled with the investigation of the thickness of the plate which would allow the use of the "thin body" approximation would prove very helpful. Since the "thin body" equation is an ordinary differential equation, the resultant temperature expressions can be evaluated much more rapidly.

It would also prove interesting to define the physical system more accurately to determine the effect of several other parameters. A system could probably be constructed which would present a greater surface area to the environment to make the radiative heat loss more efficient. In the present considerations, the view factor has been assumed to be unity in all cases.

In varying the spatial characteristics of the system, the view factor would also require further investigation. These alterations should also prove helpful in attempting to remove excess heat by the use of convection, such as was attempted through the use of two parallel plates with a flow of gas between them.

Similarly, it would also be possible to undertake a more thorough investigation of the double plate case. The temperature of the gas flowing through the channel between the plates should be followed, as well as the variation of the heat transfer coefficient. In the same vein, the variation of the sink temperature on the amount of heat removed as well as the temperature distribution should prove of interest. This would be true for the double plate case as well as each of the other physical situations which have been examined.

It should also prove of considerable interest to more closely examine the flux levels on the temperature and thermal stresses after certain predetermined times of reactor operation. Both the magnitude of the energy flux and the distribution of this energy would have a considerable effect on the temperature response of any of the systems which have been considered in this study or those which have been discussed above.

Another possibility which should prove useful in the structural considerations of nuclear rockets is the incidence of a plane flux beam on the side of a metal rod or other cylindrical supporting member. The solution of the resultant partial differential equation in cylindrical geometry and the use of any of several ordinary boundary conditions, presents a two dimensional system which is not easily solved by conventional methods. The use of Laplace transforms may prove useful in attempting to express the

discontinuous boundary conditions which might commonly be used. However, the use of numerical techniques, again coupled with the aid of a high speed digital computer would probably be found most helpful.

The magnitude of the maximum thermal stresses found for the metals investigated are well within the elastic limits. The metals examined are quite common, however, and their properties should be subjected to more thorough scrutiny. An examination of the inelastic qualities of these and other common metals would seem in order. Of special interest would be the creep of structural members caused by a cyclic temperature change which would occur when a reactor is operated for a short time and then shut down, periodically.

ACKNOWLEDGEMENT

The author wishes to express sincere gratitude to Dr. J. O. Mingle, under whose direction this work has been performed, for his guidance and assistance throughout the course of this study. I also wish to thank Professor J. R. Fagan for his advice concerning several of the more refined details of this work. Appreciation is also expressed to Dr. P. G. Kirmser and Dr. C. A. Halijak for their assistance in dealing with specific aspects of the mathematical background and to Dr. S. T. Parker and the staff of the Kansas State University computing center for their co-operation with the use of the IBM 1620 digital computer. Most sincere gratitude is also extended to Dr. W. R. Kimel, Head of the Department of Nuclear Engineering, for his guidance and encouragement during the course of this study.

BIBLIOGRAPHY

- (1) Avery, R.
Reactor Physics Constants. ANL-5800, 1958.
- (2) Besserer, C. W.
Missile Engineering Handbook. Princeton: Van Nostrand. 1958.
- (3) Bonilla, C. F.
Nuclear Engineering. New York: McGraw-Hill. 1957.
- (4) Carslaw, H. A. and J. C. Jaeger.
Conduction of Heat in Solids. London: Oxford University Press.
1959.
- (5) Epel, L. G.
Transient Temperature in Infinite Plates, Infinite Cylinders,
and Spheres Following a Simultaneous Step Change in Internal
Heat Generation Rate, Coolant Temperature and Heat Transfer
Coefficient. ORNL-2597, 1958.
- (6) Etherington, H.
Nuclear Engineering Handbook. New York: McGraw-Hill. 1958.
- (7) Fagan, J. R.
Private Communication. Kansas State University, Manhattan,
Kansas. February 1962.
- (8) Goldstein, H.
Fundamental Aspects of Reactor Shielding. Reading, Mass.:
Addison Wesley. 1959.
- (9) Grotenhuis, M.
Lecture Notes on Reactor Shielding. ANL-6000, 1959.
- (10) Gubareff, G. G., J. E. Janssen, and R. H. Torborg.
Thermal Radiation Properties Survey. Honeywell Research Center.
1960.
- (11) Hildebrand, F. B.
Introduction to Numerical Analysis. New York: McGraw-Hill. 1957.
- (12) Lottes, P. A.
Nuclear Reactor Heat Transfer. ANL-6469, 1961.
- (13) Maienschein, F. C., R. W. Peelle, W. Zobel, and T. A. Love.
Gamma Rays Associated with Fission. Geneva: Proceedings of the
Second United Nations International Conference on the Peaceful
Uses of Atomic Energy. v. 15. 1958.

- (14) Marks, L. S.
Mechanical Engineers Handbook. New York: McGraw-Hill. 1951.
- (15) Mickley, H. S., T. R. Sherwood, and C. E. Reed.
Applied Mathematics in Chemical Engineering. New York:
McGraw-Hill. 1957.
- (16) Mingle, J. O.
Structural Aspects of Gamma Heating in Nuclear Rockets. Aeorjet
General Corp. 1961.
- (17) Mingle, J. O.
Private Communication. Kansas State University, Manhattan,
Kansas. 1961.
- (18) Richtmyer, R. D.
Difference Methods for Initial Value Problems. New York:
Interscience Publishers. 1957.
- (19) Sears, F. W., and M. W. Zemansky.
University Physics. Cambridge: Addison Wesley. 1955.
- (20) Stanton, R. G.
Numerical Methods for Science and Engineering. Englewood Cliffs:
Prentice Hall. 1961.
- (21) Timoshenko, S., and J. N. Goodier.
Theory of Elasticity. New York: McGraw-Hill. 1951.
- (22) Unterberg, W.
Thin Body Temperature Transients Due to Gamma Heating in
Aerospace. North American Aviation (Rocketdyne Division). 1961.
- (23) Wylie, C. R. Jr.
Advanced Engineering Mathematics. New York: McGraw-Hill. 1960.

APPENDICES

APPENDIX A

Derivation of the Temperature Distribution and Thermal Stresses in a Flat Plate with Insulation at One Face and Radiation Heat Loss at the Other Face

The partial differential equation for the temperature distribution in the flat plate shown in Fig. 16 is

$$\frac{\partial^2 \theta}{\partial x^2} + \frac{H}{k} = \frac{1}{\alpha} \frac{\partial \theta}{\partial t} \quad (\text{A-1})$$

The heat generation term, H , is given by Bonilla (3) as $\mu I e^{-\mu x}$, where the absorption coefficient,

μ , is such that it considers the effect of buildup through the plate. Although this is not truly a constant, it can be represented in that manner for thin systems such as are being considered here. The boundary conditions for this system are

$$-k \left(\frac{\partial \theta}{\partial x} \right)_{x=0} = 0 \quad (\text{A-2})$$

$$-k \left(\frac{\partial \theta}{\partial x} \right)_{x=L} = h_r \theta \quad (\text{A-3})$$

and the initial condition is

$$\theta \Big|_{t=0} = 0 \quad (\text{A-4})$$

where h_r is the equivalent gray body convective radiation coefficient, defined by



FIG. 16.
CO-ORDINATE SYSTEM

$$\frac{q}{A} = h_r(T - T_o) = \epsilon \sigma (T^4 - T_o^4) \quad (A-5)$$

The assumption is first made that Θ may be written as

$$\Theta(x,t) = X(x) + \tau(x,t) \quad (A-6)$$

Then operating on Eq.(A-6) with (A-1) yields

$$\frac{\partial^2 X}{\partial x^2} + \frac{\partial^2 \tau}{\partial x^2} + \frac{\mu I e^{-\mu x}}{k} = \frac{1}{\alpha} \frac{\partial \tau}{\partial t} \quad (A-7)$$

Eq. (5) shows that such an equation may be solved by separating this equation into two equations in X and τ alone and setting them both equal to zero. This leaves

$$\frac{\partial^2 X}{\partial x^2} + \frac{\mu I e^{-\mu x}}{k} = 0 \quad (A-8)$$

$$\frac{\partial^2 \tau}{\partial x^2} = \frac{1}{\alpha} \frac{\partial \tau}{\partial t} \quad (A-9)$$

Integrating Eq.(A-8) twice, the solution becomes

$$X = -\frac{I e^{-\mu x}}{\mu k} + C_1 x + C_2 \quad (A-10)$$

In order to solve for the constants C_1 and C_2 it is necessary to transform the boundary conditions so they are compatible with the system of equations being solved. For Eq.(A-8) these are

$$-k \left. \frac{\partial X}{\partial x} \right|_{x=0} = 0 \quad (A-11)$$

$$-k \left. \frac{\partial X}{\partial x} \right|_{x=L} = h_r X|_{x=L} \quad (A-12)$$

In the case of Eq.(A-9) they become

$$-k \frac{\partial \tau}{\partial x} \Big|_{x=0} = 0 \quad (\text{A-13})$$

$$-k \frac{\partial \tau}{\partial x} \Big|_{x=L} = h_r \tau \Big|_{x=L} \quad (\text{A-14})$$

The initial condition now becomes

$$\tau = -X \quad (\text{A-15})$$

Applying Eq.(A-11) and (A-12) to (A-10), there results

$$C_1 = -\frac{I}{k} \quad (\text{A-16})$$

$$C_2 = \frac{I}{h_r}(1 - e^{-\mu L}) + \frac{I}{k\mu}(\mu L + e^{-\mu L}) \quad (\text{A-17})$$

Thus

$$X = \frac{I}{k\mu}(e^{-\mu L} - e^{-\mu x}) + \frac{I}{k}(L - x) + \frac{I}{h_r}(1 - e^{-\mu L}) \quad (\text{A-18})$$

which is the steady state temperature distribution. Eq.(A-9) may be solved by again separating variables in such a manner that

$$\tau = U(t) S(x) \quad (\text{A-19})$$

Operating on Eq.(A-19) with (A-9) yields

$$\frac{1}{S} \frac{\partial^2 S}{\partial x^2} = \frac{1}{XU} \frac{\partial U}{\partial t} \quad (\text{A-20})$$

This is a familiar eigenvalue problem and has solutions only when both sides of the equation are equal to the same constant $-\lambda^2$. These solutions are

$$U = e^{-\alpha \lambda^2 t} \quad (\text{A-21})$$

$$S = C_3 \sin \lambda x + C_4 \cos \lambda x \quad (\text{A-22})$$

From which

$$\tau = (C_3 \sin \lambda x + C_4 \cos \lambda x) e^{-\alpha \lambda^2 t} \quad (\text{A-23})$$

Applying Eq.(A-13) to (A-23), C_3 is found to be zero. Then applying Eq. (A-14) to (A-23), the eigenvalue is given by

$$\tan \lambda L = \frac{h_r}{k\lambda} \quad (\text{A-24})$$

There are a countable infinity of roots (λ_n) to this transcendental equation. Using this information and applying Eq.(A-15) to (A-23) gives

$$-\sum_{n=1}^{\infty} C_4 (\cos \lambda_n x)(1) = \frac{T}{k\mu} (e^{-\mu L} - e^{-\mu x}) + \frac{T}{k} (L - x) + \frac{T}{h_r} (1 - e^{-\mu L}) \quad (\text{A-25})$$

Multiplying both sides of Eq.(A-25) by the orthogonal function $\cos \lambda_n x$ and integrating over the period of orthogonality yields, after some trigonometric manipulation

$$C_4 = -\frac{2T\mu}{k\lambda_n^2(\lambda_n^2 + \mu^2)} \left[\frac{\mu(k^2\lambda_n^2 + h_r^2) + \lambda_n^2(h_r k - k\mu)e^{-\mu L} \sec \lambda_n L}{k^2\lambda_n^2 L + h_r^2 L + h_r k} \right] \quad (\text{A-26})$$

From which

$$\tau = -\frac{2T\mu \cos \lambda_n x}{k\lambda_n^2(\lambda_n^2 + \mu^2)} \left[\frac{\mu(k^2\lambda_n^2 + h_r^2) + \lambda_n^2(h_r k - k\mu)e^{-\mu L} \sec \lambda_n L}{k^2\lambda_n^2 L + h_r^2 L + h_r k} \right] e^{-\alpha \lambda_n^2 t} \quad (\text{A-27})$$

and the temperature is found to be

$$\theta = \frac{I}{h\mu} (e^{-\mu L} - e^{-\mu x}) + \frac{I}{k} (L - x) + \frac{I}{h_r} (1 - e^{-\mu L})$$

$$- \sum_{n=1}^{\infty} \frac{2 I \mu \cos \lambda_n x}{k \lambda_n^2 (\lambda_n^2 + \mu^2)} \left[\frac{\mu (k^2 \lambda_n^2 + h_r^2) + \lambda_n^2 (h_r k - k^2 \mu) e^{-\mu L} \sec \lambda_n L}{k^2 \lambda_n^2 L + h_r L + h_r k} \right] e^{-\lambda_n^2 t} \quad (\text{A-28})$$

which satisfies the assumption concerning the separability of θ .

It is possible to arrive at this same equation by transforming the partial differential equation and the boundary conditions from the time domain to the Laplace domain. Eq.(A-1) then becomes

$$\frac{\partial^2 \bar{\theta}}{\partial x^2} + \frac{\mu I e^{-\mu x}}{k s} = \frac{1}{s} (s \bar{\theta} - \theta(0)) \quad (\text{A-29})$$

where $\bar{\theta}$ is the transform of θ and also where $\theta(0)$ is zero.

The transformed boundary conditions are

$$-k \frac{\partial \bar{\theta}}{\partial x} \Big|_{x=0} = 0 \quad (\text{A-30})$$

$$-k \frac{\partial \bar{\theta}}{\partial x} \Big|_{x=L} = h_r \bar{\theta} \Big|_{x=L} \quad (\text{A-31})$$

Applying these conditions results in the equation

$$\theta = \frac{s \mu I}{s k (s - \lambda_n^2)} \left\{ e^{-\mu x} + \mu (s/\lambda_n^2)^{-1/2} \sinh(x \sqrt{s/\lambda_n^2}) \right.$$

$$\left. - \left[\frac{h_r \mu (s/\lambda_n^2) \sinh(L \sqrt{s/\lambda_n^2}) + (h_r - \mu k) e^{-\mu L} + \mu k \cosh(L \sqrt{s/\lambda_n^2})}{h_r \cosh(L \sqrt{s/\lambda_n^2}) + (L \sqrt{s/\lambda_n^2}) \sinh(L \sqrt{s/\lambda_n^2})} \right] \cosh(x \sqrt{s/\lambda_n^2}) \right\} \quad (\text{A-32})$$

which, when inverted back into the time domain, yields Eq.(A-28) above.

Timoshenko and Goodier (21) show that for a temperature distribution in the \underline{x} direction, the thermal stresses in the \underline{y} and \underline{z} directions are given by

$$\sigma_y = \sigma_z = \frac{\alpha E}{1-\nu} \left\{ -\theta + \frac{1}{L} \int_0^L \theta dx + \frac{12(x-L/2)}{L^3} \int_0^L (x-L/2) \theta dx \right\} \quad (A-33)$$

The first term within the brackets, σ_I , is simply the negative of Eq.(A-28).

The second term becomes

$$\sigma_{II} = \frac{I}{k\mu} \left[e^{-\mu L} + \frac{1}{\mu L} (e^{-\mu L} - 1) \right] + \frac{IL}{2k} + \frac{I}{h_r} (1 - e^{-\mu L}) - \sum_{n=1}^{\infty} \frac{G_n}{\lambda_n L} \sin \lambda_n L \quad (A-34)$$

where G_n is defined by

$$G_n = \frac{2I\mu e^{-\alpha \lambda_n^2 L}}{k \lambda_n^2 (\lambda_n^2 + \mu^2)} \left[\frac{\mu (k^2 \lambda_n^2 + h_r^2) + \lambda_n^2 (h_r k - k^2 \mu) e^{\mu L} \sec \lambda_n L}{k^2 \lambda_n^2 L + h_r^2 L + h_r k} \right] \quad (A-35)$$

Similarly, the third term is

$$\begin{aligned} \sigma_{III} = \frac{12(x-L/2)}{L^3} & \left\{ \frac{I}{k\mu} \left[\frac{L}{2\mu} (1 + e^{-\mu L}) + \frac{1}{\mu^2} (e^{-\mu L} - 1) \right] - \frac{IL^3}{12k} \right. \\ & \left. - \sum_{n=1}^{\infty} G_n \left[\frac{L \sin \lambda_n L}{\lambda_n} + \frac{(\cos \lambda_n L - 1)}{\lambda_n^2} - \frac{L \sin \lambda_n L}{2} \right] \right\} \end{aligned} \quad (A-36)$$

Combining these three terms yields the final equation

$$\begin{aligned} \sigma_y = \sigma_z = \frac{\alpha E}{1-\nu} & \left\{ (e^{-\mu L} - 1) \left(1 + \frac{12(x-L/2)}{\mu L^2} \right) \left(\frac{I}{k\mu^2 L} \right) + \frac{I e^{-\mu x}}{k\mu} + \frac{6I(x-L/2)}{k\mu^2 L^2} (1 + e^{-\mu L}) \right. \\ & \left. + \sum_{n=1}^{\infty} G_n \left[\cos \lambda_n x - \frac{\sin \lambda_n L}{\lambda_n L} - \frac{12(x-L/2)}{L^3} \left(\frac{L \sin \lambda_n L}{2 \lambda_n} + \frac{(\cos \lambda_n L - 1)}{\lambda_n^2} \right) \right] \right\} \end{aligned} \quad (A-37)$$

APPENDIX B

Derivation of the Temperature Distribution and Thermal Stresses in a Flat Plate with Decaying Internal Heat Generation

The partial differential equation describing the conditions for this physical case is

$$\frac{\partial^2 \theta}{\partial x^2} + \frac{\mu I(t) e^{-\mu x}}{k} = \frac{1}{\alpha} \frac{\partial \theta}{\partial t} \quad (\text{B-1})$$

where the time dependent flux, $I(t)$, is given by Lottes (12) as

$$I(t) = I(0) \left\{ 0.1(t+10)^{-0.2} - 0.087(t+2 \times 10^7)^{-0.2} - 0.0025 e^{-\left(\frac{t}{2 \times 10^4}\right)} - 0.0013 e^{-\left(\frac{t}{290,000}\right)} \right. \\ \left. - \left[0.1(t+t_s+10)^{-0.2} - 0.087(t+t_s+2 \times 10^7)^{-0.2} - 0.0025 e^{-\left(\frac{t+t_s}{2 \times 10^4}\right)} - 0.0013 e^{-\left(\frac{t+t_s}{290,000}\right)} \right] \right\} \quad (\text{B-2})$$

where t is the time after shutdown and t_s is the time of reactor operation, both times being in seconds. In such a form Eq.(B-1) is not readily solved by the separation of variables technique. If the Laplace transformation is utilized, the resulting equation in the Laplace domain is

$$\frac{\partial^2 \bar{\theta}}{\partial x^2} = \frac{1}{\alpha} (s \bar{\theta} - \theta(0)) - \frac{\mu}{k} e^{-\mu x} \mathcal{L}\{I(t)\} \quad (\text{B-3})$$

where $\bar{\theta}$ is the transform of θ . The initial condition $\theta(0)$ is given by

$$\theta(0) = \theta(x, t_s) \quad (\text{B-4})$$

and $\mathcal{L}\{I(t)\}$ is the Laplace transform of Eq.(B-2). The transformed boundary conditions are

$$-k \left(\frac{\partial \bar{\theta}}{\partial x} \right)_{x=0} = 0 \quad (\text{B-5})$$

$$-k \frac{\partial \bar{\theta}}{\partial x} \Big|_{x=1} = h_r \bar{\theta} \Big|_{x=1} \quad (\text{B-6})$$

where h_r is again the equivalent convective radiation coefficient, given by

$$\frac{q}{A} = h_r (T - T_o) = \epsilon \sigma (T^4 - T_o^4) \quad (\text{B-7})$$

The solution to this system of equations is

$$\begin{aligned} \bar{\theta} = & \left\{ \frac{I \mathcal{L} \mu^2}{s(s - \mathcal{L} \mu^2)} \left[\frac{\frac{h_r e^{-\mu L}}{k} - e^{-\mu L} + \frac{h_r (s/\mathcal{L})}{k} \sinh(L\sqrt{s/\mathcal{L}}) + \cosh(L\sqrt{s/\mathcal{L}})}{k\sqrt{s/\mathcal{L}} \sinh(L\sqrt{s/\mathcal{L}}) + h_r \cosh(L\sqrt{s/\mathcal{L}})} \right] \right. \\ & + \frac{\mathcal{L} \{I(t)\} \mu^2 \mathcal{L}}{(s - \mathcal{L} \mu^2)} \left[\frac{1 - \frac{\mu h_r}{k} - \cosh(L\sqrt{s/\mathcal{L}}) - \frac{h_r (s/\mathcal{L})}{k} \sinh(L\sqrt{s/\mathcal{L}})}{k\sqrt{s/\mathcal{L}} \sinh(L\sqrt{s/\mathcal{L}}) + h_r \cosh(L\sqrt{s/\mathcal{L}})} \right] \\ & + \sum_{n=1}^{\infty} \frac{G_n \mathcal{L}}{(s + \lambda_n^2 \mathcal{L})} \left[\frac{h_r \cos \lambda_n L - k \lambda_n \sin \lambda_n L}{k\sqrt{s/\mathcal{L}} \sinh(L\sqrt{s/\mathcal{L}}) + h_r \cosh(L\sqrt{s/\mathcal{L}})} \right] \Big\} \cosh(x\sqrt{s/\mathcal{L}}) \\ & + \frac{\mathcal{L}}{k} \left\{ \left[\frac{\mu^2 \mathcal{L} \{I(t)\} - I}{s - \mathcal{L} \mu^2} \right] + \frac{I}{s} \right\} \frac{\sinh(x\sqrt{s/\mathcal{L}})}{\sqrt{s/\mathcal{L}}} \\ & + \frac{\mathcal{L}}{k\mu} \left[\frac{\mu^2 \mathcal{L} \{I(t)\} - I}{s - \mathcal{L} \mu^2} \right] e^{-\mu x} - \frac{\mathcal{L} I x}{s k} - \sum_{n=1}^{\infty} \frac{G_n \mathcal{L} \cos \lambda_n x}{s + \lambda_n^2 \mathcal{L}} \\ & + \frac{I \mathcal{L}}{s \mu h_r k} \left[\mu (h_r L + k) + e^{-\mu L} (h_r - \mu k) \right] \end{aligned} \quad (\text{B-8})$$

where G_n is given by Eq.(A-35) and also where

$$\begin{aligned} \mathcal{L} \{I(t)\} = & I \left\{ s^{0.8} e^{s'} E_{0.2}(s') - \frac{0.087(2 \times 10^7)^{-0.2}}{s} - \frac{0.0025}{s + 1/2040} - \frac{0.0013}{s + 1/290,000} \right. \\ & \left. - \left[s^{0.8} e^{s''} E_{0.2}(s'') - \frac{0.087(2 \times 10^7)^{-0.2}}{s} - \frac{0.0025 e^{-(\frac{t}{2040})}}{s + 1/2040} - \frac{0.0013 e^{-(\frac{t}{290,000})}}{s + 1/290,000} \right] \right\} \end{aligned} \quad (\text{B-9})$$

in which s' is the Laplacian variable corresponding to the time $t' = t/10$ and s'' is that corresponding to the time $t'' = t/(t_s + 10)$. In addition

$$E_p(s) = \int_0^\infty e^{-\xi} \xi^{-s} d\xi \quad (\text{B-10})$$

It is now necessary to take the inverse of Eq.(B-8) in order to transfer the equation back into the time domain and find the temperature distribution.

Although this is straight forward theoretically, practically the fractional orders in Eq.(B-9) present difficulty. Therefore, a satisfactory solution was attempted by resorting to the use of numerical techniques.

Richtmyer (18) presents a discussion of the methods available and their limitations. Written in finite difference form, Eq.(B-1) becomes

$$\frac{\psi(\theta_{i,n+1}'' - 2\theta_{i,n}'' + \theta_{i,n-1}'') + (1-\psi)(\theta_{i,n+1}' - 2\theta_{i,n}' + \theta_{i,n-1}')}{(\Delta x)^2} + \frac{\mu I[n+1]\Delta t}{k} e^{-\mu j \Delta x} \quad (\text{B-11})$$

$$= \frac{1}{\mathcal{H}} \left[\frac{\theta_{i,n+1}'' - \theta_{i,n}'}{\Delta t} \right]$$

where ψ is a real constant $0 \leq \psi \leq 1$. For a known temperature distribution at time $n\Delta t$, this system may be solved for the $(n+1)$ st time increment at any given $x = j\Delta x$ for each of J increments. The constant ψ is chosen as the value which eliminates first order errors and still retains absolute stability. This value is

$$\psi = \frac{1}{2} - \frac{(\Delta x)^2}{12\mathcal{H}\Delta t} \quad (\text{B-12})$$

The boundary condition at the inside face is

$$-k \frac{\partial \theta}{\partial x}_{x=0} = 0 \quad (\text{B-13})$$

which would be written in finite difference form as

$$-k \left[\frac{\theta_1^n - \theta_0^n}{\Delta x} \right] = 0 \quad (\text{B-14})$$

However, Eq.(B-13) is really a symmetry boundary condition and it is more correct to write this equation in finite difference form as

$$-k \left[\frac{\theta_1^n - \theta_{-1}^n}{\Delta x} \right] \quad (\text{B-15})$$

The other spatial boundary condition is

$$-k \left[\frac{\theta_J^n - \theta_{J-1}^n}{\Delta x} \right] = h_r \theta_J^n \quad (\text{B-16})$$

The initial condition is

$$\theta_j^0 = \theta(j \Delta x) \quad (\text{B-17})$$

at the time of shutdown. Since the distribution at time $n \Delta t$ is known, it is possible to use Eq.(B-11) to set up a series of equations which may be solved for the temperature distribution at time $(n+1) \Delta t$. Using ten increments, this may be put in matrix form as written symbolically below

$$\begin{aligned} \left[\frac{(\Delta x)^2}{\alpha \Delta t} + 2\psi \right] \theta_j^{n+1} - 2\psi \theta_{j+1}^{n+1} &= \Gamma_j \quad j=1 \\ \left[\frac{(\Delta x)^2}{\alpha \Delta t} + 2\psi \right] \theta_j^{n+1} - \psi(\theta_{j-1}^{n+1} + \theta_{j+1}^{n+1}) &= \Gamma_j \quad j=2-9 \\ \left[\frac{(\Delta x)^2}{\alpha \Delta t} + \psi \left(2 - \frac{1}{(1 + \frac{h_r \Delta x}{k})} \right) \right] - \psi \theta_{j-1}^{n+1} &= \Gamma_j \quad j=10 \end{aligned} \quad (\text{B-18})$$

It is also necessary to express the thermal stress distribution in a free plate by means of some numerical technique, since an analytical expression for the temperature distribution is not available. This may be accomplished by expanding Eq.(9) through the use of Simpson's rule. Thus, it is found that when the plate is divided into ten equal increments, there results

$$\int_0^L \theta dx = (\theta_1 + 4\theta_2 + 2\theta_3 + 4\theta_4 + \dots + 2\theta_9 + 4\theta_{10} + \theta_{11})\left(\frac{L}{30}\right) \quad (B-19)$$

and

$$\begin{aligned} \int_0^L (x - L/2) \theta dx = & \left[\theta_1 \left(-\frac{L}{2}\right) + 4\theta_2 (\Delta x - L/2) + 2\theta_3 (2\Delta x - L/2) + 4\theta_4 (3\Delta x - L/2) \right. \\ & \left. + \dots + 4\theta_8 (7\Delta x - L/2) + 2\theta_9 (8\Delta x - L/2) + 4\theta_{10} (9\Delta x - L/2) + \theta_{11} \left(\frac{L}{2}\right) \right] \end{aligned} \quad (B-20)$$

whence, the final expression for the thermal stress in a free plate at each of the j mesh points becomes

$$\begin{aligned} \sigma_y = \sigma_z = -E\epsilon''_y + \frac{1}{30} (\theta_1 + 4\theta_2 + 2\theta_3 + 4\theta_4 + 2\theta_5 + 4\theta_6 + 2\theta_7 + 4\theta_8 + 2\theta_9 + 4\theta_{10} + \theta_{11}) \\ + \frac{0.4}{L^2} \left[j\Delta x - \frac{L}{2} \right] \left[(\theta_{11} - \theta_1) \left(\frac{L}{2}\right) + 4\theta_2 (\Delta x - L/2) + 2\theta_3 (2\Delta x - L/2) \right. \\ \left. + 4\theta_4 (3\Delta x - L/2) + 2\theta_5 (4\Delta x - L/2) + 2\theta_7 (6\Delta x - L/2) + 4\theta_8 (7\Delta x - L/2) \right. \\ \left. + 2\theta_9 (8\Delta x - L/2) + 4\theta_{10} (9\Delta x - L/2) \right] \end{aligned} \quad (B-21)$$

APPENDIX C

Derivation of the Temperature Distribution in Parallel Plates with a Constant Gamma Photon Flux, Insulation at the Inner Face, Gas Flow Between the Plates and Radiation Heat Loss from the Outside Face

The inside plate presents essentially the same problem as was solved in Appendix A. However, in this case the heat loss from the outer face of the plate is by convection to a gas flowing between the two plates. This boundary condition is then

$$-k_1 \left(\frac{\partial \theta_1}{\partial x_1} \right)_{x_1=L_1} = h_1 \theta_1 \Big|_{x_1=L_1} \quad (C-1)$$

where the subscript one is used to denote those quantities particular to the first plate. Similarly, the subscript two will be used for the second plate.

The solution of Eq.(A-1) using the boundary conditions given by Eq.(A-6) and (C-1), and the initial condition given by Eq.(A-10) is

$$\theta_1 = \frac{I_1}{k_1 \mu_1} (e^{-\mu_1 L_1} - e^{-\mu_1 x_1}) + \frac{I_1}{k_1} (L_1 - x_1) + \frac{I_1}{h_1} (1 - e^{-\mu_1 L_1}) \quad (C-2)$$

$$- \sum_{n=1}^{\infty} \frac{2 I_1 \mu_n \cos \lambda_n x_1}{k_1 \lambda_n^2 (\lambda_n^2 + \mu_1^2)} \left[\frac{\mu_1 (k_1 \lambda_n^2 + h_1) + \lambda_n (h_1 k_1 - k_1^2 \mu_1) e^{-\mu_1 L_1} \sec \lambda_n L_1}{k_1^2 \lambda_n^2 L_1 + h_1^2 L_1 + h_1 k_1} \right] e^{-\lambda_n^2 x_1} e^{-\lambda_n^2 t}$$

In the case of the second plate, the flux incident on the inside face is given by

$$I_2 = I_1 e^{-\mu_1 L_1} \quad (C-3)$$

The temperature distribution is again expressed by the partial differential

equation

$$\frac{\partial^2 \theta_2}{\partial x_2^2} + \frac{\mu_2 I_2 e^{-\mu_2 x_2}}{k_2} = \frac{1}{\alpha_2} \frac{\partial \theta_2}{\partial t} \quad (C-4)$$

The assumption is also again made that this equation can be separated into the form

$$\theta_2 = X_2(x_2) + \tau_2(x_2, t) \quad (C-5)$$

Operating on Eq.(C-5) with (C-4) and then separating the resultant into two equations in X_2 and τ_2 and setting each of these equal to zero again leads to

$$\frac{\partial^2 X_2}{\partial x_2^2} + \frac{\mu_2 I_2 e^{-\mu_2 x_2}}{k_2} = 0 \quad (C-6)$$

$$\frac{\partial^2 \tau_2}{\partial x_2^2} = \frac{1}{\alpha_2} \frac{\partial \tau_2}{\partial t} \quad (C-7)$$

These equations are solved in the same manner as was shown in Appendix A, and yield the equations

$$\tau_2 = (C_1 \sin \lambda_2 x_2 + C_2 \cos \lambda_2 x_2) e^{-\alpha_2 \lambda_2 t} \quad (C-8)$$

$$X_2 = -\frac{I_2 e^{-\mu_2 x_2}}{k_2 \mu_2} + C_3 x_2 + C_4 \quad (C-9)$$

The boundary conditions for the second plate are

$$-k_2 \left. \frac{\partial \theta_2}{\partial x_2} \right|_{x_2=0} = h_r \theta_2 \Big|_{x_2=0} \quad (C-10)$$

$$-k_2 \left. \frac{\partial \theta_2}{\partial x_2} \right|_{x_2=L_2} = h_r \theta_2 \Big|_{x_2=L_2} \quad (C-11)$$

where h_r is again given by Eq.(A-13).

For Eq.(C-8) the transformed boundary conditions are

$$-k_2 \left. \frac{\partial \tau_2}{\partial x_2} \right|_{x_2=0} = h_2 \tau_2 \Big|_{x_2=0} \quad (C-12)$$

$$-k_2 \left. \frac{\partial \tau_2}{\partial x_2} \right|_{x_2=L_2} = h_r \tau_2 \Big|_{x_2=L_2} \quad (C-13)$$

For Eq.(C-9) they are

$$-k_2 \left. \frac{\partial X_2}{\partial x_2} \right|_{x_2=0} = h_2 X_2 \Big|_{x_2=0} \quad (C-14)$$

$$-k_2 \left. \frac{\partial X_2}{\partial x_2} \right|_{x_2=L_2} = h_r X_2 \Big|_{x_2=L_2} \quad (C-15)$$

The initial condition is

$$\theta_2 \Big|_{t=0} = 0 \quad (C-16)$$

which now becomes

$$\tau_2 = -X_2 \quad (C-17)$$

Applying Eq.(C-14) to (C-9) gives

$$-k_2 \left(\frac{I_2}{k_2} + C_3 \right) = h_2 \left(-\frac{I_2}{k_2 \mu_2} + C_4 \right) \quad (C-18)$$

And applying Eq.(C-15) to (C-9) gives

$$-k_2 \left(\frac{I_2 e^{-\mu_2 L_2}}{k_2} + C_3 \right) = h_r \left(-\frac{I_2 e^{-\mu_2 L_2}}{k_2 \mu_2} + C_3 L_2 + C_4 \right) \quad (C-19)$$

These last two equations may be solved simultaneously to yield

$$C_3 = \frac{h_r h_2 \frac{I_2}{k_2 \mu_2} (1 - e^{-\mu_2 L_2}) + I_2 (h_2 e^{-\mu_2 L_2} + h_r)}{k_2 h_r + k_2 h_2 + h_2 h_r L_2} \quad (C-20)$$

$$C_1 = I_2 e^{-\mu_2 L_2} \left(\frac{1}{k_2 \mu_2} + \frac{1}{h_r} \right) + \left[\frac{h_2 h_r \frac{I_2}{k_2 \mu_2} (1 - e^{-\mu_2 L_2}) + I_2 (h_2 e^{-\mu_2 L_2} + h_r)}{k_2 h_r + k_2 h_2 + h_2 h_r L_2} \right] \left[\frac{k_2}{h_2} + L_2 \right] \quad (C-21)$$

This reveals the steady state solution to be

$$X_2 = -\frac{I_2 e^{-\mu_2 x_2}}{k_2 \mu_2} + I_2 e^{-\mu_2 L_2} \left(\frac{1}{k_2 \mu_2} - \frac{1}{h_r} \right) + \left[\frac{h_r h_2 \frac{I_2}{k_2 \mu_2} (1 - e^{-\mu_2 L_2}) + I_2 (h_2 e^{-\mu_2 L_2} + h_r)}{k_2 h_r + k_2 h_2 + h_2 h_r L_2} \right] \left[L_2 - x_2 + \frac{k_2}{h_r} \right] \quad (C-22)$$

Then substituting Eq.(C-8) into (C-12) gives

$$C_1 = \frac{h_2}{\lambda_2} C_2 \quad (C-23)$$

And operating on Eq.(C-8) with (C-13) and making the substitution established in Eq.(C-23) there results the transcendental equation

$$\tan \lambda_{n2} L_2 = \frac{k_2 \lambda_{n2} (h_r + h_2)}{k_2^2 \lambda_{n2}^2 - h_r h_2} \quad (C-24)$$

where λ_{n2} represents the countable infinity of roots to this equation.

Carslaw and Jaeger (4) show that if the steady state solution, $X = f(x_2)$, can be developed in an infinite series such that

$$f(x_2) = \sum_{n=1}^{\infty} C_{2n} X_{n2} \quad (C-25)$$

where X_{n2} is of the same form as the spatially dependent part of τ_2 , then the solution to τ_2 is given by

$$\tau_2 = \sum_{n=1}^{\infty} C_{2n} X_{n2} e^{-x_2 \lambda_{n2}} \quad (C-26)$$

where C_{2n} is found from the orthogonal properties, and is given by

$$C_{2n} = \frac{\int_0^{L_2} f(x_2) X_{n2} dx_2}{\int_0^{L_2} X_{n2} dx_2} \quad (C-27)$$

and the denominator remains to be evaluated.

From the solution for the spatially dependent part of τ_2

$$\frac{d^2 X_{n2}}{dx_2^2} + \lambda_{n2}^2 X_{n2} = 0 \quad (C-28)$$

This is first put into the form

$$\lambda_{n2}^2 \int_0^{L_2} X_{n2}^2 dx_2 = - \int_0^{L_2} X_{n2} \frac{d^2 X_{n2}}{dx_2^2} dx_2 \quad (C-29)$$

from which this is evaluated as

$$\lambda_{n2}^2 \int_0^{L_2} X_{n2}^2 dx_2 = - \left[X_{n2} \frac{dX_{n2}}{dx_2} \right] \Big|_{x_2=0}^{x_2=L_2} + \int_0^{L_2} \left(\frac{dX_{n2}}{dx_2} \right)^2 dx_2 \quad (C-30)$$

Substituting Eq.(C-23) into the spatially dependent part of (C-8) and multiplying both sides of the equation by λ_{n2} , results in

$$\lambda_{n2} X_{n2} = \frac{h_2}{k_2} \cos \lambda_{n2} x_2 + \lambda_{n2} \sin \lambda_{n2} x_2 \quad (C-31)$$

Taking the derivative of X_{n2} yields

$$\frac{dX_{n2}}{dx_2} = - \frac{h_2}{k_2} \sin \lambda_{n2} x_2 + \lambda_{n2} \sin \lambda_{n2} x_2 \quad (C-32)$$

Squaring the above two equations, there results immediately

$$\lambda_{n2}^2 X_{n2}^2 + \left(\frac{dX_{n2}}{dx_2} \right)^2 = \lambda_{n2}^2 + \left(\frac{h_2}{k_2} \right)^2 \quad (C-33)$$

Operating on both sides of this equation by $\int_0^{L_2} dx_2$ gives

$$\lambda_{n2}^2 \int_0^{L_2} X_{n2}^2 dx_2 + \int_0^{L_2} \left(\frac{dX_{n2}}{dx_2} \right)^2 dx_2 = \left[\lambda_{n2}^2 + \left(\frac{h_2}{k_2} \right)^2 \right] L_2 \quad (C-34)$$

Adding Eq.(C-30) to (C-34) produces

$$2\lambda_{n_2}^2 \int_0^{L_2} X_{n_2}^2 dx_2 = L \left[\lambda_{n_2}^2 + \left(\frac{h_2}{k_2} \right)^2 \right] - \left[X_{n_2} \frac{dX_{n_2}}{dx_2} \right] \Big|_{x_2=0}^{x_2=L_2} \quad (C-35)$$

Eq.(C-14) may be rearranged to

$$\frac{dX_{n_2}}{dx_2} = \frac{h_2}{k_2} X_{n_2} \quad (C-36)$$

and then

$$\left(\frac{dX_{n_2}}{dx_2} \right)^2 = \left(\frac{h_2}{k_2} \right)^2 X_{n_2}^2 \quad (C-37)$$

which shows, from Eq.(C-33), that

$$X_{n_2}^2 = 1 \quad (C-38)$$

and also by substitution from (C-36), at $x_2 = 0$

$$\left[X_{n_2} \frac{dX_{n_2}}{dx_2} \right] = \frac{h_2}{k_2} \quad (C-39)$$

Similarly, Eq.(C-15) becomes

$$\frac{dX_{n_2}}{dx_2} = -\frac{h_2}{k_2} X_{n_2} \quad (C-40)$$

from which

$$\left(\frac{dX_{n_2}}{dx_2} \right)^2 = \left(\frac{h_2}{k_2} \right)^2 X_{n_2}^2 \quad (C-41)$$

Substituting this into Eq.(C-33) shows that

$$X_{n_2} = \frac{\lambda_{n_2}^2 + \left(\frac{h_2}{k_2} \right)^2}{\lambda_{n_2}^2 + \left(\frac{h_1}{k_1} \right)^2} = \frac{\lambda_{n_2}^2 k_2^2 + h_2^2}{\lambda_{n_2}^2 k_1^2 + h_1^2} \quad (C-42)$$

Then substituting first from Eq.(C-40) and then from (C-42), there results

at $x_2 = L_2$

$$\left[X_{n_2} \frac{dX_{n_2}}{dx_2} \right] = - \left(\frac{h_r}{k_2} \right) \left(\frac{\lambda_{n_2}^2 k_2^2 + h_r^2}{\lambda_{n_2}^2 k_2^2 + h_r^2} \right) \quad (C-43)$$

Consequently,

$$\left[X_{n_2} \frac{dX_{n_2}}{dx_2} \right] \Big|_{x_2=0}^{x_2=L_2} = - \left[\left(\frac{h_r}{k_2} \right) \left(\frac{\lambda_{n_2}^2 k_2^2 + h_r^2}{\lambda_{n_2}^2 k_2^2 + h_r^2} \right) + \frac{h_r}{k_2} \right] \quad (C-44)$$

Then from Eq.(C-35), there results

$$\int_0^{L_2} X_{n_2}^2 dx_2 = \frac{1}{2\lambda_{n_2}} \left[\frac{L_2}{k_2} (\lambda_{n_2}^2 k_2^2 + h_r^2) + \frac{(\lambda_{n_2}^2 k_2^2 + h_r^2)(h_r)}{k_2(\lambda_{n_2}^2 k_2^2 + h_r^2)} + \frac{h_r}{k_2} \right] \quad (C-45)$$

For the evaluation of the numerator of Eq.(C-27), Eq.(C-22) is rearranged to the form

$$f(x_2) = X_2 = R_1 e^{-\mu_2 x_2} + R_2 x_2 + R_3 \quad (C-46)$$

where

$$\left. \begin{aligned} R_1 &= - \frac{I_2}{k_2 \mu_2} \\ R_2 &= - \left[\frac{h_2 h_r \frac{I_2}{k_2 \mu_2} (1 - e^{-\mu_2 L_2}) + I_2 (h_2 e^{-\mu_2 L_2} + h_r)}{k_2 h_r + k_2 h_2 + h_2 h_r L_2} \right] \\ R_3 &= I_2 e^{-\mu_2 L_2} \left(\frac{1}{k_2 \mu_2} - \frac{1}{h_r} \right) - R_2 \left(\frac{k_2}{h_r} + L_2 \right) \end{aligned} \right\} \quad (C-47)$$

Performing the indicated integration on Eq.(C-27) yields

$$\begin{aligned}
& \int_0^{L_2} \left(\frac{h_2}{k_2 \lambda_{n_2}} \cos \lambda_{n_2} x_2 + \sin \lambda_{n_2} x_2 \right) \left(R_1 e^{-\mu_2 x_2} + R_2 x_2 + R_3 \right) dx_2 \\
&= \frac{R_2}{\lambda_{n_2}^2} \left\{ \left(\cos \lambda_{n_2} x_2 + \lambda_{n_2} x_2 \sin \lambda_{n_2} x_2 \right) - \frac{h_2}{k_2 \lambda_{n_2}} \left(\lambda_{n_2} x_2 \cos \lambda_{n_2} x_2 - \sin \lambda_{n_2} x_2 \right) \right\} \Bigg|_{x_2=0}^{x_2=L_2} \\
&+ R_1 \left\{ \frac{e^{-\mu_2 x_2} (\lambda_{n_2} \sin \lambda_{n_2} x_2 - \mu_2 \cos \lambda_{n_2} x_2)}{(\lambda_{n_2}^2 + \mu_2^2)} \right. \\
&+ \left. \left[\frac{e^{-\mu_2 x_2} (-\mu_2 \sin \lambda_{n_2} x_2 - \lambda_{n_2} \cos \lambda_{n_2} x_2)}{(\lambda_{n_2}^2 + \mu_2^2)} \right] \right\} \Bigg|_{x_2=0}^{x_2=L_2} \\
&+ \frac{R_3}{\lambda_{n_2}} \left(-\frac{h_2}{k_2 \lambda_{n_2}} \cos \lambda_{n_2} x_2 + \sin \lambda_{n_2} x_2 \right) \Bigg|_{x_2=0}^{x_2=L_2}
\end{aligned} \tag{C-48}$$

Which may be separated and written as

$$\begin{aligned}
& \int_0^{L_2} f(x_2) X_{n_2} dx_2 = \cos \lambda_{n_2} L_2 \left[\frac{R_2}{\lambda_{n_2}} - \frac{R_3 h_2}{k_2 \lambda_{n_2}^2} - \frac{R_2 h_2 L_2}{\lambda_{n_2}^2 k_2} - \frac{R_1 e^{-\mu_2 L_2}}{(\lambda_{n_2}^2 + \mu_2^2)} \left(\mu_2 + \frac{h_2}{k_2} \right) \right] \\
&+ \sin \lambda_{n_2} L_2 \left[\frac{1}{\lambda_{n_2}} (R_3 + R_2 L_2) - \frac{R_2 h_2}{k_2 \lambda_{n_2}^2} + \frac{R_1 e^{-\mu_2 L_2}}{(\lambda_{n_2}^2 + \mu_2^2)} \left(\lambda_{n_2} - \frac{\mu_2 h_2}{k_2 \lambda_{n_2}} \right) \right] \tag{C-49} \\
&+ \frac{R_3 h_2}{k_2 \lambda_{n_2}^2} - \frac{R_2}{\lambda_{n_2}^2} + \frac{R_1 \mu_2}{(\lambda_{n_2}^2 + \mu_2^2)} + \frac{R_1 \mu_2}{k_2 (\lambda_{n_2}^2 + \mu_2^2)}
\end{aligned}$$

Then substituting (C-27) into (C-26) to solve for τ_2 , there results

$$\theta_2 = R_1 e^{-\mu_2 x_2} + R_2 x_2 + R_3$$

$$+ \sum_{n=1}^{\infty} \left[\left\{ \cos \lambda_{n2} L_2 \left[-\frac{R_3 h_2}{k_2 \lambda_{n2}} + \frac{R_2}{\lambda_{n2}^2} \left(1 - \frac{h_2 L_2}{k_2} \right) - \frac{R_1 e^{-\mu_2 L_2}}{(\lambda_{n2}^2 + \mu_2^2)} \left(\mu_2 + \frac{h_2}{k_2} \right) \right] \right. \right. \\ \left. \left. + \sin \lambda_{n2} L_2 \left[\frac{R_3}{\lambda_{n2}} + R_2 \left(\frac{L_2}{\lambda_{n2}} - \frac{h_2}{k_2 \lambda_{n2}^3} \right) + \frac{R_1 e^{-\mu_2 L_2}}{(\lambda_{n2}^2 + \mu_2^2)} \left(\lambda_{n2} - \frac{\mu_2 h_2}{k_2 \lambda_{n2}} \right) \right] \right\} \right] \quad (C-50)$$

$$+ \frac{R_1 \left(\mu_2 + \frac{h_2}{k_2} \right)}{(\lambda_{n2}^2 + \mu_2^2)} + \frac{R_3 h_2}{k_2 \lambda_{n2}^2} - \frac{R_2}{\lambda_{n2}^2} \left\{ \frac{h_2}{k_2 \lambda_{n2}^2} \sin \lambda_{n2} x_2 + \cos \lambda_{n2} x_2 \right\}$$

$$\left\{ \left[\frac{L_2}{k_2^2} (\lambda_{n2}^2 k_2^2 + h_2) + \frac{(\lambda_{n2}^2 k_2^2 + h_2)(h_2)}{k_2 (\lambda_{n2}^2 k_2^2 + h_2)} + \frac{h_2}{k_2} \right] \frac{1}{2 \lambda_{n2}} \right\}$$

Considering the case where $h_2 = 0$, this solution should reduce to the solution obtained in Appendix A. This is found to be the case and is, in part, a verification of the present solution.

APPENDIX D

Description and Explanation of the IBM 1620 FORTRAN Program to Find the Temperature Distribution and the Thermal Stresses in a Plate with Insulation at One Face and Radiative Heat Loss at the Other Face when Subjected to a Constant Gamma Photon Flux at the First Face

The equation for the temperature distribution which must be solved is

$$\theta = \frac{I}{k\mu} (e^{-\mu L} - e^{-\mu x}) + \frac{I}{k} (L - x) + \frac{I}{h_r} (1 - e^{-\mu L})$$

$$- \sum_{n=1}^{\infty} \frac{2I\mu \cos \lambda_n x}{k\lambda_n^2 (\lambda_n^2 + \mu^2)} \left[\frac{\mu (h_r^2 + k^2 \lambda_n^2) + \lambda_n^2 (k h_r - k^2 \mu) e^{-\mu L} \sec \lambda_n L}{k^2 \lambda_n^2 L + h_r^2 L + k h_r} \right] e^{-\lambda_n^2 x} \quad (D-1)$$

In order to find a numerical solution to this equation, it is first necessary to complete two iterations. The first is for λ_n which is found from the transcendental equation

$$\lambda_n \tan \lambda_n L = \frac{h_r}{k} \quad (D-2)$$

It is also necessary to find the correct value for h_r , which is a function of the surface temperature and is given by

$$h_r = \frac{\epsilon \sigma (T^4 - T_o^4)}{T - T_o} \quad (D-3)$$

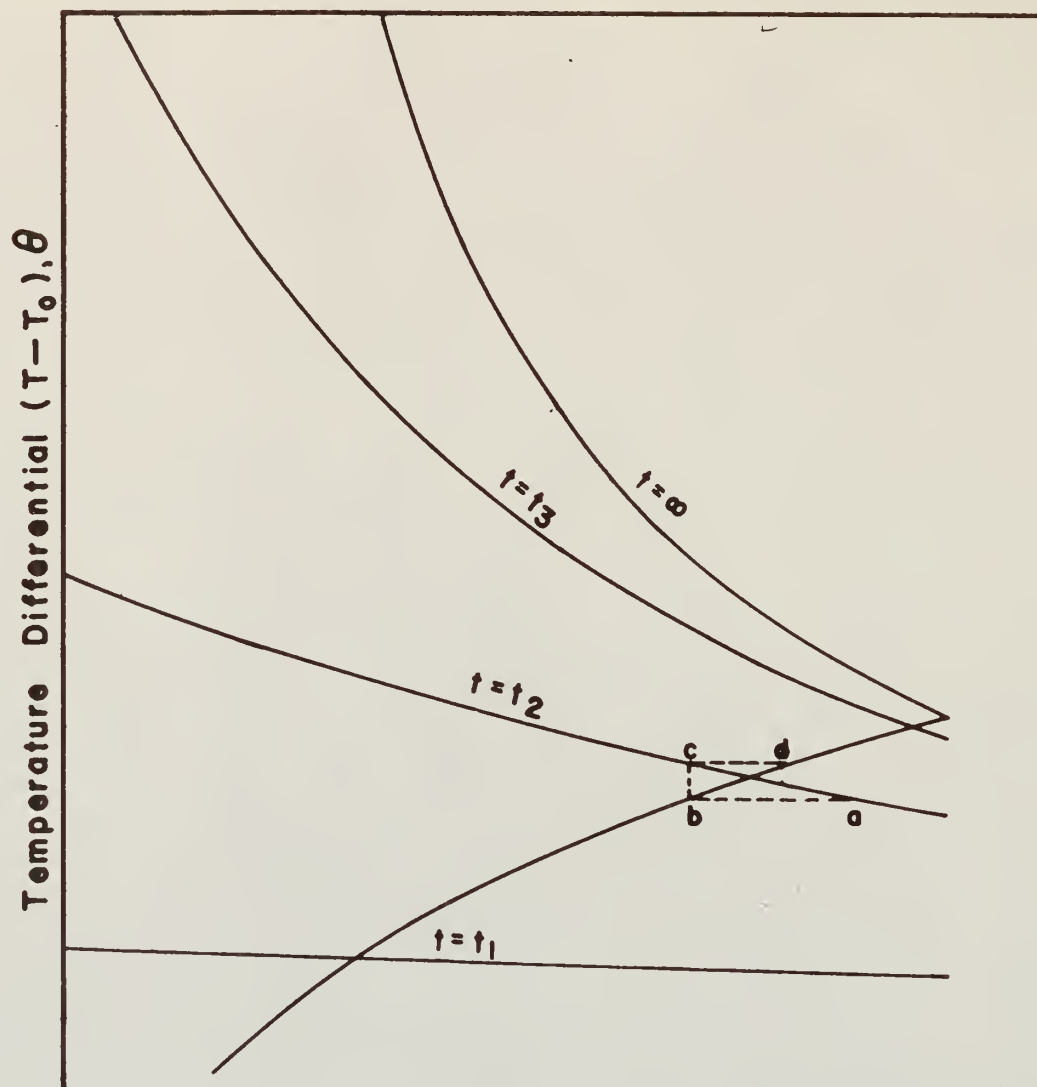
as well as by Eq.(D-1) above.

It is possible to carry out these two iterations simultaneously. A value for h_r is first assumed, from which each of the λ 's may be found. For the physical cases considered here, it was found that the first two solutions to Eq.(D-2) were sufficient to give accurate answers. Using these values, θ may then be calculated from Eq.(D-1). The temperature obtained is used in Eq.(D-3), and this calculated value for h_r is compared with the

assumed value. Before a reasonable number can be chosen for the next trial, however, it is advisable to further investigate Eq.(D-1) and (D-3). Figure 17 gives a qualitative description of these two equations. It can be seen that if point a is the first approximation, calculation with Eq.(D-1) will bring the system to point b. This value of h_r can then be used as the next estimate from which a new temperature is found, as well as a new h_r (point d). It becomes rather obvious from Fig. 17 that the continuation of this process would take considerable more time to find a reasonably close estimate for the true h_r as time increased and the temperature rose. However, the iteration process is easily amended at this point to shorten the time necessary to obtain a satisfactory answer. The graph used is that shown in Fig. 18.

The value for h_r is the assumed value, and Δh_r is the difference between this assumed value and the value finally calculated from Eq.(D-3). Point a is the first assumed value and the difference between a and b is Δh_r . Point c is the second assumed value and the second Δh_r is from c to d. Point e denotes the true value of h_r . A linear approximation can be used to estimate the point at which the true h_r exists ($\Delta h_r = 0$). This point, f, is then used as the first assumption in the next set of trials which proceed in exactly the same manner. The convergence to five significant figures, which was deemed sufficient for these calculations, is quite rapid.

When the best value of h_r is found, it is possible to calculate the temperature distribution and the thermal stress distribution in the plate. Since many of the "constants" used in these equations are truly temperature dependent, it is necessary to adjust these with each iteration. A linear approximation for these constants was found (2) and the average temperature



Equivalent Convective Radiation Coefficient, h_r
 FIG. 17. SKETCH OF h_r vs Θ

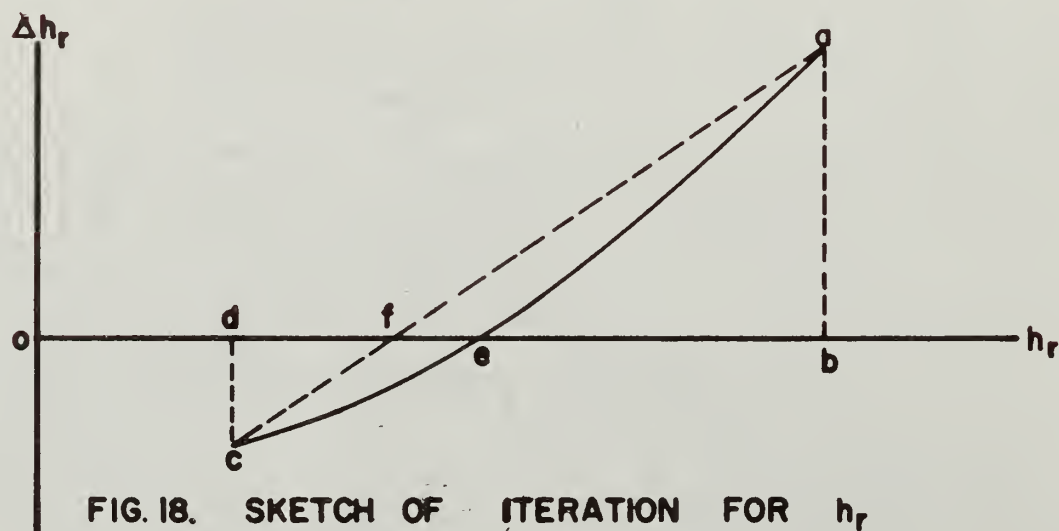


FIG. 18. SKETCH OF ITERATION FOR h_r

of the plate was used in the adjustment.

In calculating the thermal stresses, it was found that the use of floating point arithmetic in the FORTRAN program caused a loss of significant figures when Eq.(9) was used, because of the subtraction of almost equal numbers which were generated. Consequently, the following approach was taken to overcome this difficulty.

The thermal stress equation for a free plate is

$$\sigma_y = \sigma_z = \frac{\alpha E}{1-\nu} \left\{ \frac{I}{\lambda \mu} \left[(e^{-\mu L} - 1) \left(\frac{1}{\mu L} + \frac{12(\kappa - L/2)}{L(\mu L)^2} \right) + e^{-\mu x} + \frac{6(\kappa - L/2)(1 + e^{-\mu L})}{L(\mu L)} \right] \right. \\ \left. + \sum_{n=1}^{\infty} G_n \left[\cos \lambda_n x - \frac{\sin \lambda_n L}{\lambda_n L} - \frac{12(\kappa - L/2)}{L^3} \left(\frac{L \sin \lambda_n L}{2 \lambda_n} + \frac{\cos \lambda_n L - 1}{\lambda_n^2} \right) \right] \right\} \quad (D-4)$$

Consider first, the transient portion of this expression. The first two terms within the square brackets can be expanded, using a Maclaurin series, to yield

$$\cos \lambda_n L - \frac{\sin \lambda_n L}{\lambda_n L} = (\lambda_n L)^2 \left(\frac{1}{3!} - \frac{y^2}{2!} \right) - (\lambda_n L)^4 \left(\frac{1}{5!} - \frac{y^4}{4!} \right) \\ + (\lambda_n L)^6 \left(\frac{1}{7!} - \frac{y^6}{6!} \right) - (\lambda_n L)^8 \left(\frac{1}{9!} - \frac{y^8}{8!} \right) + \dots \quad (D-5)$$

where $y = x/L$. Four terms here were sufficient for the systems under consideration. The latter part of the transient portion of the equation is expanded in the same manner. After some manipulation, this becomes

$$- \frac{12(\kappa - L/2)}{L^3} \left(\frac{L \sin \lambda_n L}{2 \lambda_n} + \frac{\cos \lambda_n L - 1}{\lambda_n^2} \right) \\ = (y - 1/2)(\lambda_n L)^2 \left(\frac{1}{2} - \frac{(\lambda_n L)^2}{30} + \frac{(\lambda_n L)^4}{1120} - \frac{(\lambda_n L)^6}{75,600} + \dots \right) \quad (D-6)$$

Now considering the steady state portion of Eq.(D-4), the quantity within

the square brackets may be rearranged to

$$\begin{aligned} & (e^{-\mu L} - 1) \left(\frac{1}{\mu L} + \frac{12(x - L/2)}{L(\mu L)^2} \right) + e^{-\mu x} + \frac{6(x - L/2)(1 + e^{-\mu L})}{L(\mu L)} \\ & = \frac{(y - 1/2)}{\mu L} \left[6(1 + e^{-\mu L}) + \frac{12}{\mu L}(e^{-\mu L} - 1) \right] + \frac{e^{-\mu L} - 1}{\mu L} + e^{-\mu x} \end{aligned} \quad (D-7)$$

These last two terms are expanded to

$$\frac{e^{-\mu L} - 1}{\mu L} + e^{-\mu x} = \frac{\mu}{2!}(L - 2x) - \frac{\mu^2}{3!}(L^2 - 3x^2) + \frac{\mu^3}{4!}(L^3 - 4x^3) - \dots \quad (D-8)$$

the general expression for which is

$$\frac{e^{-\mu L} - 1}{\mu L} + e^{-\mu x} = (-1)^{m+1} \frac{\mu^m}{(m+1)!} (L^m - (m+1)x^m) \quad m = 1, 2, \dots \quad (D-9)$$

The first two terms within the square brackets of Eq.(D-7) yield

$$6(1 + e^{-\mu L}) + \frac{12}{\mu L}(e^{-\mu L} - 1) = (\mu L)^2 \left(\frac{6}{2!} - \frac{12}{3!} \right) - (\mu L)^3 \left(\frac{6}{3!} - \frac{12}{4!} \right) + \dots \quad (D-10)$$

and the general expression is

$$6(1 + e^{-\mu L}) + \frac{12}{\mu L}(e^{-\mu L} - 1) = (\mu L)^2 (-1)^{m+1} \left(\frac{6}{(m+1)!} - \frac{12}{(m+2)!} \right) \quad m = 1, 2, \dots \quad (D-11)$$

Whence the final stress equation is written as

$$\begin{aligned} \sigma_y = \sigma_z &= \frac{\alpha E}{1-\nu} \left\{ \sum_{m=2}^{\infty} \frac{I}{k\mu} \left[(y - 1/2)(\mu L)^{m+1} (-1)^{m+1} \left(\frac{6}{(m+1)!} - \frac{12}{(m+2)!} \right) + (-1)^{m+1} \frac{(\mu L)^m}{(m+1)!} (1 - (m+1)y^m) \right] \right. \\ &+ \sum_{n=1}^{\infty} G_n (\lambda_n L)^2 \left[\left(\frac{y}{2} - \frac{1}{12} - \frac{y^2}{2} \right) - \frac{(\lambda_n L)^2}{6} \left(\frac{y}{5} - \frac{1}{20} - \frac{y^4}{4} \right) \right. \\ &\left. \left. + \frac{(\lambda_n L)^4}{112} \left(\frac{y}{10} - \frac{1}{36} - \frac{7y^6}{45} \right) - \frac{(\lambda_n L)^6}{3,628,800} (4y + 8 - 90y^8) + \dots \right] \right\} \end{aligned} \quad (D-12)$$

When the final values for h_r and the temperature distribution and thermal stresses have been determined at a given time, it is possible to speed

the iteration for h_r at the succeeding time by using the finite difference approximation for the subsequent temperature and then using the radiation boundary condition to calculate h_r . The final equation is

$$\begin{aligned} T_o'' - T_o' = & \frac{(t_n - t_o)(T_o' - T_o'')}{t_1 - t_o} + \frac{(t_n - t_o)(t_n - t_1)}{t_2 - t_o} \left[\frac{T_o'' - T_o'}{t_2 - t_1} - \frac{T_o' - T_o''}{t_1 - t_o} \right] \\ & + \frac{(t_n - t_o)(t_n - t_1)(t_n - t_2)}{t_3 - t_o} \left\{ \frac{1}{t_3 - t_1} \left[\frac{T_o''' - T_o''}{t_3 - t_2} - \frac{T_o'' - T_o'}{t_2 - t_1} \right] - \frac{1}{t_2 - t_1} \left[\frac{T_o'' - T_o'}{t_2 - t_1} - \frac{T_o' - T_o''}{t_1 - t_o} \right] \right\} \end{aligned} \quad (D-13)$$

where the knowledge of the outside temperature of the plate at four previous times is necessary to satisfy the equation. However, somewhat less accurate approximations can also be found when only two or three of these previous temperatures are known by using either the first two or first three terms of this expression.

The program also includes several sense switches which allow control of the output data. When switch 2 is turned ON during the time of the iteration for h_r , the output data will contain one line with the transient and steady state portions of the free plate thermal stress respectively. This is followed by a second line containing the distance from the origin, temperature, free plate stress, and steady state portion of the temperature. This data is printed for each of the desired number of increments across the plate. The last line contains the constants λ_1 , λ_2 , G_1 and G_2 respectively. If the switch 2 is turned OFF, the line containing the transient and steady state portions of the free plate stress are omitted and the free plate stress in the succeeding line is printed as zero. The remainder of the printed output remains the same.

During the running of the program, switches 1 and 3 are set in the OFF position. When switch 3 is turned ON, the program will complete the data

point it is presently in the process of calculating. After printing the data discussed above, the constants and other data which were used as input, will be punched in whatever form they are presently in use in the program. These cards are then available for use as the first several cards of input data when it is desired to continue the program at a later time. This essentially allows continuous running of the program, even if an interruption should occur. Since the primary purpose of these programs is to find the continuous temperature response of the plate during reactor operation and also during the time after shutdown, switch 1 may be turned ON, and the additional data necessary to the finite difference program will be punched out. Thus this program is both continuous within itself, and also completely compatible with the finite difference program described in Appendix E.

If either switch 3 or switches 1 and 3 are ON, the program will stop when these data cards have been punched out. If it is desired to obtain the punched card output described above, and also to continue the program after obtaining these cards, switch 4 is turned ON and the program proceeds in the normal manner. This switch essentially allows one to obtain continuous punched card output for any number of times at which the reactor might be shut down.

The input data cards to this program contain the following:

1. The coefficient of thermal expansion, the base temperature, an initial estimate of the value \mathcal{O} and the thermal conductivity.
(1 card)
2. The temperature dependent intercept of the emissivity, the number of increments being considered across the thickness of the plate, an initial estimate of the quantity $\alpha E/(1 - \nu)$ and the equivalent gray body convective radiation coefficient. (1 card)

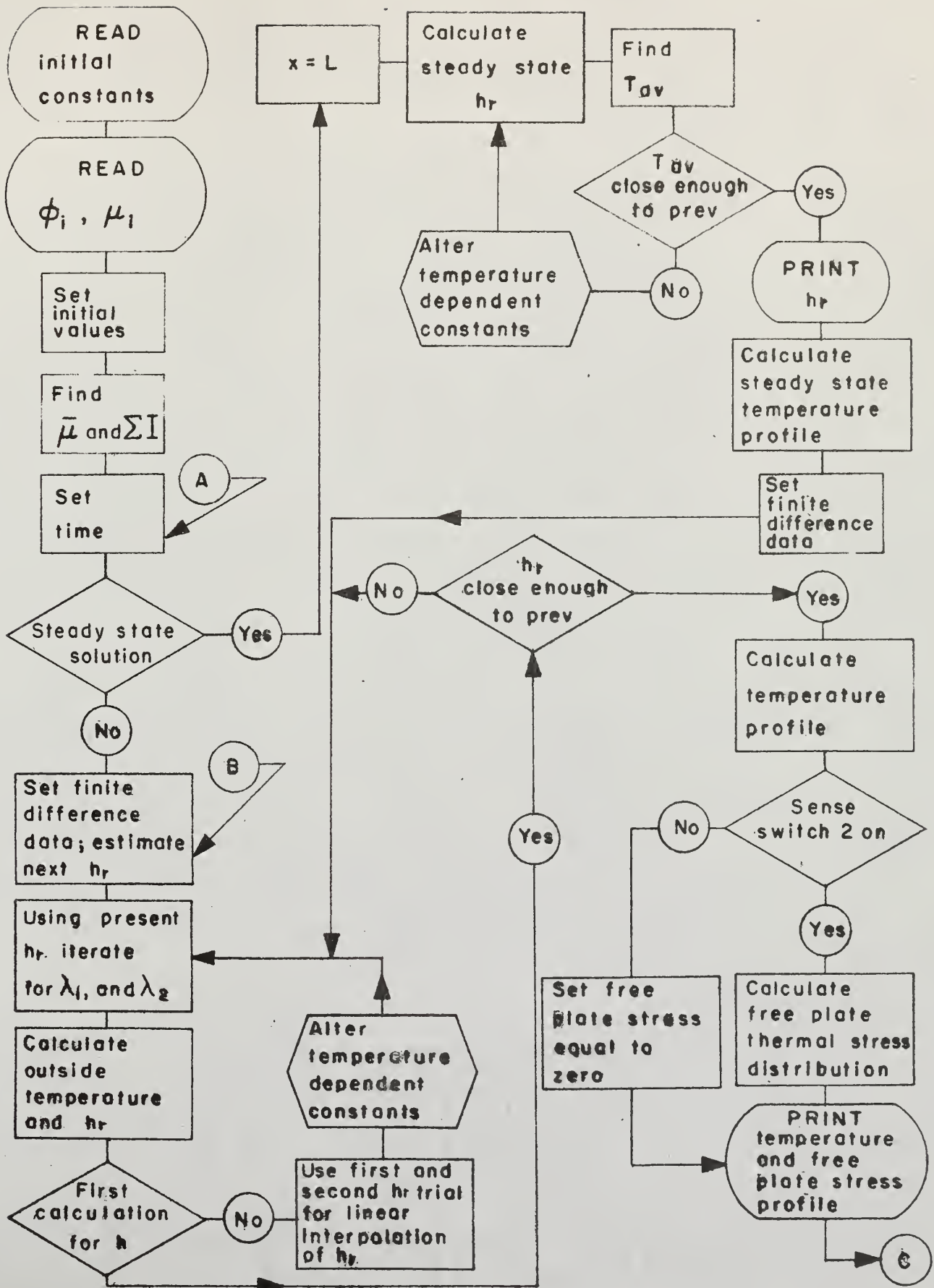
3. The temperature dependent intercepts of the modulus of elasticity, the coefficient of thermal expansion, the thermal conductivity and the density of the material at 40°F. (1 card)
4. The temperature dependent slopes of the modulus of elasticity, the coefficient of thermal expansion, the thermal conductivity and the value of the heat capacity. (1 card)
5. The initial values of the modulus of elasticity, Poisson's ratio, the time of operation at which the calculation is started and the temperature dependent slope of the emissivity. (1 card)
6. The time increment between two successive sets of calculations, an estimate of the value of h_r at steady state and the inside temperature at the time of the previous calculation. (1 card)
7. The four previous outside temperatures and the times at which these occurred. The earliest time considered has the subscript one, and each of the other data points available follows it. If less than four data points are available, the latter data cards for which numbers are not available can be set at any number and data set 8 may be appropriately set to allow the program to note this fact and proceed in the proper manner. (4 cards)
8. The first number is that mentioned above, and is set at the number of previous outside temperatures known. It is assumed that one data point is always known and that in the absence of the correct temperature this value is set at the base temperature at zero time. The number in the card allows the calculation of the steady state temperature distribution before the time dependent solution proceeds if it is set equal to zero. If the number one or any higher

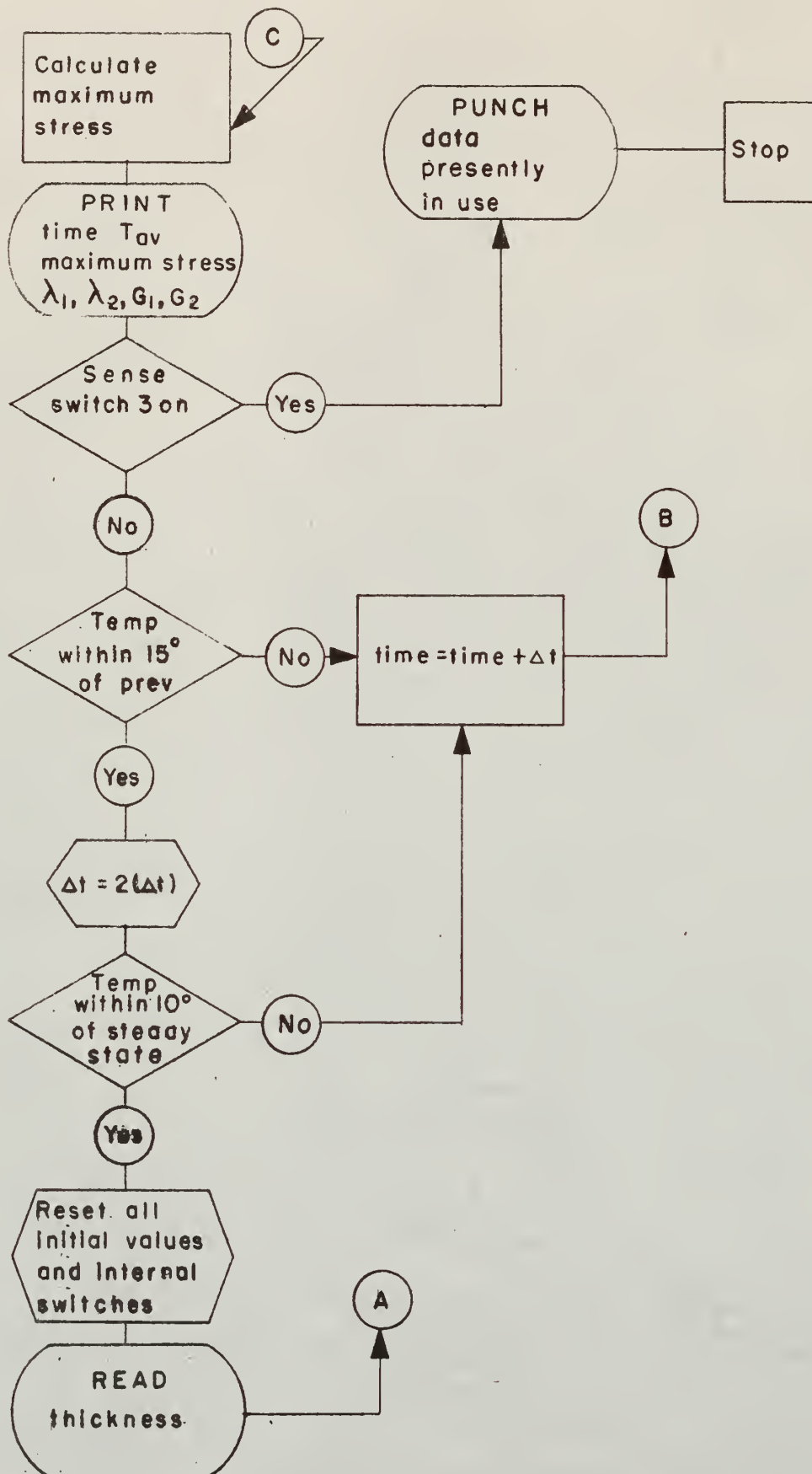
number is inserted, the time dependent solution proceed immediately at whatever time desired. (1 card)

9. The flux and the absorption coefficient for each of the eight energy groups considered. (8 cards)

10. The thickness of the plate being examined. (1 card)

The flow chart for this program and the FORTRAN source deck statements appear on the following pages.





```

1  FORMAT(E15.8,E15.8,E15.8,E15.8)
   DIMENSION FLUX(8),U(8),VALUE(2),ALAM(2),OUT(4),T(4),GRB(2),OLD(11)
250 FORMAT(I2,I2)
   READ1,ALPHA,TO,AKAP,COND
   READ1,EPSB,DIV,STCOF,HR
   READ1,ELSTB,ALPHB,CONDB,DENSB
   READ1,ELSTM,ALPHM,CONDM,CP
   READ1,ELST,V,TIME,EPSM
   READ1,DELT,HRSTD,TEMP
   DO256I=1,4
256 READ1,OUT(I),T(I)
   READ250,M,LL
   DO255I=1,8
255 READ1,FLUX(I),U(I)
   2 READ1,EL
   KK=1
   LLL=0
   KKK=0
   EPS=EPSB
   TBSAV=TO
   SIGMA=1.7123E-09
   PI=3.1415927
   3 TIME=TIME+DELT
   II=11
   PREV=TEMP
   MM=0
   IF(1-LL)300,300,54
   4 N=1
   TRY1=0.1
   TRY2=1.
   5 DIFF1=HR/(COND*TRY1)-(SIN(TRY1*EL)/COS(TRY1*EL))
   DIFF2=HR/(COND*TRY2)-(SIN(TRY2*EL)/COS(TRY2*EL))
   CURVE=(DIFF1-DIFF2)/(TRY1-TRY2)
   TRCPT=DIFF1-CURVE*TRY1
   SET=(-TRCPT/CURVE)
   TEST=SET-TRY2
   IF(TEST)10,40,15
10  TEST=(-TEST)
15  IF((TEST/SET)-1.E-06)40,40,20
20  TRY1=TRY2
   TRY2=SET
   GO TO 5
40  ALAM(N)=SET
   VALUE(N)=SET*EL
   IF(2-N)54,54,42
42  N=N+1
   TRY1=0.1+PI/EL
   TRY2=1.+PI/EL
   GO TO 5
54  X=EL
50  IF(1-LL)58,58,75
58  DO60J=1,2
   GRB(J)=0.

```

```

DO60I=1,8
TRCON=2.*U(I)*FLUX(I)/(COND*(ALAM(J)**2)*((ALAM(J)**2)+(U(I)**2)))
TRN1=U(I)*((HR**2)+((ALAM(J)**2)*(COND**2)))
TRN2=(ALAM(J)**2)*((COND*HR)-(U(I)*(COND**2)))
TRN3=(TRN2)*EXP((-U(I))*EL)/COS(VALUE(J))
TRN=TRN1+TRN3
TRD=HR**2*EL+HR*COND+COND**2*EL*ALAM(J)**2
TREXP=AKAP*(ALAM(J)**2)*TIME
IF(180.-TREXP)61,61,60
60 GRB(J)=GRB(J)+TRCON*TRN*EXP(-TREXP)/TRD
61 SUM=0.
DO63I=1,2
63 SUM=SUM+COS(ALAM(I)*X)*GRB(I)
70 STDY=0.
DO73I=1,8
STD1=FLUX(I)*(EXP(-U(I)*EL)-EXP(-U(I)*X))/(COND*U(I))
STD2=FLUX(I)*(EL-X)/COND
STD3=FLUX(I)*(1.-EXP(-U(I)*EL))/HR
73 STDY=STDY+STD1+STD2+STD3
IF(STDY-SUM)110,110,77
77 STDY=STDY+TO
IF(1-LL)74,74,400
74 TEMP=STDY-SUM
IF(EL-X)100,100,80
75 TPART=0.0
DO76I=1,8
PARTT=FLUX(I)*(1.-EXP(-U(I)*EL))
76 TPART=TPART+PARTT
78 TEMP=(TPART/(EPS*SIGMA))+TO**4)**0.25
GO TO 100
80 IF(SENSE SWITCH 2)81,84
81 SIGST=0.
Y=X/EL
BEND=Y-0.5
DO218I=1,8
RR=1.
SS=2.
PP=6.
STR2=0.
UL=(U(I)*EL)**2
YY=Y*Y
R=2.
200 S=R+1.
P=R+2.
RR=RR*(-R)
SS=SS*(-S)
PP=PP*(-P)
STR11=6./SS-12./PP
STR1=UL*(-YY/RR+BEND*STR11+1./SS)
STR2=STR2+STR1
SAVE=STR2
IF(STR1)201,202,202
201 STR1=(-STR1)

```

```

202 IF(SAVE)203,204,204
203 SAVE=(-SAVE)
204 IF(STR1/SAVE-1.E-06)215,215,213
213 R=R+1.
    UL=UL*U(I)*EL
    YY=YY*Y
    GO TO 200
215 STR3=STR2*FLUX(I)/U(I)
218 SIGST=SIGST+STR3
    SIGST=SIGST*STCOF/COND
220 STSUM=0.
    DO225I=1,2
    ST1=(Y/2.-1./12.-Y**2/2.)
    ST2=(Y/5.-1./20.-Y**4/4.)*VALUE(I)**2/6.
    ST3=(Y/10.-1./36.-7.*Y**6/45.)*VALUE(I)**4/112.
    ST4=(90.*Y**8-8.-4.*Y)*VALUE(I)**6/3628800.
225 STSUM=STSUM+GRB(I)*VALUE(I)**2*(ST1-ST2+ST3+ST4)
    STSUM=STCOF*STSUM
    STRSS=SIGST+STSUM
    PRINT1,STSUM,SIGST
    GO TO 86
84 STRSS=0.
86 PRINT1,X,TEMP,STRSS,STDY
    OLD(II)=TEMP
    II=II-1
    IF(X)85,85,90
85 STRMX=(-STCOF*THETA)
    PRINT1,TIME,TBAR,STRMX
    PRINT1,ALAM(1),ALAM(2),GRB(1),GRB(2)
    IF(SENSE SWITCH 3)91,89
89 IF((TEMP-PREV)-15.)92,92,3
91 PUNCH1,ALPHA,TO,AKAP,COND
    PUNCH1,EPSB,DIV,STCOF,HR
    PUNCH1,ELSTB,ALPHB,CONDB,DENSB
    PUNCH1,ELSTM,ALPHM,CONDM,CP
    PUNCH1,ELST,V,TIME,EPSM
    PUNCH1,DELT,HRSTD,TEMP
    DO97I=1,4
97 PUNCH1,OUT(I),T(I)
    PUNCH250,M,LL
    IF(SENSE SWITCH1)98,999
98 DO94I=1,8
94 PUNCH1,FLUX(I)
    DO96I=1,11
96 PUNCH1,OLD(I)
    IF(SENSE SWITCH 4)89,999
92 DELT=2.0*DELT
    IF((STDY-TEMP)-10.)95,3,3
95 M=0
    LL=0
    TEMP=TO
    OUT(1)=TO
    TIME=0.

```



```

      DELT=0.01
      GO TO 2
90  X=X-(EL/DIV)
      GO TO 61
100 HR2=EPS*SIGMA*((TEMP**4)-(TO**4))/(TEMP-TO)
      IF(1-MM)115,115,102
102 IF(2-KK)110,110,105
105 IF(1-LL)106,106,158
106 HRA=HR
      DEL1=HR-HR2
      DELSV=DEL1
      IF(DEL1)107,120,109
107 DEL1=(-DEL1)
109 IF(DEL1/HR-5.E-05)120,108,108
108 KK=2
      GO TO 160
110 HRB=HR
      DEL2=HR-HR2
      DELL=DELSV+DEL1
      IF(DELL)113,112,113
112 DEL1=DELSV
      IF(HRA-HRB)113,120,113
113 SLOPE=(DEL1-DEL2)/(HRA-HRB)
      IF(SLOPE)114,120,114
114 B=DEL1-SLOPE*HRA
      HRSAB=(-B/SLOPE)
      KKK=1
      KK=1
      GO TO 160
115 IF(HRSTD-HR2)116,116,117
116 HR=(HR+HRSTD)/2.
      GO TO 118
117 HR=HR2
118 MM=0
      GO TO 4
120 PRINT1,HR
      IF(2-M)121,119,80
119 OUT(2)=TEMP
121 IF(3-M)123,122,80
122 OUT(3)=TEMP
123 IF(4-M)124,124,80
124 OUT(4)=TEMP
      GO TO 80
158 HR=HR2
160 TBAR2=0.
      IF(1-LL)161,161,164
161 DO162J=1,2
      TRM5=GRB(J)*SIN(VALUE(J))/VALUE(J)
162 TBAR2=TBAR2+TRM5
164 TBAR1=0.
      DO163I=1,8
      TRM11=FLUX(I)*(1./HR-1./(COND*EL*U(I)**2))
      TRM1=(1.-EXP(-U(I)*EL))*TRM11

```

```

TRM2=FLUX(I)*EXP(-U(I)*EL)/(COND*U(I))
TRM3=FLUX(I)*EL/(2.*COND)
163 TBAR1=TBAR1+TRM1+TRM2+TRM3
    THETA=TBAR1-TBAR2
    TBAR=THETA+TO
    IF(1-LL)172,172,168
168 TBVAL=TBSAV-TBAR
    IF(TBVAL)169,180,171
169 TBVAL=(-TBVAL)
171 IF((TBVAL/TBAR)-1.E-06)180,180,172
172 TBSAV=TBAR
    COND=CONDB+CONDM*(TBAR-460.0)
    ALPHA=ALPHB+ALPHM*(TBAR-460.)
    DENS=DENSB/(1.0+3.*ALPHA*(TBAR-500.0))
    AKAP=COND/(DENS*CP)
    EPS=EPSB+EPSM*(TBAR-500.)
    IF(TBAR-500.0)173,175,175
173 ELST=ELSTB
    GO TO 174
175 ELST=ELSTB+ELSTM*(TBAR-560.0)
174 STCOF=ELST*ALPHA/(1.0-V)
    IF(1-LLL)130,130,181
181 IF(1-KKK)177,177,176
176 IF(2-KK)178,178,179
177 HR=HRSAV
    KKK=0
    GO TO 179
178 HR=HR2
179 IF(1-LL)4,4,78
180 PRINT1,HR
    HRSTD=HR
    GO TO 70
300 MM=1
    IF(2-M)310,310,305
305 T(2)=TIME
    M=M+1
    MM=0
    GO TO 4
310 TEMP=OUT(1)+(TIME-T(1))*(OUT(2)-OUT(1))/(T(2)-T(1))
    IF(3-M)320,320,313
313 T(3)=TIME
    M=M+1
    GO TO 100
320 TMP21=(OUT(3)-OUT(2))/(T(3)-T(2))-(OUT(2)-OUT(1))/(T(2)-T(1))
    TEMP=TEMP+TMP21*(TIME-T(1))*(TIME-T(2))/(T(3)-T(1))
    IF(4-M)330,330,323
323 T(4)=TIME
    M=M+1
    GO TO 100
330 TMP31=(OUT(4)-OUT(3))/(T(4)-T(3))-(OUT(3)-OUT(2))/(T(3)-T(2))
    TMP32=(1./(T(4)-T(2)))*TMP31
    TMP33=(1./(T(3)-T(2)))*TMP21
    TMP34=(TIME-T(1))*(TIME-T(2))*(TIME-T(3))/(T(4)-T(1))

```

```
TEMP=TEMP+TMP34*(TMP32-TMP33)
DO335I=1,3
J=I+1
OUT(I)=OUT(J)
335 T(I)=T(J)
T(4)=TIME
OUT(4)=TEMP
GO TO 100
400 PRINT1,STDY,X
IF(X)402,402,405
402 LL=1
GO TO 300
405 X=X-(EL/DIV)
GO TO 70
END
```

APPENDIX E

Description and Explanation of the IBM 1620 FORTRAN Program to Calculate the Temperature Distribution and Thermal Stresses in a Plate with Insulation at One Face and Radiative Heat Loss at the Other Face, when Subjected to a Time Dependent Gamma Photon Beam at the First Face

The presence of the time dependent heat generation term in this system makes it expedient to resort to the use of numerical techniques in its solution. The partial differential equation describing this system is

$$\frac{\partial^2 \theta}{\partial x^2} + \frac{H(x,t)}{k} = \frac{1}{\alpha} \frac{\partial \theta}{\partial t} \quad (E-1)$$

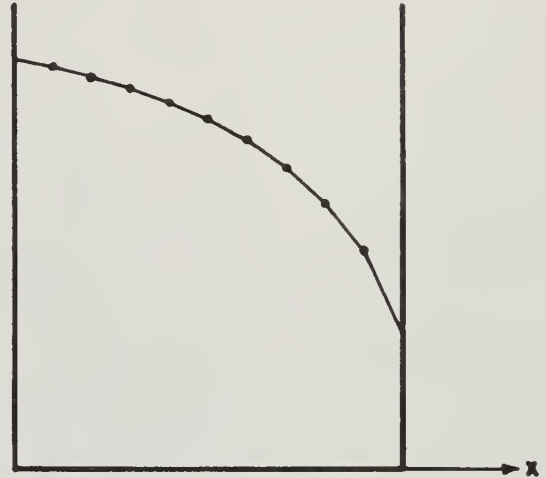


FIG. 19.

In finite difference form, this equation **TEMPERATURE DISTRIBUTION** is written as

$$\frac{\psi(\theta_{i+1}^{n+1} - 2\theta_i^{n+1} + \theta_{i-1}^{n+1}) + (1-\psi)(\theta_{i+1}^n - 2\theta_i^n + \theta_{i-1}^n)}{(\Delta x)^2} + \frac{\mu I(t) e^{-\mu_j \Delta x}}{k} = \frac{1}{\alpha} \left[\frac{\theta_i^{n+1} - \theta_i^n}{\Delta t} \right] \quad (E-2)$$

which may be solved for the $(n+1)$ st time increment at each of the j mesh points across the thickness of the plate as shown in Fig. 19. The value of ψ lies between zero and one and gives an optimum result when chosen as (18)

$$\psi = \frac{1}{2} - \frac{(\Delta x)^2}{12 \alpha \Delta t} \quad (E-3)$$

Analysis of the resulting system of equations yields the matrix found in Appendix B.

This matrix can be solved by any one of a number of methods. The one chosen was the Crout reduction. A special subroutine, called CRAM, has been written to solve an augmented matrix by the Crout reduction. The subroutine carries 20 significant digits in its solution and yields answers which are quite accurate in the eight significant digits reported in the FORTRAN output. The use of this extra accuracy was deemed necessary when an ordinary Crout reduction was found to have round off errors whose magnitude increased as the iteration progresses. It was found that after two or three time increments the answers obtained by normal methods were completely meaningless.

In the solution of the temperature distribution at each time increment, the procedure is much the same as was used in the solution to Eq.(D-1). A value of h_r is first assumed. The matrix was solved for the outside temperature and h_r was then checked against the radiation boundary condition. The value of h_r found from this boundary condition was used as the next estimate and was again checked. Then a linear approximation was used as the first of the next two assumptions for h_r . When the assumed value came within the specified proximity of the boundary condition, the iteration was considered complete.

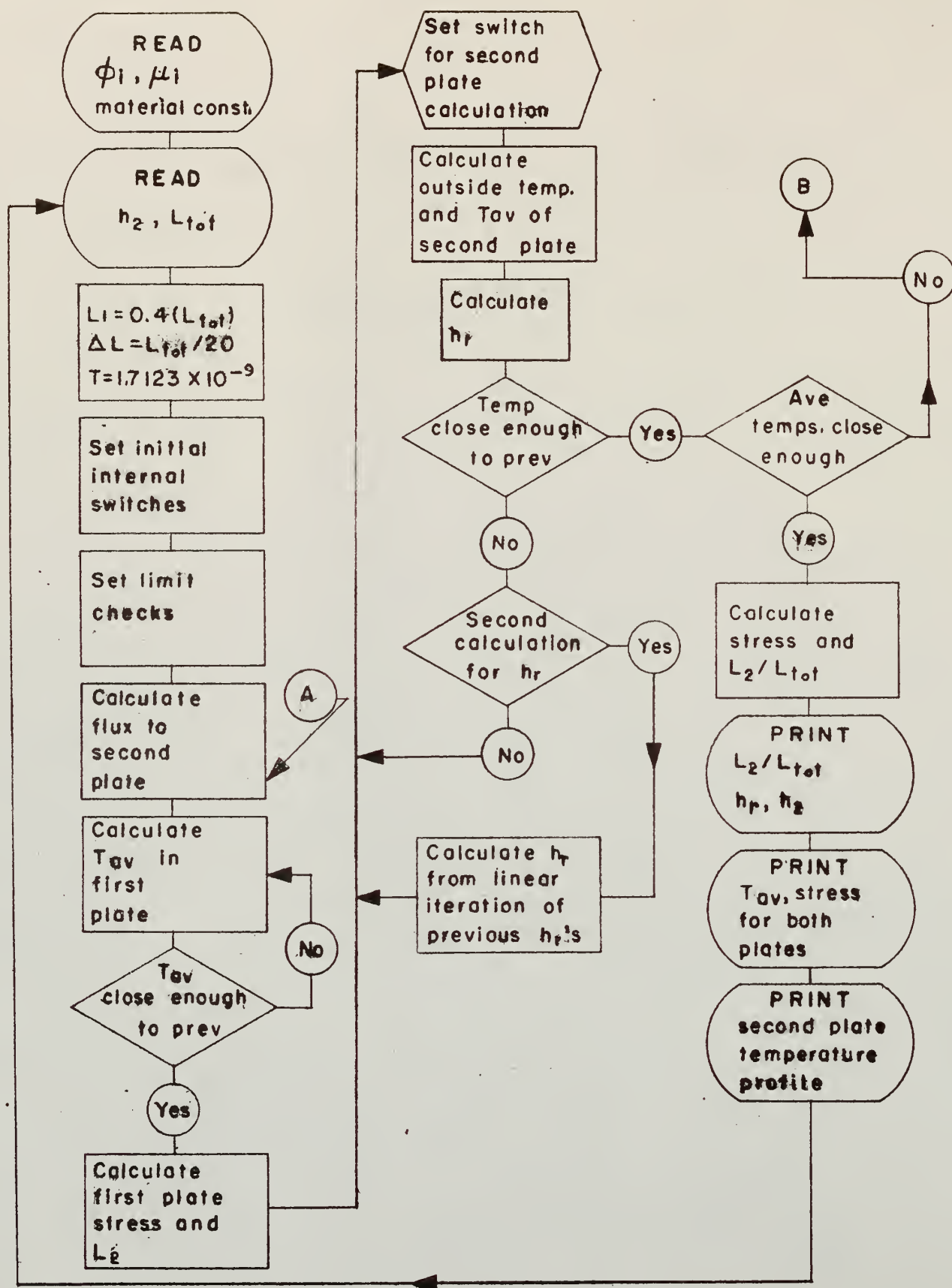
The insertion of the constants into the matrix first requires the solution of Eq.(B-2) to find the gamma photon flux at the time of interest. Since many of the matrix coefficients are temperature dependent, it is necessary to alter them after each trial for h_r has been completed, in the same manner as was done in Appendix D.

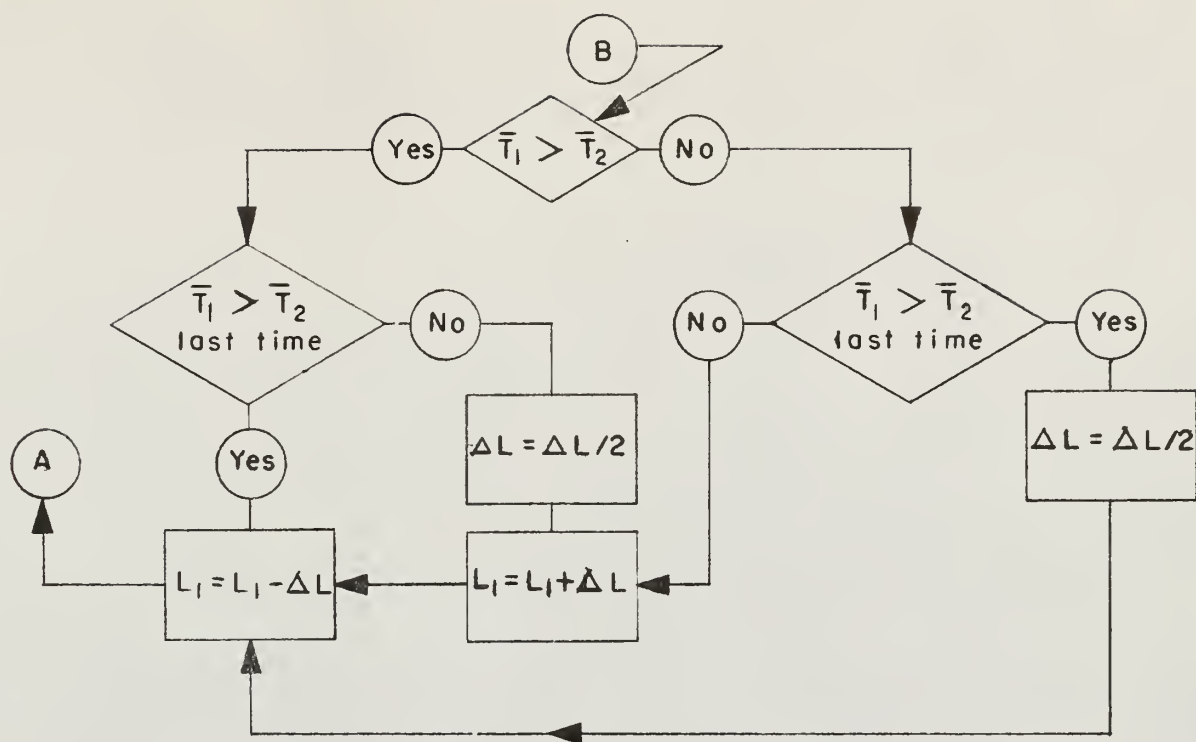
When the true value of h_r had been found, the free plate thermal stress was calculated by the use of Simpson's rule, as shown in Eq.(B-21). The temperature, the free plate thermal stress and the distance from the origin

are printed as output after the value for h_r has been printed. The last printed line contains the time, the average temperature and the average maximum thermal stress for a perfectly restrained plate. The choice as to when the calculations were complete was completely arbitrary, depending on how closely each case was desired to be investigated. Consequently, switch 2 may be turned ON at any time to terminate the program at the completion of the calculation then in progress. After completion, the program will again start at the beginning with a new set of input data. Switch 1 was also included in the program so that the time increment could be doubled at any desired time by turning the switch ON.

The entire input to this program consists of the punched card output from the program described in Appendix D. A single card is put at the front of the input data and contains the absorption coefficient at 1.05 Mev. for the material being examined. The size of the plate being considered is put on a data card and follows the remainder of the input data.

The flow chart for this program and the FORTRAN source deck statements appear on the following pages.





```

    DIMENSION SAV(10,11),FOR(11),OLD(11),FLUX(8),U(8),T(4),OUT(4)
1  FORMAT(E15.8,E15.8,E15.8,E15.8)
    READ1,U
3  READ1,ALPHA,TO,AKAP,COND
    READ1,EPSTB,DIV,STCOF,HR
    READ1,ELSTB,ALPHB,CONDB,DENSTB
    READ1,ELSTM,ALPHM,CONDM,CP
    READ1,ELST,V,TIME,EPSTM
    READ1,DELT,HRSTD,TEMP
    DO4I=1,8
4  READ1,FLUX(I)
    DO5I=1,11
5  READ1,OLD(I)
    TAU=TIME*3600.
    Z=0.
    EPS=EPSTB
    SIGMA=1.7123E-09
    READ1,EL
    DELX=EL/DIV
    FLUXX=0.
    DO7I=1,8
7  FLUXX=FLUXX+FLUX(I)
    GO TO 300
12 TIME=TIME+DELT
    PREV=OLD(11)
    Z=Z+DELT*3600.
    ZT=Z+TAU
    FFLUX=.1*(1./((Z+10.)**(.2))-1./((ZT+10.)**(.2)))
    FFLUX=FFLUX+.087*(1./((Z+2.E+07)**(.2))-1./((ZT+2.E+07)**(.2)))
    FFLUX=FFLUX-.0025*(EXP(-Z/2040.)-EXP(-ZT/2040.))
    FFLUX=FLUXX*(FFLUX-.0013*(EXP(-Z/290000.)-EXP(-ZT/290000.)))
15 BNDRY=(1.+HR*DELX/COND)
    PSI=0.5-DELX**2/(12.*AKAP*DELT)
    RATIO=DELX**2/(DELT*AKAP)
    RAPSI=RATIO+2.*PSI
    DIFF=1.-PSI
    FLCON=U*FFLUX*DELX**2/COND
    DO30I=1,10
    DO30J=1,11
30 SAV(I,J)=0.
    DO20I=2,10
    SAV(I,11)=DIFF*(OLD(I+1)-2.*OLD(I)+OLD(I-1))+RATIO*(OLD(I)-TO)
    H=I-1
20 SAV(I,11)=SAV(I,11)+FLCON*EXP(-H*U*DELX)
    SAV(1,11)=DIFF*(2.*OLD(2)-2.*OLD(1))+RATIO*(OLD(1)-TO)+FLCON
    M=1
    SAV(1,1)=RAPSI
    SAV(1,2)=-2.*PSI
    DO40I=2,9
    SAV(I,I-1)=-PSI
    SAV(I,I)=RAPSI
40 SAV(I,I+1)=-PSI
    SAV(10,9)=-PSI
    SAV(10,10)=RATIO+(2.-1./BNDRY)*PSI

```

```

      FOR(1)=CRAM(10.)
80  FOR(11)=FOR(10)/BNDRY
      TEMP=FOR(11)+TO
100  HR2=EPS*SIGMA*((TEMP**4)-(TO**4))/(TEMP-TO)
      IF(1-MM)115,115,102
102  IF(2-KK)110,110,106
106  HRA=HR
      DEL1=HR-HR2
      DELSV=DEL1
      IF(DEL1)107,120,109
107  DEL1=(-DEL1)
109  IF(DEL1/HR-1.E-05)120,108,108
108  HR=HR2
      KK=2
      GO TO 200
110  HRB=HR
      DEL2=HR-HR2
      DELL=DELSV+DEL1
      IF(DELL)113,112,113
112  DEL1=DELSV
      IF(HRA-HRB)113,120,113
113  SLOPE=(DEL1-DEL2)/(HRA-HRB)
      IF(SLOPE)114,120,114
114  B=DEL1-SLOPE*HRA
      HR=(-B/SLOPE)
      KK=1
      GO TO 200
115  HR=HR2
      MM=0
      GO TO 15
120  PRINT1,HR
      M=0
      GO TO 200
160  TBAR=STR2+TO
      CONDB=CONDB+CONDM*(TBAR-460.0)
      ALPHB=ALPHB+ALPHM*(TBAR-460.0)
      DENS=DENSB/(1.0+3.*ALPHA*(TBAR-500.0))
      AKAP=COND/(DENS*CP)
      EPS=EPSB+EPSM*(TBAR-500.)
      IF(TBAR-500.0)173,175,175
173  ELST=ELSTB
      GO TO 174
175  ELST=ELSTB-ELSTM*(TBAR-500.0)
174  STCOF=ELST*ALPHA/(1.-V)
      GO TO 15
190  DEL=0.
      DO192I=1,11
      X=DEL*DELX
      DEL=DEL+1.0
      OLD(I)=FOR(I)+TO
192  PUNCH1,OLD(I),STRES(I),X
      IF(2-N)182,181,193
181  OUT(2)=TEMP
182  IF(3-N)184,183,193

```

```

183 OUT(3)=TEMP
184 IF(4-N)185,185,193
185 OUT(4)=TEMP
    STMAX=STR2*STCOF
193 PUNCH1,TIME,TBAR,STMAX
    IF(SENSE SWITCH 2)3,250
250 IF(SENSE SWITCH 1)251,12
251 DELT=2.*DELT
    GO TO 12
200 STR2=FOR(1)+4.*(FOR(2)+FOR(4)+FOR(6)+FOR(8)+FOR(10))
    STR2=(STR2+2.*(FOR(3)+FOR(5)+FOR(7)+FOR(9))+FOR(11))/30.
    IF(1-M)160,160,202
202 STR31=(FOR(11)-FOR(1))*EL/2.
    STR32=4.*((9.*DELX-EL/2.)*FOR(2)+(DELX-EL/2.)*FOR(10))
    STR33=2.*((8.*DELX-EL/2.)*FOR(3)+(2.*DELX-EL/2.)*FOR(9))
    STR34=4.*((7.*DELX-EL/2.)*FOR(4)+(3.*DELX-EL/2.)*FOR(8))
    STR35=2.*((6.*DELX-EL/2.)*FOR(5)+(4.*DELX-EL/2.)*FOR(7))
    STR37=STR31+STR32+STR33+STR34+STR35
    R=0.
    DO205I=1,11
    STRES(I)=STCOF*(STR2-FOR(I)+.4*(R*DELX-EL/2.)*STR37/EL**2)
205 R=R+1.
    GO TO 190
300 MM=1
    IF(1-N)310,310,305
305 T(2)=TIME
    N=N+1
    MM=0
    GO TO 15
310 TEMP=OUT(1)+(TIME-T(1))*(OUT(2)-OUT(1))/(T(2)-T(1))
    IF(2-N)320,320,313
313 T(3)=TIME
    N=N+1
    GO TO 100
320 TMP21=(OUT(3)-OUT(2))/(T(3)-T(2))-(OUT(2)-OUT(1))/(T(2)-T(1))
    TEMP=TEMP+TMP21*(TIME-T(1))*(TIME-T(2))/(T(3)-T(1))
    IF(3-N)330,330,323
323 T(4)=TIME
    N=N+1
    GO TO 100
330 TMP31=(OUT(4)-OUT(3))/(T(4)-T(3))-(OUT(3)-OUT(2))/(T(3)-T(2))
    TMP32=(1./(T(4)-T(2)))*TMP31
    TMP33=(1./(T(3)-T(2)))*TMP21
    TMP34=(TIME-T(1))*(TIME-T(2))*(TIME-T(3))/(T(4)-T(1))
    TEMP=TEMP+TMP34*(TMP32-TMP33)
    DO335I=1,3
    J=I+1
    OUT(I)=OUT(J)
335 T(I)=T(J)
    T(4)=TIME
    OUT(4)=TEMP
    GO TO 100
END

```

APPENDIX F

An Explanation and Description of the IBM 1620 FORTRAN
Program to Equate the Steady State Maximum Thermal Stress
and Find the Temperature Distribution in the Outer Plate

The consideration used to equate the maximum thermal stress in the two plates was an equality of the average temperatures within certain tolerance limits, which were arbitrarily chosen. The equation for the average steady state temperature in the first plate is

$$\bar{\theta}_1 = \frac{I_1}{k_1 \mu_1} e^{-\mu_1 L_1} + \left(\frac{I_1}{h_1} - \frac{I_1}{k_1 \mu_1^2 L_1} \right) (1 - e^{-\mu_1 L_1}) + \frac{I_1 L_1}{k_1 \mu_1} \quad (F-1)$$

In the outer plate the average steady state temperature is given by

$$\bar{\theta}_2 = -\frac{R_1 e^{-\mu_2 L_2}}{\mu_2 L_2} + \frac{R_2 L_2}{2} + R_3 \quad (F-2)$$

where

$$R_1 = -\frac{I_2}{k_2 \mu_2}$$

$$R_2 = -\frac{h_r h_2 \frac{I_2}{k_2 \mu_2} (1 - e^{-\mu_2 L_2}) + I_2 (h_2 e^{-\mu_2 L_2} + h_r)}{k_2 h_r + k_2 h_2 + h_2 h_r L_2} \quad (F-3)$$

$$R_3 = I_2 e^{-\mu_2 L_2} \left(\frac{1}{k_2 \mu_2} - \frac{1}{h_r} \right) - R_2 \left(\frac{k_2}{h_2} + L_2 \right)$$

and also where

$$I_2 = I_1 e^{-\mu_1 L_1} \quad (F-4)$$

The maximum thermal stress for the completely restrained plate is given
by

$$\sigma_{max} = -\frac{\alpha E}{1-\nu}(\bar{\theta}) \quad (F-5)$$

and in the present case this has been altered slightly to give the average maximum thermal stress. This is

$$\bar{\sigma}_{max} = -\frac{\alpha E}{1-\nu}(\bar{\bar{\theta}}) \quad (F-6)$$

so that a single uniform stress is present at the ends of the plate. It is easily seen that the maximum stress in each plate is equal when the average temperature in the plates are equal. The two temperatures were considered equal when the quantity $\Delta T/T$ is less than 10^{-4} .

The steady state temperatures are a function of the thickness of each of the two plates for some fixed total thickness of the two plates. Hence, it is necessary to iterate for the correct thickness. This is done by assuming some initial percentage of the total thickness is in the first plate. If the average temperature in the first plate is higher than that of the second plate, its thickness is decreased by some fixed increment until the average temperature in the first plate is less than that of the second.

At this point, the increment is halved and the thickness of the plate is increased until the temperature is again greater in the first plate. The increment is again halved and the iteration then proceeds in the opposite direction. This procedure continues until the limits have been reached. If the initial estimate yields a lower average temperature in the first plate, the iteration proceeds in the opposite order from that described above.

When the iteration has been completed, the temperature distribution in the second plate is calculated. It was not thought necessary to calculate

the distribution in the first plate since this is essentially the same as the case of the single plate previously considered. The temperature distribution in the second plate is given by

$$\theta_2 = R_1 e^{-\mu_2 x_2} + R_2 x_2 + R_3 \quad (F-7)$$

where R_1 , R_2 , and R_3 are the same as defined above.

The input data cards to this program consist of the following:

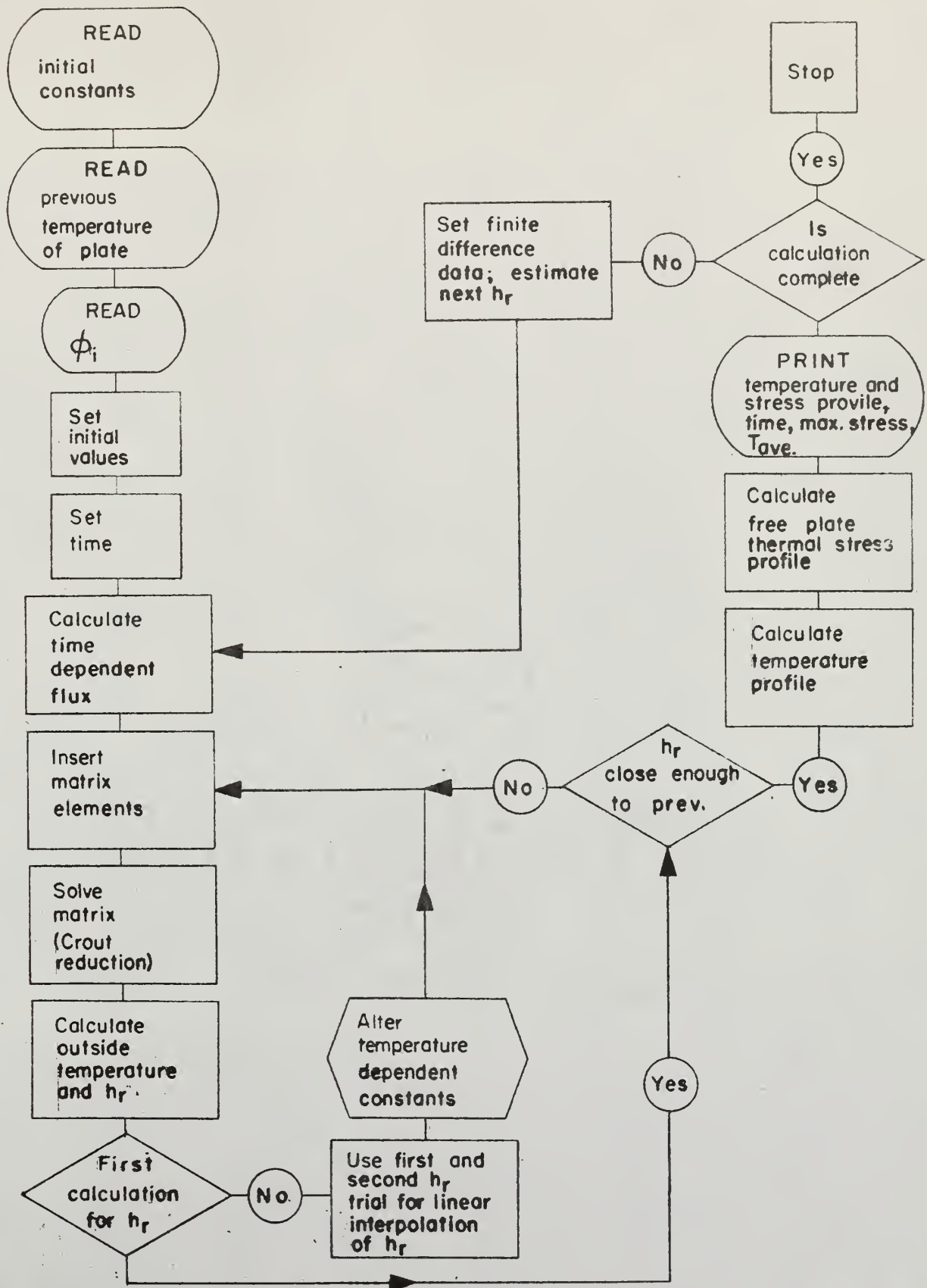
1. The flux and absorption coefficient for each of the eight energy groups employed. (8 cards)
2. The intercept and slope of the emissivity with regard to its temperature dependency, the value of the quantity $\alpha E / (1 - \nu)$ and the base temperature. (1 card)
3. The temperature dependent intercepts of the modulus of elasticity, the coefficient of thermal expansion and the conductivity, and the density of the material at 40°F. (1 card)
4. The temperature dependent slopes of the modulus of elasticity, the coefficient of thermal expansion and the conductivity, and the value of the heat capacity. (1 card)
5. The initial values of the modulus of elasticity, the coefficient of thermal expansion and the conductivity, and Poisson's ratio. (1 card)
6. The heat transfer coefficient between the plates, and an initial estimate of the equivalent gray body convective radiation coefficient, the total thickness of the two plates and the steady state temperature of a single plate of the same total thickness. (1 card)

The output data, in printed form, consists of the following:

1. The percentage of the total thickness contained in the second plate, the final equivalent convective radiation coefficient and the convection coefficient between the two plates.
2. The average temperature of the first and second plates and the average maximum thermal stress of both plates.
3. The temperature profile of the second plate.

It is also possible to follow the path of the difference between the average temperatures in the first and second plates by turning switch 2 ON. At the completion of each calculation for a given choice of thicknesses for each of the two plates, this difference will be printed.

The flow chart for this program and the FORTRAN source deck statements appear on the following pages.



```

1  FORMAT(E15.8,E15.8,E15.8,E15.8)
   DIMENSION FLUX(16),U(8)
   DO15I=1,8
15  READ1,FLUX(I),U(I)
   READ1,EPSB,EPSM,STCOF,TO
   READ1,ELSTB,ALPHB,CONDB,DENSB
   READ1,ELSTM,ALPHM,CONDM,CP
   READ1,ELST,ALPHA,COND,V
17  READ1,H2,HR,ELTOT,STDY
   EL=.5*ELTOT
   DELTL=ELTOT/20.
   SIGMA=1.7123E-09
   L=0
   LL=0
   M=0
   KK=1
   TBSAV=0.
   TBR22=0.
20  DO25I=1,8
   K=I+8
25  FLUX(K)=FLUX(I)*EXP(-U(I)*EL)
164 TBAR1=0.
   DO163I=1,8
   TRM11=FLUX(I)*(1./H2-1./(COND*EL*U(I)**2))
   TRM1=(1.-EXP(-U(I)*EL))*TRM11
   TRM2=FLUX(I)*EXP(-U(I)*EL)/(COND*U(I))
   TRM3=FLUX(I)*EL/(2.*COND)
163 TBAR1=TBAR1+TRM1+TRM2+TRM3
   TBAR=TBAR1+TO
168 TBVAL=TBSAV-TBAR
   IF(TBVAL)169,180,171
169 TBVAL=(-TBVAL)
171 IF(TBVAL/TBAR-1.E-06)180,180,172
172 TBSAV=TBAR
165 COND=CONDB+CONDM*(TBAR-460.0)
   IF(COND)166,166,167
166 COND=0.1
167 ALPHA=ALPHB+ALPHM*(TBAR-460.)
   DENS=DENSB/(1.0+3.*ALPHA*(TBAR-500.0))
   AKAP=COND/(DENS*CP)
   EPS=EPSB+EPSM*(TBAR-500.)
   IF(TBAR-500.0)173,175,175
173 ELST=ELSTB
   GO TO 174
175 ELST=ELSTB+ELSTM*(TBAR-560.0)
174 STCOF=ELST*ALPHA/(1.0-V)
   IF(1-LL)176,176,164
176 IF(2-KK)178,178,400
178 HR=HR2
   GO TO 400
180 STRS1=(-STCOF*TBAR1)
   EL=ELTOT-EL
   X=EL

```



```

      LL=1
      GO TO 400
100  HR2=EPS*SIGMA*((TEMP**4)-(TO**4))/(TEMP-TO)
102  IF(2-KK)110,110,106
106  HRA=HR
      DEL1=HR-HR2
      TBR21=TBAR2
      TBR2=TBR21-TBR22
      IF(TBR2)107,120,109
107  TBR2=(-TBR2)
109  IF(TBR2-5.E-02)120,108,108
108  KK=2
      GO TO 165
110  HRB=HR
      DEL2=HR-HR2
      TBR22=TBAR2
      IF(HRA-HRB)113,120,113
113  SLOPE=(DEL1-DEL2)/(HRA-HRB)
      IF(SLOPE)114,120,114
114  B=DEL1-SLOPE*HRA
      HR=(-B/SLOPE)
      KK=1
      GO TO 165
120  LL=0
      GO TO 450
400  TEMP=0.
      TBAR2=0.
      DO405 I=1,8
      K=I+8
      UL=(-U(I)*EL)
      R1=(-FLUX(K)/(COND*U(I)))
      R2N=(-R1*HR*H2*(1.-EXP(UL))+FLUX(K)*(HR+H2*EXP(UL)))
      R2=(-R2N/(COND*(HR+H2)+HR*H2*EL))
      R3=(-R2*(COND/HR+EL))+FLUX(K)*EXP(UL)*(1./(COND*U(I))-1./HR)
      TEMP=TEMP+R1*EXP(-U(I)*X)+R2*X+R3
405  TBAR2=TBAR2+R1*(EXP(UL)-1.)/UL+R2*EL/2.+R3
      TEMP=TEMP+TO
      IF(TBAR1-TBAR2-TBAR1/2.)404,464,464
404  IF(TBAR2+TO-STDY)406,406,407
406  TBAR=TBAR2+TO
      GO TO 408
407  TBAR=STDY
408  IF(1-L)505,505,100
450  TBR=TBAR1-TBAR2
      IF(SENSE SWITCH2)449,448
449  PRINT1,TBR
448  TBSV2=TBR
      IF(TBR)451,500,452
451  TBR=(-TBR)
452  IF(TBR/TBAR2-1.E-04)500,500,453
453  IF(TBSV2)455,500,465
455  IF(1-M)475,456,456
456  EL=ELTOT-EL+DELTL

```



```
M=1
GO TO 20
464 LL=0
EL=ELTOT-EL-DETL
GO TO 20
465 IF(1-M)466,475,466
466 EL=ELTOT-EL-DETL
M=2
GO TO 20
475 DETL=DETL/2.
IF(1-M)456,466,466
500 STRS2=(-STCOF*TBAR2)
ELPCT=EL/ELTOT
PRINT1,ELPCT,HR,H2
PRINT1,TBAR1,TBAR2,STRS1,STRS2
L=1
505 PRINT1,X,TEMP
IF(X)17,17,506
506 X=X-EL/10.
IF(X-EL/10.)507,400,400
507 X=0.
GO TO 400
END
```


A TRANSIENT ANALYSIS OF TEMPERATURES
AND THERMAL STRESSES IN GAMMA
HEATED MATERIALS

by

NORMAN KARL RUMPF

B. S., Lehigh University, 1959

AN ABSTRACT OF A THESIS

submitted in partial fulfillment of the

requirements for the degree

MASTER OF SCIENCE

Department of Nuclear Engineering

KANSAS STATE UNIVERSITY
Manhattan, Kansas

1963

ABSTRACT

In considering the structural aspects of nuclear rockets, it is possible to construct idealized models of structures which might be found in the vicinity of the reactor. Such a model is an infinite flat plate one face of which is subjected to a constant gamma photon flux. The temperatures and thermal stresses of both a steel and an aluminum plate are investigated. The temperatures of steel plates as thick as one inch are well below the melting point for a flux intensity of $94500 \text{ Btu/hr, ft}^2$ when radiation heat loss is the only mode of heat transfer available. For aluminum, this energy flux must be reduced by a factor of ten to keep it below the melting point.

In steel, the maximum thermal stress for a plate held in perfect restraint exceeds the yield stress after being subjected to the gamma heating for a few minutes. The aluminum must be heated for longer than one hour before the maximum thermal stress exceeds the yield stress. For a plate restrained in bending, the thermal stresses in both aluminum and steel are below the yield stress. The free plate stresses are small enough to be considered insignificant.

After shutdown of the reactor, the plate is exposed to a time dependent gamma flux. Although its magnitude is quite significant, the plate initially cools at a rate almost the same as if no additional heating were present. The cooling begins so rapidly that the temperature appears to be discontinuous with time.

Additional cooling can be provided for the plate by constructing a system which enables the other face of the plate to lose heat by convection. Two parallel plates were considered, where the total thickness of both plates was the same as that of the single aforementioned plate. Then the steady

state temperatures and thermal stresses were compared with the single plate case as the magnitude of the convection coefficient was changed. The base temperature to which heat was lost by both radiation and convection was always assumed to be 500°R .

The temperature in both steel and aluminum were found to be lower than the single plate case. In aluminum, this difference was most pronounced since it has a low emissivity and does not readily lose heat by radiation alone. The thermal stress for the case of a plate restrained in bending exhibited a minimum at the time when the heat lost from one face of the plate by radiation was equal to the heat lost from its other face by convection.

[illegible]